TECHNISCHE UNIVERSITÄT WIEN
Vienna University of Technology

DIPLOMARBEIT

Observation of GNSS satellites with VLBI antennas – From observation planning to practical implementation

ausgeführt zum Zwecke der Erlangung des akademischen Grades eines Diplom-Ingenieurs unter der Leitung von

Prof. Dr. Johannes Böhm
Technische Universität Wien,
Department für Geodäsie und Geoinformation (E120-4)

Dr.rer.nat. Alexander Neidhardt
Technische Universität München, Geodätisches Observatorium Wettzell

Dr. Lucia Plank
University of Tasmania

eingereicht an der Technischen Universität Wien
Fakultät für Mathematik und Geoinformation

von

Andreas Hellerschmied
Turnergassegasse 27/2
1150 Wien

Wien, November 2014

Acknowledgments

My greatest appreciation deserves Johannes Böhm, my supervisor at my home institution in Vienna. I want to thank him for his dedication to promote my work and for giving me the possibility to present my findings in an international frame. He enabled me, to get into contact with the VLBI community and gave me an insight into the current research. Beyond that, he introduced me to the VieVS developers group, of which I am a member now myself.

I want to express my deep gratitude to Lucia Plank. Although she moved to the other side of the globe, to Tasmania, during the time I worked on this thesis, she never stopped to support me and my work, by giving me many valuable suggestions and advice. I specially appreciate her enthusiastic character, and her contagious and unbreakable motivation.

Altogether, I spent nearly two months in Germany at the Geodetic Observatory Wettzell, to do research for this thesis topic. There, I had the unique opportunity to learn about VLBI from a completely new perspective. I had the possibility, to get deeper insights into applied VLBI data acquisition, I gathered lots of valuable experiences. For this I am grateful. I am truly thankful to Alexander Neidhardt, the head of the radio telescope group in Wettzell. He invited me to come to Wettzell for this joint project and also supported me in handling all the organizational issues.d During my research stay, he spent a lot of time and effort on our work, and he always had a sympathetic ear for my concerns. I would also like to thank the rest of the staff of the radio telescope group, in particular Jan Kodet, Christian Plötz and Gerhard Kronschnabl. They all supported me in the process of my work.

My special acknowledgment is directed to Rüdiger Haas, for the close cooperation during our experiments in early 2014 and for the subsequent analysis of the acquired data. Without his involvement, large parts of this research topic could not have been covered.

Finally I want thank my parents for their consistent support of my education and my academic career throughout my life. Without their assistance I would not be here I am now. Thank you.

Andreas Hellerschmied, November 2014

Abstract

Within this master thesis options for an operational path of carrying out VLBI observations of satellites are investigated. From scheduling, over satellite tracking, to actual data acquisition, the complete process chain is considered. One concept for VLBI satellite observations has been exemplarily realized with the radio antennas at the Geodetic Observatory Wettzell (GOW), Germany. It is based on a newly developed satellite scheduling module of the Vienna VLBI Software (VieVS) in combination with dedicated satellite tracking features provided directly by the Antenna Control Units (ACU), which were activated in the NASA Field System (FS).

Observing satellites with VLBI is a promising topic and has been discussed vividly in the VLBI community for the last few years. Despite several successful experiments, a clear strategy has not been shown so far, demonstrating a way of realizing such observations operationally. The challenges already start at the observation planning level, because the common scheduling software packages are currently not able to schedule moving satellites as targets. Additionally, the current standard data-formats used for VLBI schedule files do not provide the possibility to define satellite orbits in a suitable way. Finally, the most recent version of the FS does not yet support the generation of appropriate local control-files (SNAP files) for satellite observations, which would be required to carry out such VLBI sessions automatized. These restrictions are the reason that previous satellite observations had to be done with hand-written schedules and numerous manual interaction at the stations. Therefore, an operational path for satellite observations with VLBI is still missing.

On that account a joint project with the GOW was started to investigate concepts for an operational path for VLBI observations of satellites. VieVS was extended with a new module providing the possibility of scheduling VLBI satellite observations. Considering several observation conditions, such as the common visibility from a selected station network, the program determines a selection of satellites being potentially available for observations and presents this information to the user, who is asked to assemble an observation plan. The schedule is then saved in the VEX format, with the changing satellite positions converted to sequences of corresponding topocentric celestial coordinates. Based on these VEX files satellites can be tracked – virtually stepwise – by consecutively re-positioning the antennas in a defined time interval. Alternatively, preparations were made at Wettzell to be able to track satellites in a truly continuous fashion by making use of the satellite tracking mode provided by the ACU of Wettzell's antennas. Therefore, modifications in the station-specific code of the FS were required to enable this feature. Several successful obser-

vations of GLONASS satellites were carried out in January 2014 on the baseline Wettzell-Onsala based on the implemented concept, validating that all developments worked properly. These experiments showed that VLBI satellite observations can already be carried out nearly operationally, which is important to promote further developments and research activities in this field of VLBI.

Contents

Chapter 1

Introduction

Satellite tracking with Very Long Baseline Interferometry (VLBI) antennas has become a hot topic within the last years and was vividly discussed in the scientific community, as the increasing number of on-topic publications suggests. It offers a variety of new possibilities in terms of the improvement of geodetic products, such as the International Terrestrial Reference Frame (ITRF), and represents an important step toward a rigorous combination of different space-geodetic techniques. The latter one – the benefit of a VLBI-satellite-hybrid approach in terms of an inter-technique combination – is one of the main goals of the Global Geodetic Observing System (GGOS)[1], an initiative of the International Association of Geodesy (IAG)[2].

This work discusses approaches and strategies of how to observe radio signals from Earth satellites (GNSS satellites in our case, without restriction) with large radio antennas, as used for the geodetic VLBI. The outcome is a recommendation for a (nearly) operational way of conducting such observations with today's technical state-of-the-art means – from scheduling to data acquisition.

In the following pages I will look into the question of why satellite tracking with VLBI antennas is of interest for geodetic issues and which kind of motivations are behind. After discussing important previous work in the field of VLBI satellite observations, the tasks and objectives for this thesis are formulated.

1.1 Motivation and previous work

Global reference frames Global coordinate systems are the foundation for many technical applications, which are of great economical, social and ecological interest, such as navigation, surveying and global change monitoring. These coordinate systems serve for all kinds of measurements on and around Earth as a location reference. Under those circumstances modern geodesy

[1] http://www.ggos.org/
[2] http://www.iag-aig.org/

plays an important role as the science, which is capable of realizing such global reference systems.

On a global scale there are several reference systems in use. In terms of accessibility we distinguish between kinematically realized systems, which are applicable through positions and velocities at a certain time epoch, and dynamic reference frames, defined by ephemeris of celestial bodies or space probes, such as satellites. Furthermore we distinguish between celestial (space fixed) systems, realizing at least an approximated inertial reference frame, and terrestrial (Earth fixed) systems, which are co-rotating with the Earth. The connections between space and Earth fixed systems are established by means of the current orientation of the Earth in space, which is observed by space-geodetic techniques. The derived parameters, which describe the Earth's orientation, are referred to as Earth Orientation Parameters (EOP). The knowledge of these EOP enable the coordinate transformation between both systems.

The most important realizations of global coordinate systems, used in almost all global applications, are the International Celestial Reference Frame (ICRF) and the International Terrestrial Reference Frame (ITRF). The current realization of the ICRF (ICRF2; Fey *et al.*, 2009) is defined by positions of extragalactic radio sources (quasars) only, acquired with the Very Long Baseline Interferometry (VLBI) technique. The latest ITRF (ITRF2008, Altamimi *et al.* (2011)) is a combined product of VLBI and three space-geodetic techniques using satellites: Global Navigation Satellite Systems (GNSS), Satellite Laser Ranging (SLR) and Doppler Orbitography and Radiopositioning Integrated by Satellites (DORIS). Except for the determination of the origin, it is possible to generate a terrestrial reference frame as a VLBI-only solution, the VLBI Terrestrial Reference Frame[1] (VTRF). Nevertheless, a combined product is preferred for the ITRF realization in order to make an optimum use of the specific strengths of each space-geodetic technique.

Local frame ties. A crucial task is the combination of the single-technique solutions of all four contributing space techniques to one combined solution, the ITRF solution. This is done by establishing precise frame ties in terms of locally surveyed coordinate differences between the reference points of the antennas, or the related geodetic markers, of contributing techniques at collocation sites[2]. These terrestrially determined ties, referred to as *local ties*, play a key role at the ITRF combination. For the ITRF2008 combination, as for any ITRF combination, local ties at co-located sites are used with proper weighting in addition to the observations of the space-geodetic techniques, as described in detail in Altamimi *et al.* (2002).

Seitz *et al.* (2012) shows, that despite precise terrestrial surveying, discrepancies of up to a few centimeters occur between local ties and tie vectors determined through estimates of the contributing space-geodetic techniques. According to that, either local ties, or space geodesy estimates, or both, are imprecise or flawed. These discrepancies could have several causes, e.g.

[1] The VTRF is based on VLBI station coordinates and is calculated by applying No Net Translation (NNT) and No Net Rotation (NNR) conditions. Further information is available at http://ccivs.bkg.bund.de/quarterly/vtrf

[2] "A collocation site is defined by the fact that two or more space geodesy instruments are occupying simultaneously or subsequently very close locations which are very precisely surveyed in three dimensions, using classical surveys or the GPS technique (Altamimi *et al.*, 2002)".

outdated local tie measurements, measurement errors, or missing variance covariance information, which is necessary for a proper weighting. In general the surveying of local tie vectors is a difficult task. One problem is, that the physical reference points of the used geodetic instruments are practically inaccessible. Therefore it involves a great deal of effort to determine the local tie vectors with a sufficient precision. Furthermore, it is difficult to precisely determine the eccentricity between the intersection of the axes of VLBI or SLR telescopes and the ground physical markers (Altamimi *et al.*, 2011). Additional problems could occur due to gravity deformations on large VLBI antennas (Sarti *et al.*, 2011). However, there is room for improvement in the establishment of inter-technique ties. In this regard Altamimi *et al.* (2011) state that,

> "*...future ITRF improvement resides in improving the consistency between local ties in co-location sites and space geodesy estimates.*"

Co-location in space. The co-location of several geodetic techniques on one satellite platform provides promising possibilities regarding frame connection with inter-technique ties. Thaller *et al.* (2011) suggested the inclusion of such *space ties* in the ITRF combination as a complement to the local ties on the Earth's surface. She already combined SLR and GNSS observations successfully using co-location in space (Thaller *et al.*, 2011).

Plank (2014) outlined the concept of a satellite, realizing a space tie, which is dedicated to the improvement of the TRF realization, as shown in Fig. 1.1. According to that, one satellite is observed simultaneously by several space-geodetic techniques. If the relative positions of the different sensors on the platform are precisely known, such a configuration can combine the frames of the involved techniques.

Assuming a rigorous co-location platform in space is intended, it has to have antennas, respectively receivers, for all four space-geodetic techniques as payload in best case. In detail retro reflectors for SLR, a DORIS receiver, a GNSS receiver and dedicated signal transmitters in the S/X-band for observations with currently regular VLBI antennas are required. A first satellite mission trying to realize such a configuration was proposed to NASA in 2011. This mission, called Geodetic Reference Antenna in Space (GRASP; Nerem & Draper, 2011), was not granted yet. Nevertheless, it was evaluated as good and has serious chances to be realized in the future with slight modifications (Plank, 2014).

Another possible scenario is to use already available infrastructure for the implementation of co-location in space, instead of launching new satellites. Many satellites, such as the satellites of the various GNSS constellations, use microwave signal for communication and for measurement purposes. Assuming that the satellite signals are located in an appropriate frequency band, it would be possible to observe them with VLBI radio antennas. This would enable a rigorous connection between e.g. the dynamic reference frame of GNSS and the kinematic frame of VLBI (Plank, 2014).

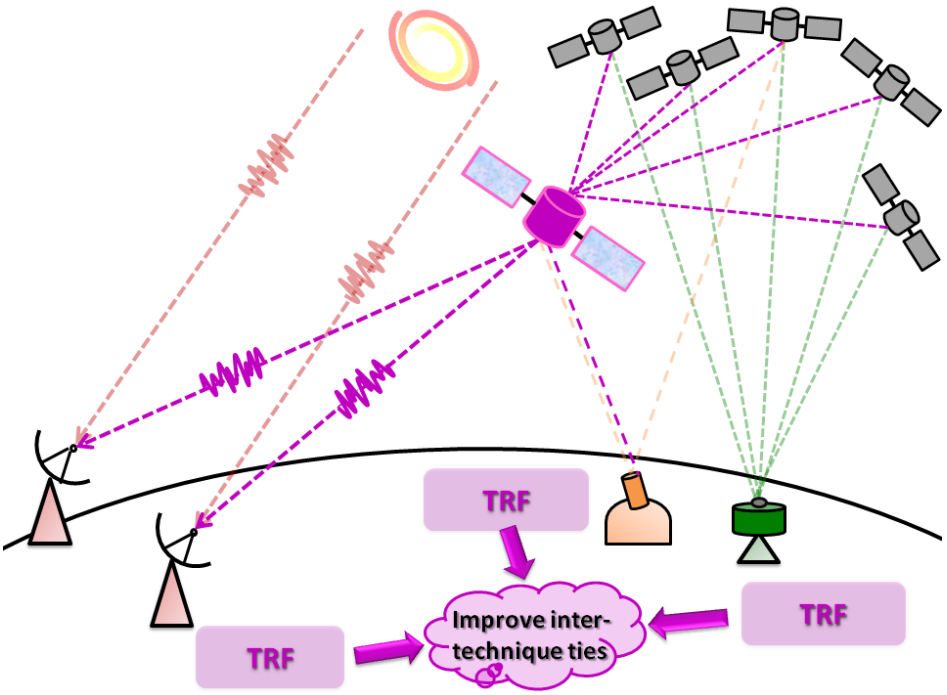

Figure 1.1: Principle of a *space tie*. A satellite is tracked simultaneously by different space-geodetic techniques (VLBI, SLR and GNSS) realizing a platform for co-location in space (Plank *et al.*, 2014).

Observation of GNSS signals with VLBI As implied above, a promising approach for the implementation of co-location in space is the observation of signals from GNSS satellites with VLBI antennas. Although GNSS satellites are not qualified to serve as a co-location platform for all four space-geodetic techniques contributing to the ITRF (due to the missing DORIS equipment and the missing SLR retro-reflectors on many GNSS satellites), they could provide a link between the reference frames of GNSS and VLBI.

Hase (1999) suggested to use VLBI observations of GNSS satellites to solve the problem of tying their signal transmitters directly into the ICRF, the most accurate realization of a quasi-inertial system. According to Dickey (2010), the determination of GNSS satellite orbits with VLBI directly in the ICRF would give the possibility to establish the position of the Earth's center of mass in the ICRF. This is not possible with classical VLBI observations of quasars.

Dickey (2010) basically proposed two approaches of how to observe GNSS satellite signals with the VLBI antennas of the International VLBI Service for Geodesy and Astrometry (IVS)[1] network:

1. **Direct observations of GNSS satellites with VLBI antennas.** The VLBI antennas themselves record the GNSS signals as standard VLBI data. Then the acquired data are correlated to determine the delay on each baseline and hence the position of each satellite as a function of time (Dickey, 2010). This approach has two obvious disadvantages: (1) The field of view

[1] http://ivscc.gsfc.nasa.gov/

of large VLBI antennas is narrow. Therefore it is necessary to track the satellite's position with the antenna during an observation, which is a problem for large telescopes. (2) The frequencies of GNSS signals[1] are below the S-band frequencies ($2100-2400MHz$), which are usually observed with the common receiver equipment of IVS stations. Solutions have to be found in order to facilitate the observation of standard sources and GNSS signals together at all IVS stations.

2. **Observations of GNSS signals with GNSS antennas near the VLBI antennas.** Standard geodetic GNSS receivers and antennas are used near the VLBI antennas, phase-stably locked to the VLBI station clock, to record GNSS signals as ordinary VLBI data. The GNSS signals are stored on the same media as signals from standard VLBI observations, which are carried out simultaneously. A precise local frame tie, connecting both antennas, is needed. As the GNSS antenna has a nearly omnidirectional characteristic, all satellites above the horizon could be observed simultaneously without tracking their positions. Correlation of the GNSS signals (using the usual VLBI schemes) would then give multiple delay peaks on each baseline, one for each satellite. With three ore more baselines the positions of all satellites could be fixed. Such an *VLBI-GPS hybrid system* is discussed in detail by e.g. Kwak *et al.* (2010). One disadvantage is that the connection between the VLBI and the GNSS frame still depends on the precise realization of local ties between the observing antennas.

1.2 Previous VLBI satellite tracking experiments

In this work, the approach of observing GNSS satellites directly with VLBI antennas is followed. Several experiments applying direct tracking were carried out in the last years.

An initial experiment took place in 2009, as described in Tornatore *et al.* (2010b). Four satellites of the GLONASS constellation were tracked simultaneously in geodetic VLBI mode by the stations Medicina (Italy), Noto (Italy) and Onsala (Sweden). The data acquisition was performed using the available L-band receivers and the standard recording equipment for geodetic VLBI, which is available at the participating stations. To follow the satellites during the observations, the antennas were positioned stepwise with a 20 seconds update interval (see Sec. 2.5.1). Unfortunately an attempt to cross-correlate the recorded data failed, because of recording problems during the data acquisition. Nevertheless, these first experiment showed, that in principle it is possible to track GNSS satellites with VLBI antennas. Tornatore *et al.* (2010b) also suggested the inclusion of the SATTRACK module (Moya Espinosa & Haas, 2007) in the official NASA Field System (see Sec. 2.2) release to simplify satellite tracking and to allow tracking in a continuous fashion as discussd in Sec. 2.5.2.

On June 28, 2010 another experiment was carried out, as described by Tornatore *et al.*

[1] GNSS L1-band frequencies are closest to the S-band: GLONASS L1 $= 1592-1609MHz$, GPS L1 $= 1575.42MHz$ (Kaplan & Hegarty, 2005).

(2010a), with the main goals to develop and test the scheduling, signal acquisition and processing routines. The VLBI stations Medicina and Onsala observed signals from two GLONASS satellites. The signals were simultaneously recorded at the two stations, were successfully cross-correlated and fringes could be found, even though the power of the satellite signals was very low at one station. The satellites were tracked stepwise with a position update-interval of 20 seconds.

A similar follow-on experiment took place on August 16, 2010 (Tornatore *et al.*, 2011 and Tornatore *et al.*, 2014). Again three GLONASS satellites were observed on the baseline Medicina-Onsala in the L-band using a stepwise tracking approach. Cross-correlation was applied successfully on the recorded signals to find fringes.

The most recent satellite VLBI experiment was carried out on January 28, 2013 on the baseline Wettzell-Onsala, where a GLONASS satellite was observed in the geodetic VLBI mode (Haas *et al.*, 2014). The goal was to test the newly developed L-band receiver system on the 20*m* radio telescope in Wettzell (Kodet *et al.*, 2013). The satellite was tracked stepwise with an antenna repositioning interval of 15 seconds on the basis of schedules generated at the Joint Institute for VLBI in Europe (JIVE). The preliminary results are described by Haas *et al.* (2014). This experiment is particularly important for the work done for this thesis, because it comprised the same VLBI stations and antennas. Hence, the experiences made back then were very helpful to plan and carry out the new satellite observations described in chapter 5.

Although the experiments described above showed, that direct VLBI observations of GNSS signals are possible and have the potential to derive the satellite position on a centimeter level, several *major problems* have been revealed in order to observe GNSS signals in geodetic VLBI mode according to Tornatore *et al.* (2014):

1. Preparation of observation plans (schedules) for satellite observations,
2. tracking of the fast moving GNSS satellites with the large VLBI radio antennas,
3. recording of the artificial GNSS radio signals with the existing VLBI station equipment, and
4. the development of appropriate algorithms for processing and correlation of the acquired satellite signals.

This points out that there is still a lot of research needed till satellite observations with VLBI can be carried out in an operational way.

1.3 Tasks and objectives

In the Section 1.2 several previous experiments, implementing direct observations of GNSS satellites with the VLBI technique, have been discussed. Although satellites have been observed successfully, a clear strategy for the realization of such experiments has not been shown by now.

The challenges already start for the planning of an observation. A schedule has to be prepared, defining which antennas have to observe a selected source simultaneously at a particular time with common visibilities of the target . This is a critical task and it is usually done by dedicated software packages. Unfortunately the standard scheduling programs for VLBI (described in Sec. 2.1.2) are not able to schedule satellites as targets routinely. Furthermore, the standard data formats for VLBI schedule files do not provide the possibility to include the required information on satellite orbits in a suitable way.

Although the most recent version of the NASA Field System[1] (FS; see Sec. 2.2) provide functions to facilitate satellite tracking with VLBI radio antennas, it does not support the generation of local command schedule files, including the necessary commands (SNAP commands; Himwich & Vandenberg, 2001) with the program DRUDG (Vandenberg, 2000; also see Sec. 2.1.2). For those reasons, a huge effort was necessary to implement satellite observations with VLBI previously. Schedules had to be generated manually and plenty of manual interactions were necessary at the stations to track the satellite orbits and to record the data appropriately.

In order to solve these flaws, a joint project with the Geodetic Observatory Wettzell, Germany (GOW, see Sec. 4.1) was started in the context of this master thesis.

The goal of this work is to investigate options for an operational path to implement satellite observations with the VLBI technique.

The whole process chain – from observation planning, to orbit tracking and data recording – has to be considered. Therefore several sub-tasks can be formulated within this project:

1. **Preparation of a software tool for the scheduling of VLBI satellite observations.** To have a software to schedule satellite observations with VLBI antennas, the Vienna VLBI Software (VieVS, Böhm *et al.*, 2012) was updated for a satellite scheduling module. The software provides the possibility to generate schedule files in the VEX format (version 1.5b1; Whitney *et al.*, 2002) feasible to conduct actual satellite observations. The scheduling of VLBI satellite sessions is discussed in Chapter 3.

2. **Implementation of functions to facilitate continuous satellite tracking in Wettzell.** The station-specific code of the Field Systems, controlling of the radio antennas have to be updated. New FS commands and station functions were added to enable satellite tracking in a continuous way, utilizing satellite orbit data in the form of NORAD Two Line Elements (TLE). These implementations are discussed in detail in Chapter 4.

3. **Carrying out actual satellite observations to validate the developments.** Four satellite observation sessions were carried out in January 2014 on the baseline Wettzell-Onsala. Several GLONASS GNSS satellites have been observed on the basis of schedules, generated

[1] The current FS version is 9.11.6.

with the new VieVS module. The newly installed satellite tracking capabilities at the station Wettzell were used. All experiments are described in detail in Chapter 5.

Chapter 2

Satellite observations with VLBI antennas

Background information, related to satellite observations with the VLBI technique, is being discussed within this chapter.

2.1 Very Long Baseline Interferometry

The Very Long Baseline Interferometry (VLBI) is a space-geodetic technique that measures the difference in arrival times of microwave signals from radio sources by cross-correlation. In the standard geodetic VLBI, the sources, which are usually extragalactic objects called quasars, are observed by globally distributed antenna networks. VLBI is exceptionally important for the realization and maintenance of the International Celestial Reference Frame (ICRF) and it makes indispensable contributions to the International Terrestrial Reference Frame (ITRF). Further, it is the only geodetic technique which is able to measure nutation parameters and the Earth rotation angle ($UT1-UTC$) directly. Hence, it is the only technique which is able to provide a full set of Earth Orientation Parameters (EOP) (Schuh & Böhm, 2013).

2.1.1 Geometric principle

The basic geometric principle of VLBI is illustrated in Fig. 2.1. Due to the large distance of billions of light years between the Earth and the observed extragalactic sources, such as quasars or radio galaxies, the arriving wavefronts can be considered as plane. Hence, the directions to the sources $\vec{s_0}$ can be considered as equal from each point on Earth. If the reception times at the stations 1 and 2 are denoted as t_1 and t_2, the observed delay time is defined as $\tau = t_2 - t_1$. The basic relation between delay time τ, baseline vector $\vec{b}$, source direction $\vec{s_0}$ and the speed of light c is represented by Equ. 2.1 (Schuh & Böhm, 2013).

$$\tau = -\frac{\vec{b} \cdot \vec{s_0}}{c} = t_2 - t_1 \tag{2.1}$$

In the geodetic VLBI two or more radio antennas are used to observe numerous radio sources distributed across the sky simultaneously in the S-band ($\sim 2.3GHz$) and the X-band ($\sim 8.4GHz$). The received radio signals are recorded on hard discs and precisely time-tagged using highly accurate and stable time signals obtained by atomic clocks on each participating station. The acquired data is then sent to particular correlation centers, where the cross-correlation is carried out for each baseline and observation to obtain the group delay observable τ. Using these delay times τ, the length of the baselines b and other geodetic and astrometric parameters can be derived accurately.

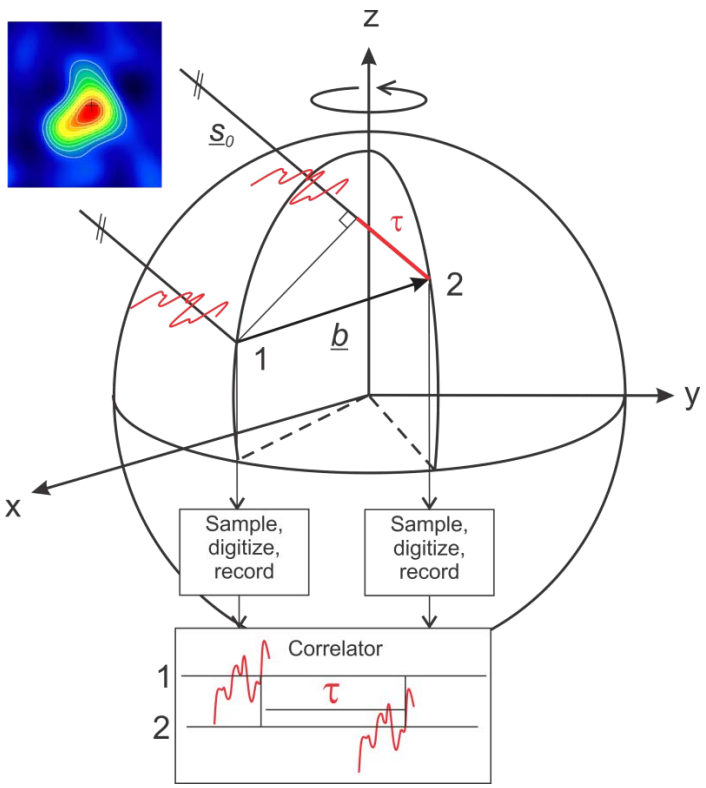

Figure 2.1: Geometric VLBI model (Schuh & Böhm, 2013). The delay time τ for a particular baseline $\vec{b}$ can be derived by cross-correlating the radio signals from extragalactic sources, acquired on the participating stations 1 and 2.

2.1.2 Data acquisition

To successfully perform VLBI observations, first of all a proper time schedule has to be prepared. An accurate observation planning is particularly important for the VLBI, because several

stations, distributed all over the world, have to observe the same radio source simultaneously. Hence, VLBI schedules define, which antennas should observe a source simultaneously at a particular time, e.g. which antennas form a scan.

A selection of suitable sources has to be made. Further, the chronological order of the observations and the period of time required for each particular observation have to be determined. The required duration of the observations, and therefore the achievable signal-to-noise-ratio (SNR), is dependent on several station specific parameters, such as antenna diameters, receiver temperatures and the recording bandwidth. Also source specific parameters have an influence, e.g. the flux densities emitted by the observed radio sources. The quality of the derived geodetic parameters also depend on the distribution of the sources over the sky and the distribution of the participating stations on the Earth's surface (Sun, 2013). The complexity of the scheduling task becomes obvious when considering the large number of different parameters, which have to be taken into account, such as scan durations, antenna slewing rates, station specific horizon masks, etc. All of them have an influence on the observation setup and finally on the quality of the derived geodetic products.

There are several software packages available for the generation of VLBI schedules, supporting various scheduling optimization strategies. The scheduling program SKED (Gipson, 2012) developed by Nancy Vandenberg and currently maintained by John Gipson at the NASA Goddard Space Flight Center (GSFC) is widely used in the VLBI community. Other program packages are SCHED (Walker, 2014), developed at the National Radio Astronomy Observatory (NRAO), which is mostly used for astronomical applications, and Vie_SCHED (Sun, 2013), a module of the Vienna VLBI Software (VieVS Böhm *et al.*, 2012). Vie_SCHED is used, for instance, to schedule VLBI sessions for the AuScope geodetic VLBI array in Australia (Lovell *et al.*, 2013) in recent times.

Such scheduling programs are usually used to generate schedule files, comprising all information which is necessary to carry out an actual VLBI session. These "global" schedule files define the complete observation timeplan, as well as the setup parameters of the station equipment at *all* participating sites, e.g. the recorder hardware setup.

There are two different file formats available in which VLBI schedule files are usually issued: SKD (Gipson, 2010) and VEX (VLBI EXperiment; Whitney *et al.*, 2002). SKD is the native format of the scheduling program SKED[1], whereas VEX is the more up-to-date format.

To carry out an actual VLBI session on the basis of a global schedule file in the VEX or SKD format, the locally necessary information has to be extracted at each participating station. This is done by the program DRUDG (Vandenberg, 2000), which comes with the NASA Field System distribution (see Sec. 2.2). The scheduling data flow is illustrated in Fig. 2.2. Prior to a VLBI session a global schedule file (VEX or SKD) is distributed to all participating stations, where DRUDG is used to generate local control files, so-called SNAP files (SNP), and the related SNAP procedure files (PRC; see Sec. 2.2 and Fig 2.3). SNAP files contain schedules of dedicated FS commands which are executed one after another by the FS according to their time tagging. Using

[1]Although VEX is also supported by SKED since 1997 (Gipson, 2010).

the synchronized, time tagged SNAP files, it is possible to perform a complete VLBI session in an automated manner by loading these files into the Field System, which processes them. Due to this routine, only a minimum of manual interactions are necessary to carry out a VLBI observation, e.g. antenna pointing tests before the observations start, disc or storage exchanges.

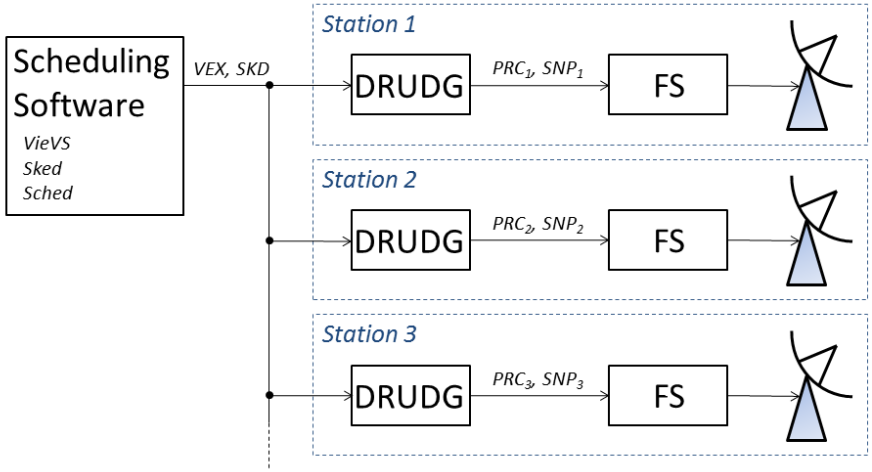

Figure 2.2: VLBI scheduling data flow. "Global" schedule files in the VEX or SKD format are generated by particular VLBI scheduling programs and distributed to all participating VLBI stations. There, the program DRUDG is used to extract the locally needed information from the "global" schedule and to generate local control files (PRC and SNP). The site-specific local control files are run with the FS at each site to carry out a VLBI session in an automated manner.

The radio signals, obtained by the VLBI antennas, are received and down-converted in the receiver system. They are transported to the data acquisition rack. There they are digitized, usually with one or two bit resolution and a high sampling rate of e.g. $256 Mbit/sec$. After applying a specific data format to the continuous data stream from the receiver in the formatter, the resulting data frames are recorded on storage packages of the Mark5 system, consisting of eight customary hard discs("eight-packs"). Because of the huge amount of data collected during a typical VLBI session[1], the data are commonly sent on eight-packs, or nowadays frequently via electronic data transfer over the internet ("eVLBI"), to a correlation center. There the cross-correlations are carried out to determine delay times for each scan.

Finally, the correlation results are used to calculate geodetic parameters (such as Earth Orientation Parameters, station coordinates, etc.) in dedicated analysis centers[2] maintained by the IVS.

[1] During a 24 hour VLBI session usually $1TB$ to $2TB$ of data is recorded.
[2] A list of all IVS analysis centers is available at: http://ivs.nict.go.jp/mirror/about/org/components/ac-list.html

2.2 NASA Field System

The VLBI Field System (FS)[1] is a suite of programs, maintained and developed by Ed Himwich at the NASA Goddard Space Flight Center (GSFC). It provides the coordinating control of VLBI observation and data acquisition (Rottmann, 2011). The FS runs on a Debian Linux platform and controls the tasks needed for the VLBI operation, e.g. handling the recording equipment, receiver calibration, antenna control, etc.

The FS operator interface is based around the concept of user-typed commands in the Standard Notation for Astronomical Procedures (SNAP; Himwich & Vandenberg, 2001) format. These basic *SNAP commands* can be used to set or monitor the state of the hardware and various system features. To facilitate the execution of recurring operations, such as various system checks, single SNAP commands can be combined to *SNAP procedures*. A SNAP procedure basically consists of the definition of a procedure name, followed by a sequence of consecutive SNAP command invocations. One or more of these SNAP procedures are defined in the *SNAP procedure files* (PRC; file ending *.prc), as illustrated in Fig. 2.3 (b). Automatic VLBI operations can be implemented by using local control files, called *SNAP files*. They are generated by the program DRUDG (as well as the related SNAP procedure files) as outlined in the VLBI data flow scheme in Fig. 2.2. These SNAP files (file ending *.snp) contain SNAP procedure invocations and distinct SNAP commands, as illustrated in Fig. 2.3 (a). Additional time-flow control commands in between are required to synchronize operations at different VLBI stations (Himwich *et al.*, 2003).

An overview of the FS architecture is given in terms of a block diagram in Fig. 2.4 (Rottmann, 2011). Each blue box represents a memory resident program, connected to each other via a shared memory. Each program has a specific task. For example, the *oprin* module reads and interprets user input and the *boss* module is the spider in the net, as it relays the commands to different programs (Moya Espinosa & Haas, 2007). It is important to note, that VLBI stations can have a inhomogeneous hardware equipment and unique antenna interfaces. This circumstance is incorporated in the FS architecture by providing various interface modules, to support the different hardware that is found at particular stations, e.g. the antenna control module (*antcn*) (Rottmann, 2011). Further, the FS distinguishes between station-independent and station-dependent software modules. The latter ones can be adopted to the specific station requirements by adding dedicated code. One of these station dependent modules is the antenna control program *antcn* (red box in Fig. 2.4). They are implemented locally for each antenna and provide a kind of a "black box" functionality for the FS, so that it has not to know how the antenna control is to be handled. *Antcn* basically provides a set of antenna operations, which are executable via SNAP commands – such as commanding a new source or an offset – independent of the details of the particular antenna (Himwich *et al.*, 2003).

[1] A complete FS documentation is available online at ftp://gemini.gsfc.nasa.gov/pub/fsdocs/

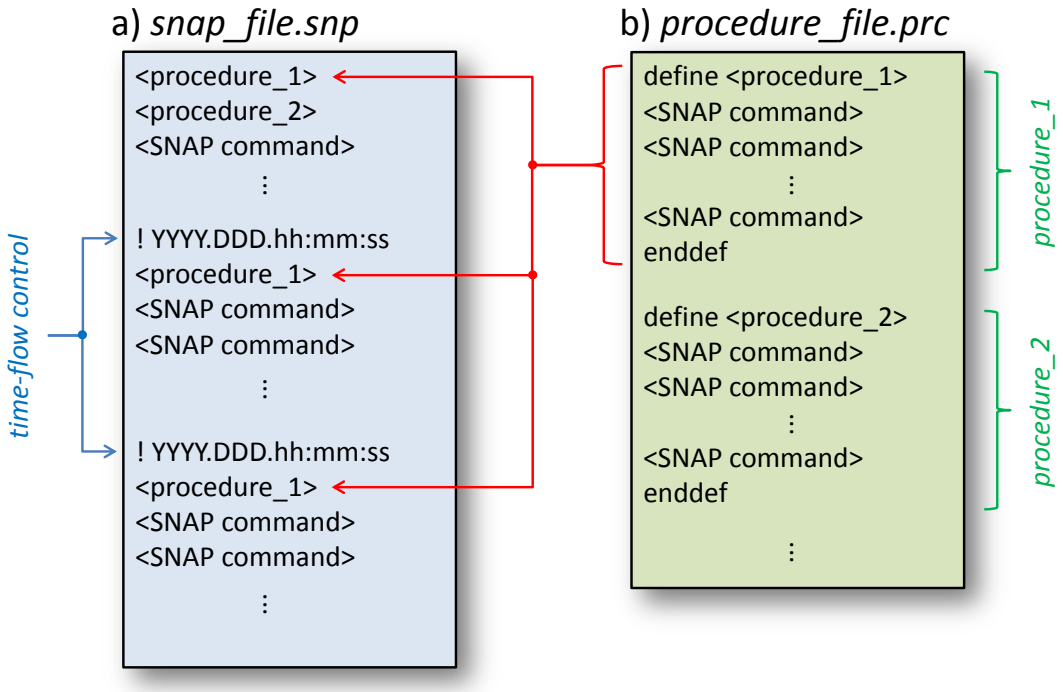

Figure 2.3: SNAP and procedure files are basically used for process automation in the VLBI. (a) A SNAP file (*.snp) consists of a sequence of SNAP procedure invocations (e.g. ⟨*procedure_1*⟩) and SNAP commands (⟨*SNAP command*⟩), which are executed by the FS line by line during an VLBI experiment. The operation timing is determined by dedicated time-flow control commands (*!YYYY.DDD.hh.mm.ss*), defining the date and the time for the execution of the next subsequent command sequence. (b) A SNAP procedure file (*.prc) is used to define an arbitrary number of SNAP procedures (e.g. *procedure_1*). Each procedure consists of a list of distinct SNAP commands, which are executed when the procedure name is called in a SNAP file or by an FS operator input.

2.3 Satellite orbit prediction

2.3.1 Demands on the orbit prediction

The precise calculation of satellite positions as a function of time is a critical and important task within the scope of VLBI satellite observations. Satellite positions are basically required for the scheduling of an observation as well as for the final tracking of a particular satellite at the time of observation. Both applications have different requirements:

Scheduling: Satellite positions are required to calculate antenna pointing directions and further, to determine whether a particular satellite is visible from a given station network, or not. Usually the observation planning is done from several days up to several weeks before the actual observations are carried out. For this reason the orbit data format has to provide the possibility to *predict* satellite orbits into future, i.e. to extrapolate orbit positions, with a sufficient accuracy.

Tracking: Precise satellite positions are needed to derive pointing directions with the purpose to

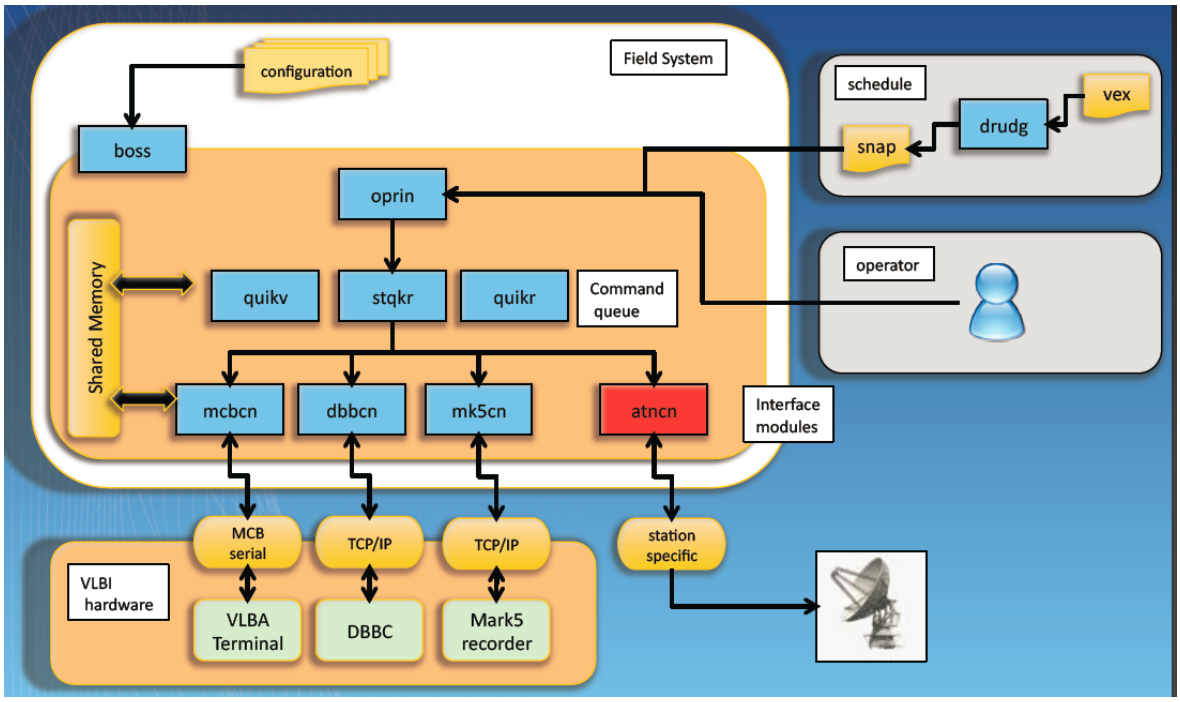

Figure 2.4: NASA Field System overview (taken from Rottmann, 2011). Blue and red boxes represent memory resident programs, communicating with each other via a shared memory. The program *drudg* (Vandenberg, 2000) is used to extract locally required information from VLBI schedule files (*vex*, Whitney *et al.*, 2002) and to generate local FS control files – so-called *snap* files (Himwich & Vandenberg, 2001). The operator interface (*oprin*) forwards commands entered directly by the user to the station quick response module (*stqkr*), which parses some of the commands and detects, which one must be forwarded to the antenna control module (*antcn*). The *antcn* module executes commands directly related to the antenna control.

guide the VLBI antennas at the time of observation. In this case, the accuracy loss due to orbit extrapolation is not a great problem, because usually there is the possibility to obtain the latest orbit data immediately before the observation starts.

However, the accuracy requirements for scheduling are fairly low, compared to the requirements for actual tracking, because the calculated satellite orbits are mainly used to decide, whether the target is visible or not (which also depends on several boundary conditions, such as the elevation angle of the local horizon, etc.). At this point it is difficult to provide concrete and reliable figures concerning the required orbit prediction accuracy for scheduling respectively for actual tracking. Further investigations in this field would be necessary, that consider the numerous influencing variables, such as various antenna and orbit characteristics, etc. Nevertheless, a first attempt to assess the influence of orbit inaccuracies on the antenna view directions can be found in Sec. 2.4.

2.3.2 Data formats for orbit prediction

In principle there are numerous sources, providing orbit information for different satellite constellations in various data formats. For example, orbit data for GNSS satellites are provided by the International GNSS Service (IGS, Dow *et al.*, 2009). It is available via standard SP3 (Standard Product 3; Spofford & Remondi, 1999) files and was used e.g. by Plank (2014) for her simulation studies on VLBI satellite observations. Although SP3 files provide the possibility to calculate satellite orbits with highest precision, there are two main deficiencies concerning VLBI satellite tracking: (1) The data, especially those with highest accuracy, become available with a certain delay. That makes it preferably suitable for post processing applications, but not for real time uses, respectively for orbit predictions to the future. (2) SP3 data are only available for GNSS satellites.

Another possibility would be to utilize the satellite orbit prediction data provided by the International Laser Ranging Service (ILRS; Perlman *et al.*, 2002) in the Consolidated Prediction Format[1] (CPF; Ricklefs, 2006). The ILRS CPF data, usually used for SLR tracking, provide daily tables of x, y, and z positions for all tracked objects, that can be interpolated for very accurate predictions. The provided prediction file for a particular satellite contains several days worth of data, usually with predictions for four days from the release date. According to Ricklefs (2006), current CPF data permit the integration of satellite positions well past the epoch of the last entry in the data file. Although the predictions show an increasing loss of accuracy, it is possible to extend the integrations several months into the future for the purpose of scheduling, as discussed by (Ricklefs, 2006), because of the fairly low accuracy requirements of this use. Nevertheless, also the CPF data has the disadvantage of a limited data availability. Orbit predictions are only available for satellites currently tracked by the ILRS[2].

The orbit data formats, described above (SP3 and CPF), provide sequences of discrete satellite positions in Cartesian coordinates (x, y, z) at certain epochs. Therefore, numerical integration, respectively interpolation, is necessary to derive positions at the epoch of interest. Another approach is followed by the Two-Line Element (TLE) data, an orbit data format specified by the North American Aerospace Defense Command (NORAD)[3]. TLE datasets are mean Keplerian orbital element sets, which allow to calculate satellite positions at a particular time with designated analytical orbit models (Simplified General Perturbation models, SGP; see Sec. 2.3.3), i.e. without time consuming numerical integrations. TLE data for thousands of space objects are made freely available for the public by NORAD via dedicated web services[4]. Therefore, NORAD TLE datasets provide the most complete source for satellite orbit data, generally available to the public.

[1] CPF files are available via anonymous ftp under ftp://cddis.gsfc.nasa.gov/pub/slr/cpf_predicts/

[2] Current ILRS missions are available at http://ilrs.gsfc.nasa.gov/missions/satellite_missions/current_missions/

[3] A detailed TLE format definition is available at http://spaceflight.nasa.gov/realdata/sightings/SSapplications/Post/JavaSSOP/SSOP_Help/tle_def.html

[4] TLE data is accessible at http://www.celestrak.com/ and https://www.space-track.org/.

2.3.3 Orbit propagation with Two-Line Element data

Basically perturbation models, as used to propagate NORAD Two-Line orbit Elements, are analytical models to calculate positions and velocities of Earth-orbiting objects. Additionally to the primary attractive force due to gravitation of an idealized spherical Earth, perturbing forces are considered to model the motion of a satellite on its orbit around the Earth. Regarding these perturbing forces, which act on the satellite's motion, we can distinguish between gravitational forces (e.g. due to the equator bulges and the non-uniform density distribution, or due to the attraction of Sun and Moon) and non-gravitational forces, such as the atmospheric drag (Kelso, 1994).

The TLE datasets generated and provided by NORAD can be directly used to predict the position and velocity vectors of satellites. To get accurate results, it is absolutely necessary to use a prediction model, which is compatible with the orbit model used to generate the TLE data originally (the TLE data are fitted to this certain model; Vallado *et al.*, 2006). Five compatible models – SGP, SGP4, SDP4, SGP8 and SDP8 – are described by Hoots & Roehrich (1980). Further details on these models are discussed by Vallado *et al.* (2006).

According to Hoots & Roehrich (1980) the NORAD elements are generated either with SGP4 or SDP4. SGP4 is the near-Earth model for satellite round-trip times of less than 225 minutes[1] and SDP4 is the deep-space model for periods greater than or equal 225 minutes. This distinction is made, because the major perturbation influences change with altitude.

Regarding the coordinate system specified for SPG4 ephemerides, Vallado *et al.* (2006) states that "the actual SGP4 model has a little need for any specific coordinate system, but when used for propagating TLE generated by DoD[2] it becomes important to use the same coordinate system as the DoD orbit determination routines use". The coordinate system for the propagated satellite positions is of particular interest, if these positions are used to derive further products (e.g. topocentric view directions), as it is done within this work. According to Vallado *et al.* (2006) the commonly accepted output coordinate system is an Earth Centered Inertial (ECI) system, which axes are referred to a True Equator and a Mean Equinox (TEME). It is described in Appx. A.1.1.1.

Associated to the paper about orbit propagation with the SGP4/SDP4 models from Vallado *et al.* (2006) there are software libraries available in different programming languages, which contain code to help implementing these models[3]. There are also different software packages available, being able to calculate satellite positions and related products based on SGP4/SDP4 propagation and NORAD TLE data[4].

[1] A round-trip time 225 minutes corresponds to a orbit height of approximately 6000km.
[2] United States Department of Defense
[3] The SPG4/SDP4 libraries are available online at http://celestrak.com/publications/AIAA/2006-6753/
[4] A list composed by T.S. Kelso is available at http://celestrak.com/software/satellite/sat-trak.asp

2.3.4 Accuracy assessment of SGP4 orbits

A big deficiency of SGP4[1] orbital data in the form of TLE datasets is, that it does not provide any information on accuracy, such as covariance estimates. To assess the suitability of different error estimation approaches, Kelso (2007) compared a SGP4 ephemeris to the high precision ephemeris available for the GPS constellation. The precise GPS satellite ephemeris is considered as an independent truth dataset of much higher accuracy than those calculated by SGP4 with TLE data. Based on this comparison the SGP4 prediction error is analyzed as a function of the prediction interval, i.e. of the time between TLE release date and propagation epoch. The comparisons were carried out for 22 GPS satellites and for a period of ± 15 days from the release date of the according TLE dataset. The prediction error assessment was based on positions, calculated in a 15 minutes interval with the SGP4 model, and on the corresponding high accuracy reference positions for the same epochs. The SGP4 prediction errors were calculated in form of radial, along-track and cross-track differences between the precise GPS positions and the SGP4 positions. For further details the author refers to the publication from Kelso (2007).

Fig. 2.5 and 2.6 depict fundamental statistical results for two representative GPS satellites (PRN10 and PRN11)[2]. In both plots the mean value of the SGP4 prediction error is shown along with a one-sigma error bar, to illustrate the bias and variance characteristic. The mean value and the variance are computed by binning the calculated propagation errors (available in a 15 minutes interval) to the closest day within the treated period.

According to the error assessment approach by Kelso (2007) the SGP4 prediction error shows the following pattern:

1. The along-track error was generally dominant, followed by the radial error and then cross-track error.

2. The along-track error showed significant biases, while there were only slight biases in the radial and cross-track direction.

3. Errors were not symmetric with respect to the propagation direction. Typically, the errors were larger at positive prediction times, i.e. when predicting positions for future epochs.

4. While the bias in general grew with propagation time, often the variance did not.

5. The mean along-track bias for all 22 GPS satellites for a propagation with 15 days old TLE data (propagation time of +15 days) is approximately 28 km with a mean one-sigma variance of about ± 8 km.

The investigations of Kelso (2007) showed significant biases between GPS high precision orbits and SGP4 orbits with the largest magnitudes in the along-track direction. The results of this

[1] From now on the term SGP4 implicitly includes the SDP4 model.
[2] Statistics for all considered satellites are available at http://www.celestrak.com/publications/AAS/07-127/

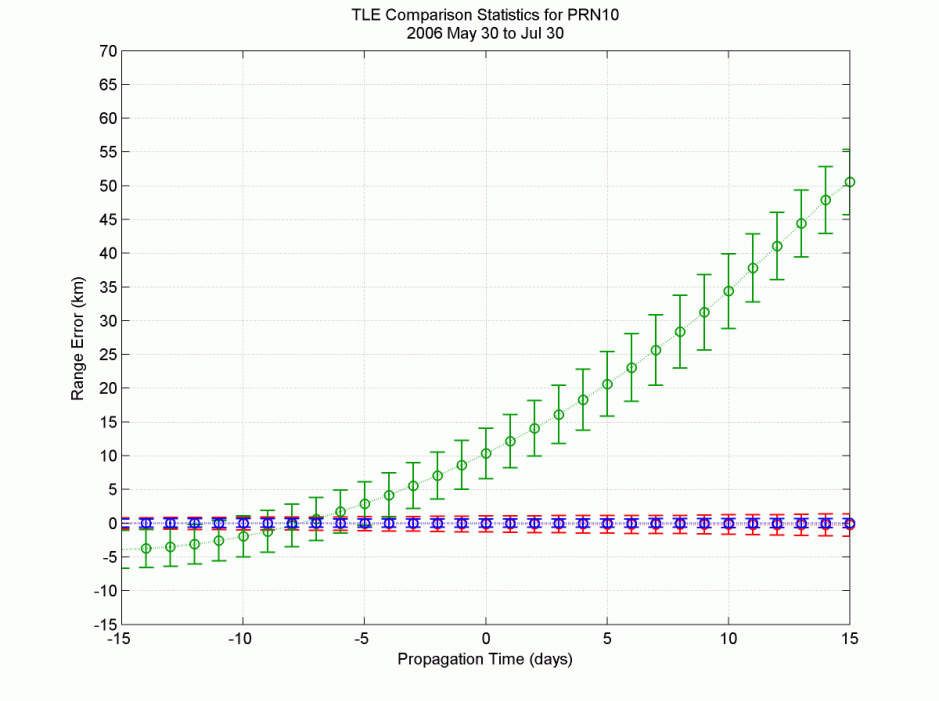

Figure 2.5: TLE comparison statistics (taken from: Kelso, 2007). The diagram illustrates the mean values of the SGP4 prediction error along with a one-sigma error bar in radial (red), along-track (green) and cross-track direction (blue) for GPS PRN10 as a function of the propagation time.

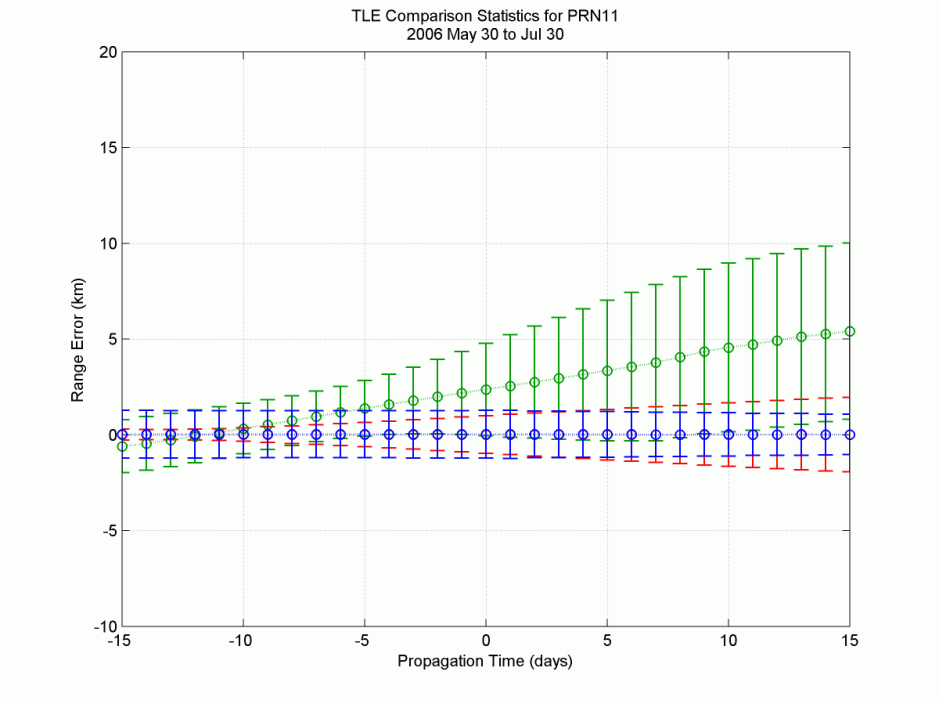

Figure 2.6: TLE comparison statistics (taken from: Kelso, 2007). The diagram illustrates the mean values of the SGP4 prediction error along with a one-sigma error bar in radial (red), along-track (green) and cross-track direction (blue) for GPS PRN11 as a function of the propagation time.

error assessment approach are used later on in Sec. 2.4 to discuss the influence of along-track orbit errors (caused by the SGP4 modelling) on the actual pointing angles of an observing antenna on the Earth's surface.

2.4 Considerations on the antenna pointing accuracy

Beamwidth. To enable a correct signal acquisition, the moving satellites have to be tracked with sufficient antenna pointing accuracy, to keep them within the antenna beam during the observation. Ideally, the observed object should be centered within the antenna beam. Hence, the narrower the beam is, the more difficult is the properly receiving from a satellite. The situation is illustrated in Fig. 2.7. A measure for the diameter of the antenna beam – more precisely of the main lobe of the antenna's radiation pattern – is referred to as *beamwidth* (BW). The beamwidth is directly proportional to the wavelength λ of the received radiation and is inversely proportional to the diameter D of the antenna's main reflector (in case of a parabolic antenna). Equ. 2.2 could be used to get a rough estimate of the beamwidth of an antenna:

$$BW\,[rad] = \frac{\lambda\,[m]}{D\,[m]}. \tag{2.2}$$

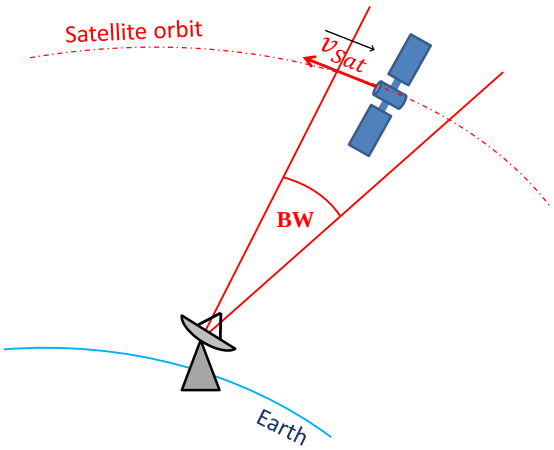

Figure 2.7: Illustration of the beamwidth BW of a radio antenna.

Assuming that L1 signals from GLONASS satellites with a wavelength of $\lambda \approx 0.188m$ are observed, Table 2.1 shows the beamwidths, calculated with Equ. 2.2, for three different VLBI radio antennas used for our experiments: The $20m$ Radio Telescope Wettzell (RTW), the $13.2m$ Twin Telescope Wettzell (TTW) and the $25m$ antenna in Onsala, Sweden (On80). We see that smaller antennas have a wider beamwidth. For the three antennas we find beamwidths between $0.43°$ and $0.81°$.

Table 2.1: Beamwidth calculated with Equ. 2.2 for three different antennas and a wavelength of $\lambda = 0.188m$ (GLONASS L1).

Antenna	**Diameter** D $[m]$	**Beamwidth** BW $[°]$
TTW	13.2	0.814
RTW	20	0.537
On80	25	0.430

Impact of orbit errors on pointing angles. A rough assessment of the impact of satellite orbit errors on the pointing accuracy of VLBI radio antennas, observing these satellites, was made.

For this estimation a simplified observation geometry is assumed, as shown in Fig. 2.8. First, the Earth is approximated as a spherical body with a radius of $R = 6378km$. It is assumed that GNSS satellites are used. The flight altitude of GLONASS satellites is $\sim 19100km$ and that of GPS satellites $\sim 20200km$. Both have nearly circular orbits (Kaplan & Hegarty, 2005). Hence, the assumption is made, that the considered satellite orbit is perfectly circular (without eccentricity) and the flight altitude is $20000km$ above the ground. Further, the orbit is situated, so that the satellite crosses the observing antenna directly in its local zenith point (elevation angle $\delta = 90°$) during an overpass. The Z-axis of a Cartesian coordinate system is aligned with the local zenith direction and the origin is located in the Earth's center. The X-axis points at the intersection between the satellite orbit and a plane, which is parallel to the antenna's local horizon and contains the Earth's center. The angle between the local horizon and the direct line of sight (LOS) from the antenna to the satellite in the X-Z-plane is referred to as elevation angle δ. Because we assume, that the satellite moves only in the X-Z-plane, the antenna's azimuth angle has not to be considered.

According to the discussion in Sec. 2.3.4, by far the largest error component of GPS satellite positions, which are calculated with the SGP4 model and NORAD TLE data, lies in the along-track direction, i.e. in the direction the satellite moves. The considered GPS satellites showed a mean along-track bias of $28km$ with a mean variance of $\pm 8km$ at a propagation time of 15 days (Kelso, 2007). The radial and cross-track components are neglected in this assessment.

Using the observation geometry described above, the impact of an along-track orbit error ΔS on the antenna's elevation angle δ could be determined. In detail, the variation of the elevation angle $\Delta\delta$, as function of the along-track orbit error ΔS and the elevation angle δ, was calculated. The result is shown in Fig. 2.9. Generally, $\Delta\delta$ gets larger as ΔS and δ increase. For an along-track error of $\Delta S = 50km$ and an elevation angle $\delta = 90°$, the impact on the elevation angle is $\Delta\delta \approx 0.145°$. The gray line represents the variation of $\Delta\delta$ as a function of δ at an along-track error of $28km$ (in compliance with the discussion in Sec. 2.3.4). For an along-track orbit error of $\Delta S = 28km$ the impact on the elevation angle of an observing antenna $\Delta\delta$ is always $< 0.0802°$.

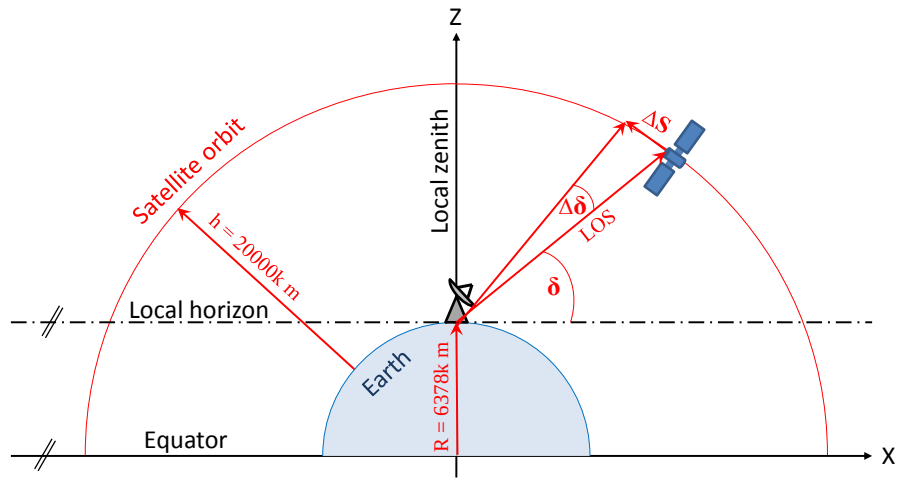

Figure 2.8: Geometric constellation used for the assessment of the impact of along-track orbit errors (ΔS) on the antenna's elevation angle ($\Delta\delta$).

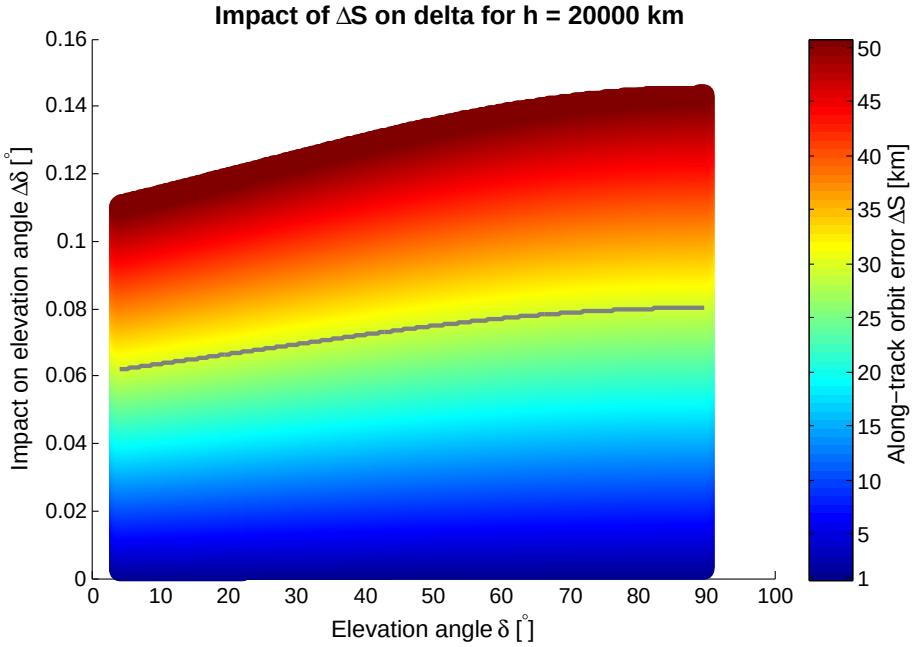

Figure 2.9: Impact on the elevation angle $\Delta\delta$ [°] as a function of the along-track orbit error ΔS [km] and the elevation angle [°] for a satellite altitude of $h = 20000km$. The gray line illustrates the change in elevation angle $\Delta\delta$ [°] for an along-track orbit error of $\Delta S = 28km$.

Feasibility of GNSS satellite observations. According to the discussion in Sec. 2.3.4, GPS satellite positions calculated with the SGP4 model and NORAD TLE data show on average an along-track bias of $28km$ at a propagation time of 15 days. The rough estimate above showed that an along-track variation of $28km$ will cause a variation in the pointing angle of an antenna observing the GPS satellite of maximum 0.08° (see gray line in Fig. 2.8). As shown in Table 2.1, the beamwidths of all considered VLBI antennas ($> 0.43°$) are by far larger than the estimated

impact of SGP4 propagation errors on the antenna pointing directions ($< 0.08°$) – even if the NORAD TLE datasets, which are used for the propagation, are as old as 15 days. This in principle means that even the viewing angle of a large VLBI antenna with an diameter of $25m$, such as the one in Onsala, is still large enough to observe GPS signals, even if substantial orbit errors are introduced by the SGP4 orbit modeling. The same assumption should apply not only for GPS satellites, but also for GLONASS satellites, because of similar orbit characteristics.

2.5 Implementation of satellite tracking with VLBI antennas

In the standard geodetic VLBI, the coordinates of radio sources (quasars) are considered to be constant during an observation for all participating antennas. Source positions are usually represented in the schedule in terms of right ascension (α) and declination (δ) angles in the ICRF frame at the standard epoch J2000.0.

If satellites should be observed directly with VLBI radio antennas, the situation is a bit different: First, Earth orbiting satellites – except such on a geostationary orbit – move fast with respect to the Earth' surface. Hence, they have to be tracked by the VLBI antennas during signal acquisition to keep the satellite within the antenna beam. Second, it is important to consider that the distance between an observing antenna and the signal source – unlike in standard VLBI observations of natural radio sources – cannot be assumed to be infinite. Therefore the incident wavefronts of satellite signals cannot be considered as plane and certain "near-field" effects need to be taken into account (Tornatore *et al.*, 2014). As illustrated in Fig. 2.10 the view directions to a quasar $\left(\vec{k}\right)$ do not differ between antennas on different locations on the Earth's surface. Due to the relatively short range between antennas and satellites – compared to quasars – view directions, represented by the vectors $\vec{k_1}$ and $\vec{k_2}$ in Fig. 2.10, are different from site to site. Therefore, a *cross-eyed observation configuration* has to be used (Duev *et al.*, 2012). This means that antennas observing the same satellite target from different locations on the Earth have to angle topocentric view directions which differ from one another (see Fig 2.10).

To enable automated satellite observations with VLBI, analogous to the observation procedure in the standard VLBI (see Sec. 2.1.2), information on the orbits of the observed satellites have to be added to the global schedule files. Then the orbit information has to be utilized by the program DRUDG to generate particular FS commands (SNAP commands) for satellite tracking and to write them into the issued local control files (SNAP and procedure files, see Sec. 2.2). The purpose of these particular satellite SNAP commands is to point the antenna at the satellite's position at the right time, i.e. to track the satellite during signal acquisition.

In the following sections two principle approaches of implementing satellite tracking with VLBI antennas are discussed in detail. Both have their specific assets and drawbacks.

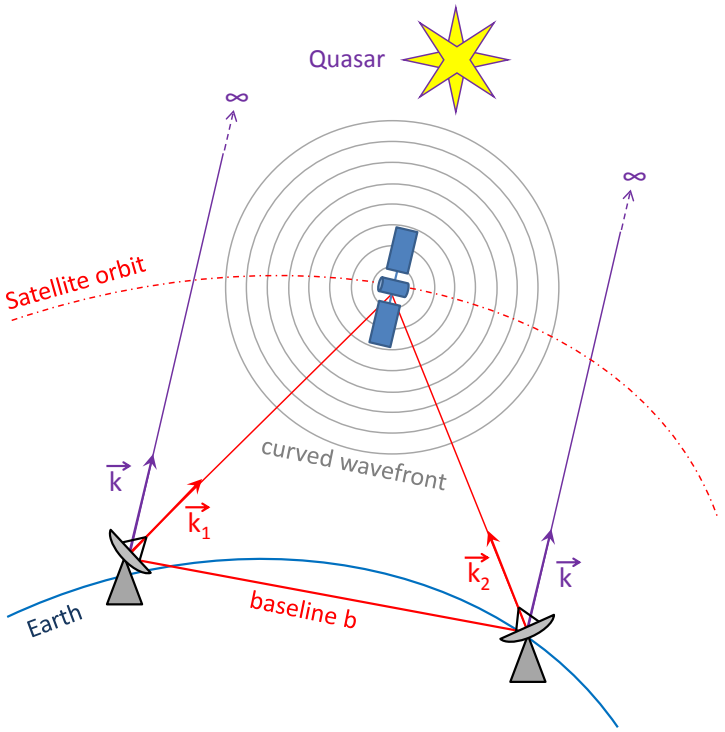

Figure 2.10: Schematic of satellite observations with VLBI. Due to the relatively short distance between source and antenna, compared to standard VLBI observations, the incident wavefront of a signal from a satellite cannot be considered as plane. It is curved and the directions of view differ between antennas on different locations $\left(\vec{k}_1 \neq \vec{k}_2\right)$. For observations to quasars, which can be considered to be at an infinite distance, the view directions from different locations on Earth $\left(\vec{k}\right)$ can be assumed as parallel.

2.5.1 Stepwise tracking approach

This approach was used for several previous VLBI satellite observation experiments as described in Sec. 1.2.

The basic idea of this approach is illustrated in Fig. 2.11. The antenna is repositioned stepwise in a defined repositioning interval, e.g. $\Delta t = 15$ seconds, to follow the satellite on its orbit. At the epoch t_1 the antenna is angled towards the position calculated for that particular epoch. The antenna remains in this position for the repositioning-interval time Δt, while the moving satellite crosses the antenna beam[1]. A signal acquisition is possible as long as the satellite remains within the beam of the observing antenna. Therefore, the satellite position for the next epoch $t_2 = t_1 + \Delta t$ has to be commanded timely in order to prevent loss of signal during the scan.

To incorporate this stepwise approach into schedule files in the currently available formats, the satellite orbit is fragmented and approximated by discrete positions at particular epochs (t_1, t_2, t_3,...). For each epoch the satellite position is defined as a distinct source, equal to the definition of a natural and stationary radio source. To implement a cross-eyed observation configuration,

[1]To be exact the antenna remains pointing at the commanded celestial coordinates during the observation, permanently correcting the topocentric pointing angles for the Earth rotation rate.

as discussed in Sec. 2.5 above, and to generate a cross-eyed schedule (Duev *et al.*, 2012), the satellite positions have to be defined in terms of topocentric right ascension (α_t) and declination (δ_t) in a topocentric equatorial coordinate system (see Appx. A.1.3).

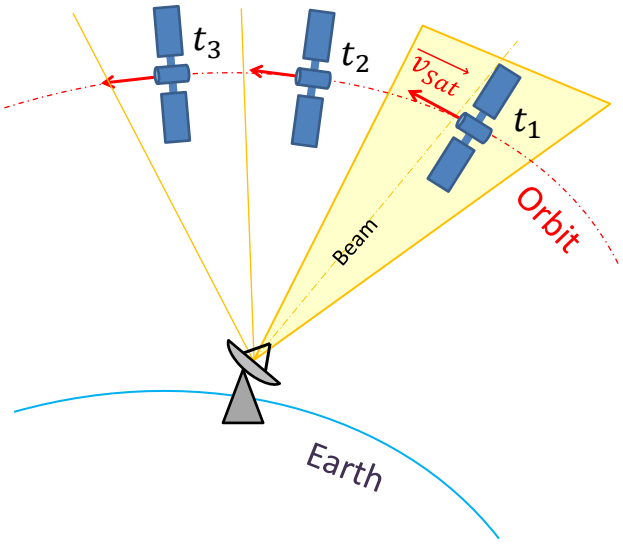

Figure 2.11: Stepwise satellite tracking approach. At epoch t_1 the antenna points to the satellite position calculated for that particular epoch and given in a topocentric equatorial coordinate system (see Appx. A.1.3). The antenna remains pointing to the commanded celestial coordinates for the reposition-interval time Δt until the next position is commanded at epoch $t_2 = t_1 + \Delta t$.

The big advantage of this stepwise tracking approach is, that it is viable with the currently available formats for schedule files (VEX 1.5b1; Whitney *et al.*, 2002 and SKD; Gipson, 2010), because the satellite sources are defined in the same manner as quasars in terms of celestial coordinates. All IVS VLBI antennas have to be capable of processing these celestial coordinates. Therefore they are in principle able to carry out such satellite observations without modifications in the local antenna steering control, if their slew speeds meet the requirements for satellite tracking.

According to Tornatore *et al.* (2011), one drawback of the stepwise tracking approach is, that the re-pointing of the radio antenna during an observation could produce some glitches in the resulting data residuals with a period equal to the repositioning-interval time Δt. This happens, because the satellite is not kept centered exactly within the antenna beam during data recording. To avoid this shortcoming Tornatore *et al.* (2011) recommends to track satellites in a continuous fashion, as discussed in the following Section (2.5.2).

2.5.2 Continuous tracking approach

Tracking satellites continuously means, that the antenna's view direction is steadily updated, so that the signal source is kept centered within the antenna beam during the whole scan.

Software for satellite tracking. To continuously track satellites, some kind of information about the orbit of the currently observed satellite is needed at the station. It is required to calculate the satellite's position and, further, to derive topocentric view directions for the particular site. How this orbit data, such as TLE[1], has to be prepared, processed and formatted to satisfy the demands of satellite tracking depends on the requirements of the local Antenna Control Unit[2] (ACU) and is therefore strictly station specific. If the ACU of a particular VLBI antenna does not have the ability to process the provided orbit data directly, a dedicated tracking software is needed in between to prepare the orbit information as required. Such tracking software can be installed on the Field System computer. Then, the station specific part of the Field System installation – mainly the antenna control program (*antcn*, see Sec. 2.2) – has to be adapted, to enable communication between the tracking software and the Field System programs. Currently the following software packages for satellite tracking with VLBI antennas are available:

SATTRACK. SATTRACK is a satellite tracking module for the Field System. It was initially developed to track Low Earth Orbiting (LEO) satellites to perform antenna pointing tests. Due to the lack of natural radio sources in the southern hemisphere, strong enough for pointing tests with small antennas, satellites that broadcast a strong signal in the X-band could be used instead. SATTRACK utilizes TLE data to calculate the necessary satellite positions (Moya Espinosa & Haas, 2007).

Field System. The Field System starting from version 9.11.2 is able to process TLE data and provides new SNAP commands intended for satellite tracking (Himwich & Gipson, 2012). The most important one has the following syntax: $satellite = \langle satellite\_name \rangle, \langle tle\_filename \rangle, \langle mode \rangle, \langle wrap \rangle$. Through the first two parameters the TLE dataset of a particular satellite with the common designation *"satellite_name"*, which is stored in a TLE library file with the filename *"tle_filename"*, is selected. "*Mode*" and "*wrap*" are optional parameters to select between different tracking modes and to specify a certain direction of motion for the cable wrap. After executing this satellite SNAP command in the FS the antenna starts to track the selected satellite, if the *antcn* module is extended with specific software.

Basically both tracking software packages, which are shown above, work very similarly, following the same principles. Prior to a satellite observation experiment the most recent TLE datasets, which are needed for an accurate orbit determination, have to be downloaded and stored in a dedicated folder on the Field System computer. Executing the provided "satellite SNAP command", which refers to a particular satellite to be tracked, in the Field System's operator input window

[1] Although there are different data formats available, providing the necessary orbit information (see Sec. 2.3.2), we only consider TLE data in this section, because TLE data is used for all further investigations and experiments in the context of this thesis.

[2] The ACU controls the antenna hardware functions (slewing, etc.). It is usually provided by the antenna manufacturer. It consists of a control computer with dedicated remote control interfaces, in connection with a Programmable Logic Control unit (PLC) that controls the antenna hardware.

(or through a SNAP file) will start the following process: The tracking software first reads the TLE dataset for the chosen satellite. Then it uses an SGP4 orbit propagator program (see Sec. 2.3.3) to calculate a very narrow sequence of satellite positions (e.g. in a one second interval). Then those positions are used to derive a stack of topocentric view directions in terms of azimuth and elevation angles (see Appx. A.1.2) or topocentric right ascension and declination (see Appx. A.1.3) for several hours (24 hours in case of the Field System tracking capability). This ephemeris stack is then available in the FS shared memory and can be used by the *antcn* interface of the Field System to guide the antenna. Another option is, to use proprietary satellite tracking solutions, if available, such as the Two-Lin Track mode of the Vertex ACU in Wettzell, which is described in Sec. 4.2.1. In this case, the station-specific code oft the FS has to be adapted to incorporate the proprietary functions.

Basically this "continuous" approach also uses discrete satellite positions to guide the VLBI antennas, but compared to the stepwise approach described above in Sec. 2.5.1, there are some differences: The main difference is, that the view directions towards the tracked satellite are commanded to the ACU of the antenna in a much narrower time sequence in the continuous approach, e.g. 1 second separation time compared to 15 seconds. Hence, the "steps" are much smaller. Due to the large inertia of the antenna structure and the fast repositioning during a continuous satellite track, the antenna moves very smoothly. The movement appears truly continuous, because the antenna does not stop, before the next position is commanded – it moves rather slowly and steadily.

In contrast to the stepwise tracking approach (see Sec. 2.5.1) a single satellite is defined as one single source in the global schedule and not as a sequence of discrete positions, approximating the orbit. Therefore, a reference to dedicated orbit data – such as TLE datasets – has to be provided in the schedule file for each particular satellite.

One problem is, that the current schedule file formats – in particular VEX 1.5b1 (Whitney *et al.*, 2002), which is used for the investigations within this thesis – do not provide the possibility to include TLE datasets, respectively references to TLE datasets, which are stored locally on the Field System computer at the station[1]. Even if satellites could be defined as sources in the global schedule, the program DRUDG, which generates the local Field System control files (SNAP and PRC files, see Sec. 2.2), currently represents a limitation. DRUDG, in the current version, is not able to write specific satellite SNAP commands to these local control files, being able to command the Field System to track a satellite continuously.

For those reasons, it is presently not possible to carry out continuous satellite tracking directly in an automatized manner, without manually modifying the local control files to include particular SNAP commands for satellite tracking. A way to implement these modifications in the control files

[1] According to personal communication with Ed Himwich, a new VEX version – "VEX2.0" – will be released in the near future, which will be able to include moving sources in terms of TLE data.

very flexibly, as realized at the VLBI station Wettzell, is presented in Sec. 4.2.4.

2.6 Antenna mount types

Within this section, various antenna mount types are discussed, including their limitations and opportunities in view towards an application for satellite tracking.

Basically, there are three different mount types, and therefore three primary antenna coordinate systems, used for VLBI antennas: the azimuth-elevation mount (*AzEl*, see Sec. 2.6.1), the equatorial mount (*HaDec*, see Sec. 2.6.2) and the X-Y mount. Because only the first two mount types are relevant for the work within this thesis, the X-Y mount is not further discussed here.

Each antenna mount type shows certain areas, so-called *keyholes*, where coordinate singularities occur, i.e. the coordinate for one axis is undefined for a particular antenna position. Although the antenna may be able to point at a particular keyhole position, it is impossible to track a target continuously throughout this position, which is particularly important related to satellite tracking. Examples for the coverage areas, resulting from such keyhole situations, are illustrated in Fig. 2.12 for (a) a AzEl and (b) a HaDec antenna mount.

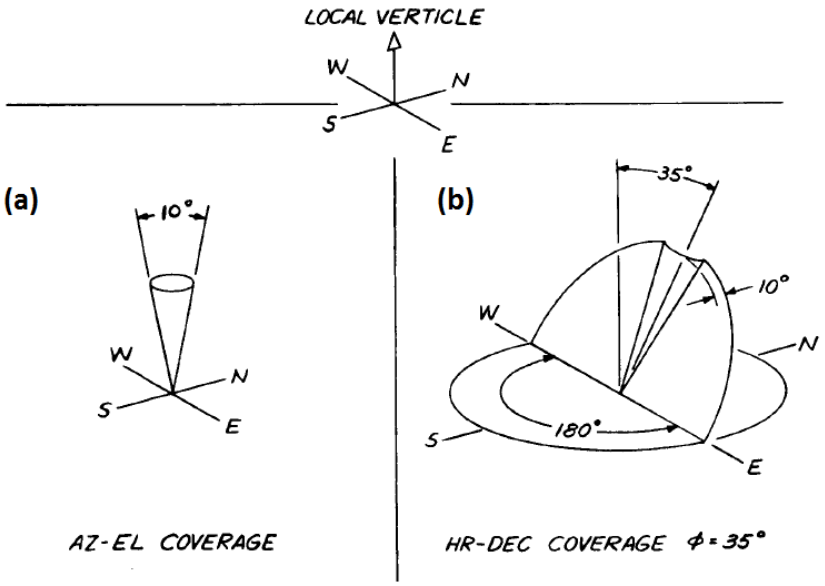

Figure 2.12: Coverage areas, resulting from coordinate singularities at particular mount dependent directions (keyholes), for different antenna coordinate systems used for VLBI antennas. (a) azimuth-elevation mount (AzEl) and (b) equatorial mount (HaDec) for an antenna located at a geographical latitude of $\phi = 35°$ (figure modified from Salzberg, 1967).

2.6.1 Azimuth - elevation mount, AzEl

The AzEl-mount is the usual antenna mount for large radio telescopes. It has a fixed vertical axis, the azimuth axis, and a moving horizontal axis, the elevation axis, that is attached to the

platform that rotates about the azimuth axis. The azimuth motion is typically ±270° relative to either north or south and the elevation motion is typically 5° to 85° (Petrachenko, 2013).

All points of azimuth can be covered at an elevation of 0°, hence, there are no horizon acquisition problems. The maximum azimuth rate occurs at an elevation of 90°, i.e. in zenith direction, which causes loss of track on overhead passes. Furthermore, the azimuth is not defined directly for the zenith direction (singularity, keyhole) (Salzberg, 1967). This finds expression in the fact, that the slew rate of the azimuth axis would have to become infinite to track a target through the zenith, i.e. the azimuth axis of the antenna would have to turn 180° instantaneously, which is certainly not possible in reality. As illustrated in Fig. 2.12 (a), the coverage area of an AzEl mount type antenna is limited in a certain area (with 10° diameter in this example) in zenith direction.

2.6.2 Equatorial mount, HaDec

The equatorial antenna mount type is no longer used for large antennas, although it was in widespread use prior to the advent of high speed real-time computers for calculating coordinate transformations. It has a fixed axis in the direction of the celestial pole, the equatorial axis, and a moving axis at right angles to the equatorial axis, the declination axis. The declination axis is attached to the part of the antenna that rotates around the equatorial axis. The axis motion and the coverage area (keyholes) are dependent on the site's latitude. Generally, the motion range is less than ±180° in hour angle (equatorial) and less than ±90° in declination (Petrachenko, 2013).

The main advantage is, that tracking of a fixed point in space becomes a matter of merely driving the hour angle at the counterspeed of the Earth's rotational rate after setting declination (Salzberg, 1967). The maximum hour angle occurs at a declination of ±90° which cause loss of track on passes going through an $azimuth = 0°$ and $elevation = 90° - \phi$, where ϕ is the geographic station latitude. The hour angle is not defined at a declination of 90° (keyhole). Keyholes also exists in the two northern quadrants, as shown in Fig. 2.12 (b), due to the mechanical design constraints for this mount type (Salzberg, 1967).

2.7 Technical restrictions for VLBI satellite observations

Major restrictions for satellite observations with VLBI antennas arise from the requirement of common visibility of the target and the capabilities of the large antennas to follow the comparatively fast moving satellites over the sky. Both aspects are discussed in the following Sections (2.7.2 and 2.7.3).

Further restrictions emerge due to the specific *characteristics of satellite signals*. In general satellite signals differ from radio signals from quasars in terms of bandwidth, frequency and flux density. To account for these signal aspects during data acquisition and analysis is also a prerequisite for successful VLBI satellite observations. Because investigating satellite signal characteristics in the context of VLBI would go beyond the scope of this thesis, the author refers to relevant lit-

erature, e.g. from Tornatore *et al.* (2008) and Tornatore & Haas (2009), where particularly the possibility of GNSS signal acquisition is discussed.

2.7.1 Satellite visibility

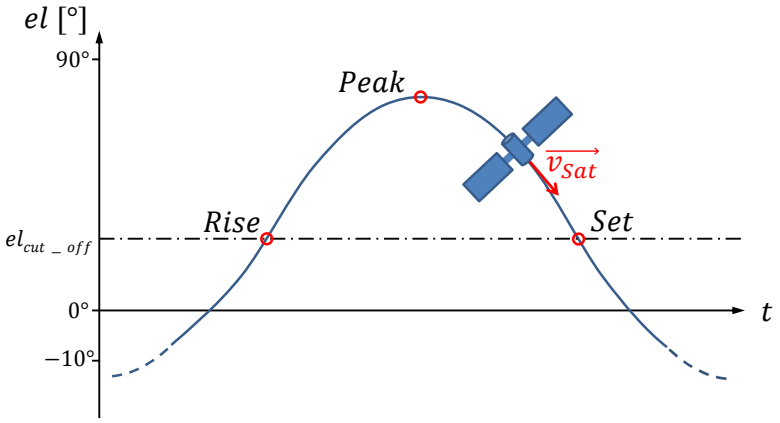

Figure 2.13: Satellite rise/peak/set. The satellite is visible between *rise* and *set* time. *Peak* refers to the maximal elevation during a passage.

A satellite counts as visible from a particular station, if its elevation angle (el) is larger than the specified cut-off elevation ($el_{cut-off}$). The situation is outlined in Fig. 2.13. Related to this, we can define three *"orbit events"*:

- **Rise** or **Arise of Sight (AOS)**: The satellite just rose above the cut-off elevation.
- **Peak**: The satellite reached the highest elevation angle during this passage (local maximum).
- **Set** or **Loss of Sight (LOS)**: The satellite just moves below the cut-off elevation (setting).

According to that, the satellite is visible between *rise* and *set* time.

2.7.2 Common visibility of satellites

One fundamental condition for VLBI observations of a satellite by a VLBI antenna network is the common visibility of the source from all participating antenna sites[1]. In general, a satellite is commonly visible from a given station network, if it is simultaneously above the cut-off elevation at all participating stations, i.e. it is between *rise* and *set* at all stations according to Fig. 2.13.

If a satellite is simultaneously visible by several stations depends on various parameters, such as the baseline length between stations and the height of the satellite on its orbit. For further details the author refers to the work of Plank (2014), where requirements for the common visibility of satellites are discussed in detail.

[1] In principle, at least from two sites, forming a baseline.

2.7.3 Antenna slew rates

During a scan in the standard geodetic VLBI the local view direction of an antenna needs to be corrected for the Earth's rotation, which results in a correction of 0.25° per minute at maximum. Antennas for geodetic VLBI are designed to rotate fast, to be able to switch fast between sources. The current IVS network includes antennas with slew rates in the range form 0.4° to 3° per second Plank (2014). The target for upcoming VLBI2010 antennas lies at 6° to 12° per second (Schuh & Behrend, 2012).

If satellite signals should be observed with VLBI, the antennas have to be capable to follow the satellite on its way over the sky. The speed of a satellite on its orbit depends mainly on the orbit height, meaning that low orbiting satellites cross the sky faster than high satellites. Furthermore, the appearing speed of a satellite for a site on the Earth's surface is dependent on the local elevation angle, which means that the required tracking speed gets faster as the elevation angle of the target gets higher. Hence, the most challenging observations are those to satellites on low overpasses close to the zenith. Also in this place the author refers to the investigations of Plank (2014) with respect to the required antenna slew rates for actual satellite tracking. Plank concluded, that the slew rates of current IVS antennas are basically sufficient to track GNSS satellites (orbit height of $\sim 20200km$), except for keyhole situations (see Sec. 2.6).

Chapter 3

Scheduling of VLBI observations to satellites with VieVS

To carry out observations of satellite signals with VLBI antennas a proper time schedule is required. It has to be prepared prior to an observation experiment. In general a VLBI observation schedule determines the timing of the whole VLBI observation constellation, as described in the Sec. 2.1.2, where the data acquisition procedure for standard geodetic VLBI is discussed. Due to the large number of different parameters influencing the observation setup, scheduling a VLBI session is a complex task. It gets even more complex, if satellite signals should be observed instead of natural radio sources. Considering that satellites orbit the Earth rather fast, the scheduling and observing become more complicated because the sources are no longer stationary targets being only subject to the Earth's rotation such as quasars. Therefore, the whole scheduling task becomes more time critical, because the source positions and, therefore, the topocentric view directions from the observing VLBI stations, change quickly in time. Furthermore, the source positions for satellites, described in a topocentric equatorial system in terms of topocentric right ascension and declination (see Appx. A.1.3), differ from site to site due to the finite source distance, as described in Sec. 2.5 and illustrated in Fig. 2.10. This "cross-eyed" observation configuration has to be considered in the schedule.

Currently a limited number of software packages is available to generate VLBI schedules, as already mentioned in Sec. 2.1.2: Program SKED (Gipson, 2010) maintained at NASA Goddard Space Flight Center (GSFC), SCHED (Walker, 2014) developed at the National Radio Astronomy Observatory (NRAO), and Vie_SCHED (Sun *et al.*, 2014). Although each of them has the capability to schedule conventional VLBI observations of quasars, the current official releases do not routinely support the scheduling of observations to satellites. Consequently, every satellite VLBI experiment leads to a huge effort at present, because the schedules have to be generated "manually", or at least software generated schedules have to be modified "manually" to implement satellite observations. To solve that deficiency, one sub-task of this work was to prepare an appropriate software tool, capable to generate fully realistic schedules for satellites. In the context of this thesis the generated schedules had to be implementable in practice for on-site experiments

in Wettzell and Onsala, as described in Chapter 5. Therefore, the schedules were fundamentally important and their correctness was a prerequisite for all following observation experiments. The specific requirements on such a scheduling software are discussed in detail in Sec. 3.1.

With the Vienna VLBI Software (VieVS; Böhm *et al.*, 2012) we have a multifunctional VLBI software on-hand, where the module Vie_SCHED Sun *et al.* (2014) already provides the ability of scheduling classical VLBI observations to quasars. So it seemed convenient to extend the already existing VieVS scheduling module for the possibility of scheduling satellites as observation targets. The newly created scheduling software is discussed in Sec. 3.2.

3.1 Requirements on the scheduling program

First, we should consider the application field in which the scheduling program should be used. Observing satellites with VLBI is still an experimental approach on its very beginning, where further research and development work is necessary to achieve operational applicability. To be able to carry out dedicated experiments an appropriate tool is needed, which helps to generate suitable schedules in a simple and quick way.

The currently available scheduling packages for standard geodetic VLBI observations to natural radio sources, such as SKED (Gipson, 2010) or Vie_SCHED (Sun *et al.*, 2014), are very sophisticated. They provide different scheduling optimization strategies, with the help of these, the source selection and the determination of the optimal observation time per scan is done fully automatically for a chosen station network and a certain observation setup. In the standard geodetic VLBI the selection of sources plays an important role, because the distribution of targets over the sky has fundamental impacts on the baseline geometry and on the feasibility to determine tropospheric parameters. As satellites are only observed in comparable small-scaled networks and not operationally so far, an optimization approach for the source distribution can still be neglected. For the calculation of appropriate observation times, which are necessary to achieve a certain signal-to-noise-ratio in the resulting data, further information would be required. Among others, additional information on the flux density of the transmitted satellite signals, as well as the level of efficiency of particular antennas and the related receiver chains would be required. The determination of such parameters for satellite observations is still a subject of research. In principle, an automatized scheduling would be possible, but appropriate strategies for the selection of satellites as targets and the determination of optimal scan times have not been examined by now.

Manual scheduling approach. For the reasons mentioned above, it seems to be the best way at this stage of development to implement a *manual scheduling approach*, meaning that the scheduler has to select the order of the satellites to be observed and the time per scan himself. The purpose of the scheduling software is, in that case, to provide all information needed to support the user in his decisions and to check his rulings for correctness; i.e. the program has to determine periods, where the observation of particular satellites from a certain station network is possible, taking into account various observation restrictions and constraints. This information has to be provided to

the user in a convenient way through graphics (satellite overpass illustrations, skyplots, etc.) and soft copy (additional detail as text). One advantage of such a "manual" approach is, that the user maintains full control over the schedule, which is an important point, particularly for research and development experiments.

Conditions for a valid satellite scan. Concerning the decision, whether a particular satellite is observable or not from a given station network at a certain time, the following *main conditions* have to be taken into account:

- **Cut-off elevation**: The cut-off elevation angle defines the minimum elevation angle for which sources are allowed to be scheduled. If a source is below the cut-off angle for a particular station, it counts as "not visible", even if it is above the horizon (above 0° elevation). Cut-off elevations could be defined in order to take limited motion ranges of antennas into account and, further, to prevent them from reaching the axis hardware limits.
- **Common view**: The source has to be visible from all participating stations (from *all* stations, if no sub-netting approach is included), i.e. it has to be above the cut-off elevation for each station. A valid baseline consists of at least two stations. The common visibility for satellite observations is discussed in detail in Sec. 2.7.2.
- **Antenna slew rate limitations**: The maximum slew rates of the axes of the observing antennas must not be exceeded, in order to ensure that the antennas are able to follow the satellite in the sky. Antenna slew rates with respect to satellite tracking are discussed in Sec. 2.7.3.
- **Sun distance**: A certain angular distance between the observed signal source and the sun has to be kept during an observation. The Sun itself is a very strong radio source. If the antenna would point directly to the Sun, the receiver equipment could be harmed, because of the strong flux density, or – at least – the measurements would probably be impaired, so that the recorded data would become useless.

If these conditions are met simultaneously at a certain epoch, the satellite target counts as *observable* for that particular time.

Generation of schedule files. The program has to be able to generate global schedule files in an appropriate file format, which can be used to carry out real satellite observations with VLBI antennas. The VEX format (Whitney *et al.*, 2002) should be used, because it is the more flexible and up-to-date format, compared to SKD – the scheduling file format used by the program SKED (Gipson, 2012). Another reason to use VEX (current version 1.5b1) is the fact, that an update to version 2.0 was already announced[1], which will include the possibility to define satellites as

[1]According to personal communication with Ed Himwich. Also see https://safe.nrao.edu/wiki/bin/view/VLBA/Vex2doc

sources explicitly in terms of corresponding TLE datasets (parameter: *source_type* = *tle* in the *$SOURCE* block). Nevertheless, the current VEX1.5b1 format does not provide that possibility. Therefore, the most convenient way of defining satellites as sources in the VEX file is to approximate the satellite orbits by discrete celestial positions, as described in Sec. 2.5.1. To implement continuous satellite tracking, as described in Sec. 2.5.2, using VEX1.5b1 formatted schedule files, a workaround has to be implemented, according to the requirements of the local satellite tracking capabilities at the stations. One possible approach, like it was realized in Wettzell, is presented in Sec. 4.2.4.

Another important demand is the feasibility to configure the used receiver setup for each observing station flexibly, e.g. the recorded frequencies, number of channels, bandwidth, etc. For this reason the information provided in the SKED catalog files[1] (Vandenberg, 1997) should be utilized. They have to be complemented by additional catalog files to define further parameters, specific to for satellite observations, which are not included in the SKED catalogs. In dedicated configuration files, a complete observation should be flexibly definable.

Inclusion into the VieVS GUI. The scheduling tool has to be easy and convenient to use. Therefore, a program with a Graphical User Interface (GUI) is preferred compared to a pure command line interface. For this reason it was decided to use the already existing VieVS package as a basis to implement a satellite scheduling software. VieVS is written in MATLAB and provides a flexible programing environment, including a GUI, with numerous useful functionalities and already existing functions to handle geodetic tasks. Therefore, the GUI menu of the VieVS scheduling module (Vie_SCHED, Sun *et al.*, 2014) was modified to add new satellite scheduling functions. The implementation of the scheduling tool with VieVS is described in Sec. 3.2.

Reliability. A final important point is the reliability of the program. The generated schedules have to be absolutely correct and actually observable as issued. This is a prerequisite for the feasibility of observations, which will be carried out on the basis of these schedules (e.g. as those described in Chap. 5).

3.2 VieVS satellite scheduling module

Initially it was planned to create a small program to generate schedules in terms of VEX files to carry out GNSS observation experiments on the baseline Wettzell–Onsala (as described in Chap. 5). Later, during the software development, it was decided to include the satellite scheduling tool as a module to the VieVS package. The first version was programed in a short period of time in autumn 2013, after the author's first research stay in Wettzell. Several small updates were added as required. Basically, all the requirements described in Sec. 3.1 have been considered and implemented. Eventually, the created VieVS satellite scheduling module, as it is now, can be used

[1] They are available online via anonymous ftp at ftp://gemini.gsfc.nasa.gov/pub/sked/catalogs/

very flexibly to generate schedules for numerous satellites in arbitrary orbits (low/medium/high Earth orbits, geostationary, etc.) in combination with various VLBI station networks. Also the varying station equipment can be taken into account in a flexible way.

The next Section (3.2.1) will give an overview of the basic program concepts and the workflow, followed by descriptions of specific technical aspects of the program in the following section (3.2.2).

3.2.1 Workflow and program overview

Workflow. The VieVS satellite scheduling workflow is illustrated in Fig. 3.1. Before the actual scheduling starts, the required *input data* (a), in the form of catalog, configuration and TLE files, have to be prepared. A detailed description is given in Sec. 3.2.1.1. When the scheduling program is executed, these files are loaded.

In the *VieVS GUI* (b) several satellite scheduling parameters have to be set, as discussed in Sec. 3.2.1.2, to determine the desired observation configuration. Then the program calculates the available observation periods for the chosen session parametrization and provides this information to the user with *a graphic and a text based interface* (c), as described in Sec. 3.2.1.3. Depending on the application and this auxiliary information, it may be necessary to refine the selection of scheduling parameters. The easiest way to find an appropriate parametrization is, to run the software iteratively, until the presented auxiliary information indicates, that a proper observation setup was found. This can be done without starting the actual scheduling process and VEX file generation.

Finally, if all scheduling parameters are set properly and a pre-selection of observable satellites was made, the *scheduler interface* (d) in the MATLAB Command Window can be started to determine the exact chronological sequence of satellite observations (see Sec. 3.2.1.4). If the collocation of satellite scans is finished, *VEX formatted schedule files* (e) are generated, as discussed in Sec. 3.2.1.5, providing the possibility to actually carry out the observations as scheduled.

Program overview, based on a simple example. The items (a) to (d) in Fig. 3.1 are described in detail in the following sub-sections, where all shown figures are created according to a *simple example*: The task is to generate VEX files for a $15min$ satellite scan in the time between $9:00$ and $13:00$ on August 31, 2014, for the baseline Onsala-Wettzell. The observation availability of the satellites GLONASS-721, GLONASS-731 and GLONASS-735 should be examined and one of them has to be selected for the scan. The cut-off angle is $5°$ and the minimum Sun distance is $15°$. It is assumed, that the station equipment setup for Wettzell and Onsala is already defined properly in the corresponding catalog and configuration files.

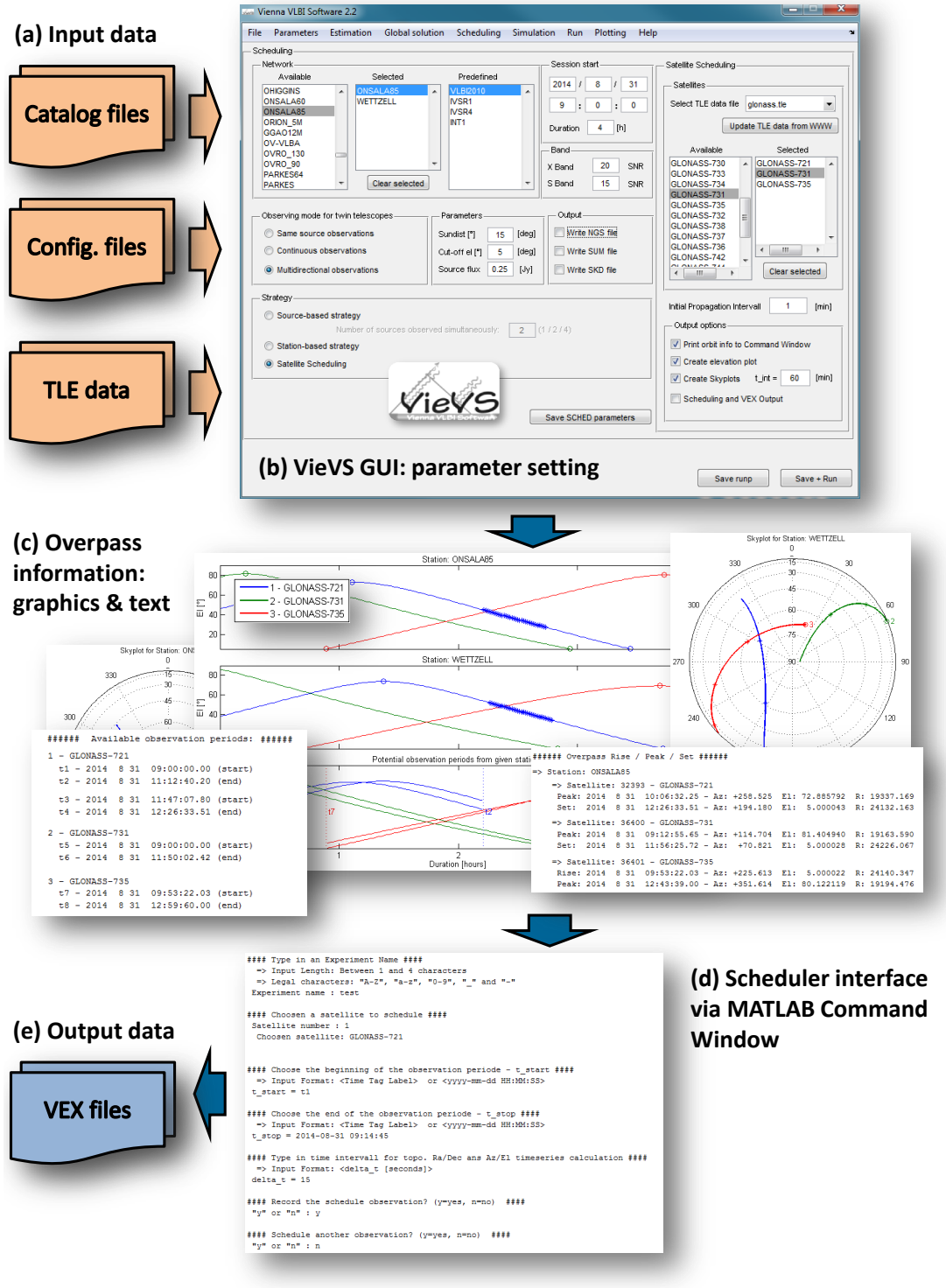

Figure 3.1: Workflow and overview of the VieVS satellite scheduling module. (a) Input data in terms of catalog, configuration and TLE files are loaded on program start. (b) In the GUI various scheduling parameters have to be set. (c) The available observation periods for the chosen satellite/station constellation are calculated and presented by different output by means of graphics and text. (d) In the scheduler interface single satellite scans are combined to one schedule as requested. (e) Finally, VEX files are generated for the scheduled observations.

3.2.1.1 Input data

When the program is started, the necessary input data (3.1, (a)) are loaded from particular directories in the VieVS file system. Several *SKED catalog files*[1] (Vandenberg, 1997) provide the required basic information about the available VLBI stations, such as station names, station coordinates, station equipment and antenna properties. Separate, VieVS-specific *VEX catalog files* have been set up to predefine various receiver and observation settings for the generation of VEX files.

Raw TLE files, which are provided for the download by dedicated websites[2] in the most recent version, build the basis for the maintaining of a local TLE data library, which is then used for all orbit propagation purposes. The raw TLE files comprise single TLE datasets[3] for numerous satellites of a particular type or for a certain application purpose in one file (e.g. all available GNSS or remote sensing satellites). The raw TLE files can contain datasets for hundreds of satellites Hence, they are often very confusing. For this reason, there is the possibility to extract TLE data for particular satellites from the raw files and to collect them in *local TLE files*. Such local files can be used to maintain a kind of a local database, containing only data, which are needed for specific tasks. These local TLE files are loaded by VieVS and the contained satellites occur in the GUI of the satellite scheduling module. The scheduling tool also provides a function, which is accessible in the GUI to download the most recent raw TLE data files and to use them to update the local TLE files automatically.

Several *configuration files* are used for different purposes. For example, to define the online resources for the latest raw TLE datasets and the update procedure for the automatic TLE update routine, described before. Another configuration file is used to define the receiver and observation setup for particular VLBI stations for the generation of VEX files by combining the information, which is provided in the catalog files. One file defines the RF carrier frequencies of particular satellites – information which is also needed for the VEX file generation.

3.2.1.2 VieVS GUI

The already existing GUI of the VieVS scheduling module Vie_SCHED (Sun *et al.*, 2014) was modified and updated to incorporate the user interface of the new satellite scheduling module. The GUI is used to set various user-definable *satellite scheduling parameters*, as listed below (see Fig. 3.2):

1. Selection of the VLBI station network.

2. Date and time of the session start and its duration. The available observation periods for the chosen parameters are then calculated for the selected time.

[1] They are available online via anonymous ftp at ftp://gemini.gsfc.nasa.gov/pub/sked/catalogs/.

[2] http://www.celestrak.com/ is recommended as resource for *raw* NORAD TLE data.

[3] Actually with three lines per dataset, not with two, as the name suggests. An additional line is added for the satellite name, which is followed by two lines containing the actual orbit data.

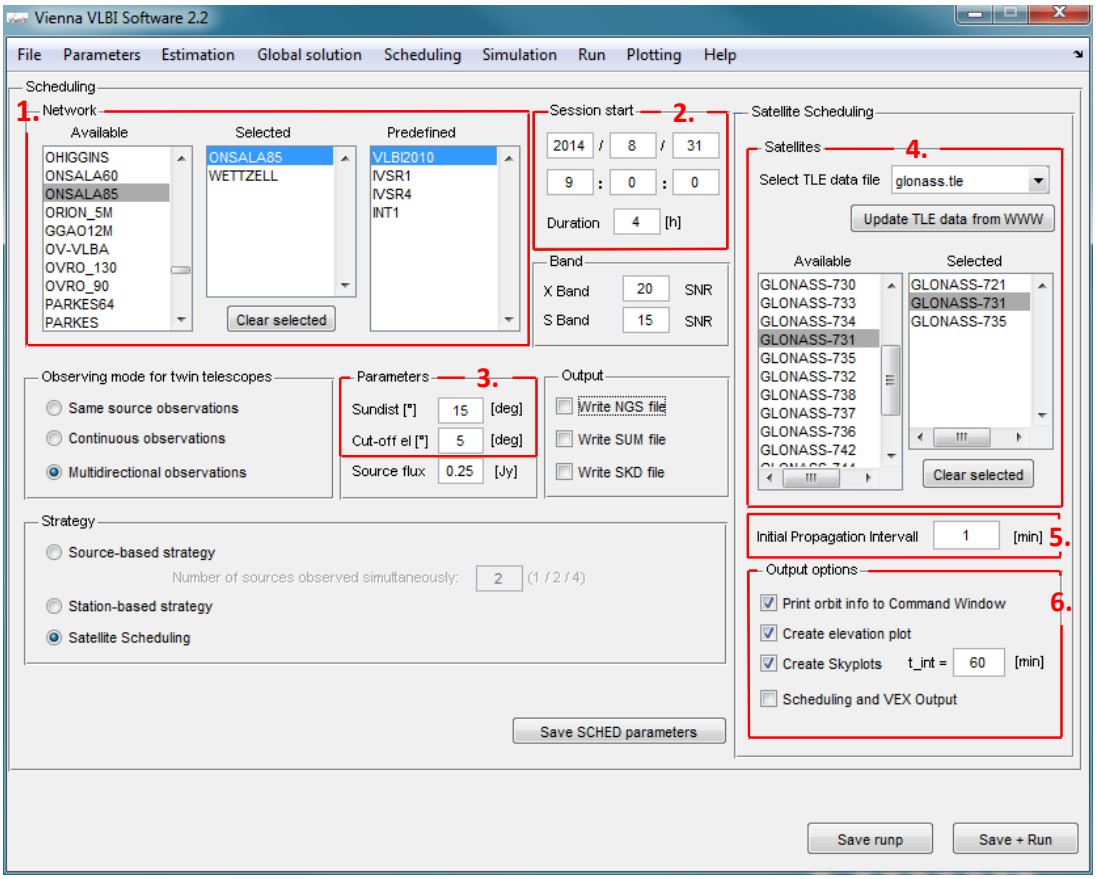

Figure 3.2: VieVS satellite scheduling GUI. Various parameters (marked with red boxes and described in Sec. 3.2.1.2) have to be set before the initial calculation of the available observation periods can be started, respectively before the schedule can be generated. All parameters are set according to the example given on page 37.

3. Observation restrictive parameters such as the minimum sun distance and the cut-off elevation.

4. Selection of satellites: In a drop-down list, one of the available local TLE files can be selected. All satellites, for which TLE datasets are contained in the chosen file, are listed in a list-box, from where they can be selected. An update function provides the ability to automatically update all available TLE datasets for the most recent version, downloaded from the internet.

5. Initial orbit propagation interval: All initial calculations (satellite visibility, etc.) are carried out for discrete steps, separated by the chosen time interval.

6. Output options: Through check boxes, it can be selected, how the calculated auxiliary scheduling information is presented. For more details see Sec. 3.2.1.3. Only, if the checkbox *"Scheduling and VEX output"* is selected, the scheduler interface (see Sec. 3.2.1.4), which is used for the selection of satellites and the observation timing, opens in the MATLAB

Command Window and VEX files are generated in the end. Otherwise, only the calculated information is presented, which is helpful to find an appropriate observation setup, before the real assembly of observations is scheduled.

After setting all necessary parameters, the calculation of the available observation periods can be started via the GUI by pressing the *"Save + Run"* button.

3.2.1.3 Satellite passage information

According to the selection in the GUI, a different auxiliary output is generated to basically show the user, for which time period and under which topocentric view angles the selected satellites are observable. The conditions for a valid scan are taken into account, as discussed in Sec. 3.1.

Elevation plot. The most meaningful and important graphical output is the *elevation plot*. Fig. 3.3 shows an illustration, according to the observation setup, shown in Fig. 3.2. One subplot per VLBI station is created to show the topocentric elevation angles of all selected satellites as a function of time. This is particularly important for the scheduling, because the fundamental condition, whether a satellite is observable, depends on the requirement that it has to be above the defined cut-off elevation angle. This plot also indicates the three *orbit events* (rise, peak, set), as defined in Sec. 2.7.1 (Fig. 2.13) with markers. Further, the corresponding parts of the elevation diagrams are highlighted, where at least one of the conditions for a valid satellite scan (see Sec. 3.1) is violated. One additional sub-plot on the very bottom summarizes the information and illustrates the periods for each satellite, in which an observation from the whole station network is possible, i.e. periods where none of the observation conditions is violated at any station. Vertical lines with time tags (t_x) mark each point in time, where a particular satellite becomes observable or is not observable anymore. During the further scheduling process, described in Sec. 3.2.1.4, the user can refer to these times via the tags.

Skyplots. Skyplots provide additional information about the satellite transits, seen from particular stations. Additionally to the elevation angle, shown in the elevation plot, also the azimuth angle is visible here. Time marks, by means of asterisks printed in a defined time interval on the satellite tracks, provide a time reference. Fig. 3.4 shows the skyplots generated for the observation setup, shown in Fig. 3.2.

Orbit details in the Command Window. As additional option, details about the satellite passes can be printed to the MATLAB Command Window. The exactly determined time of the orbit events – rise, peak and set (see Sec. 2.7.1) – with the corresponding pointing directions (azimuth and elevation) can be displayed for each station. Further, the available observation periods are printed by means of the start and end time of each period, denoted by a time tag (t_x), like the example

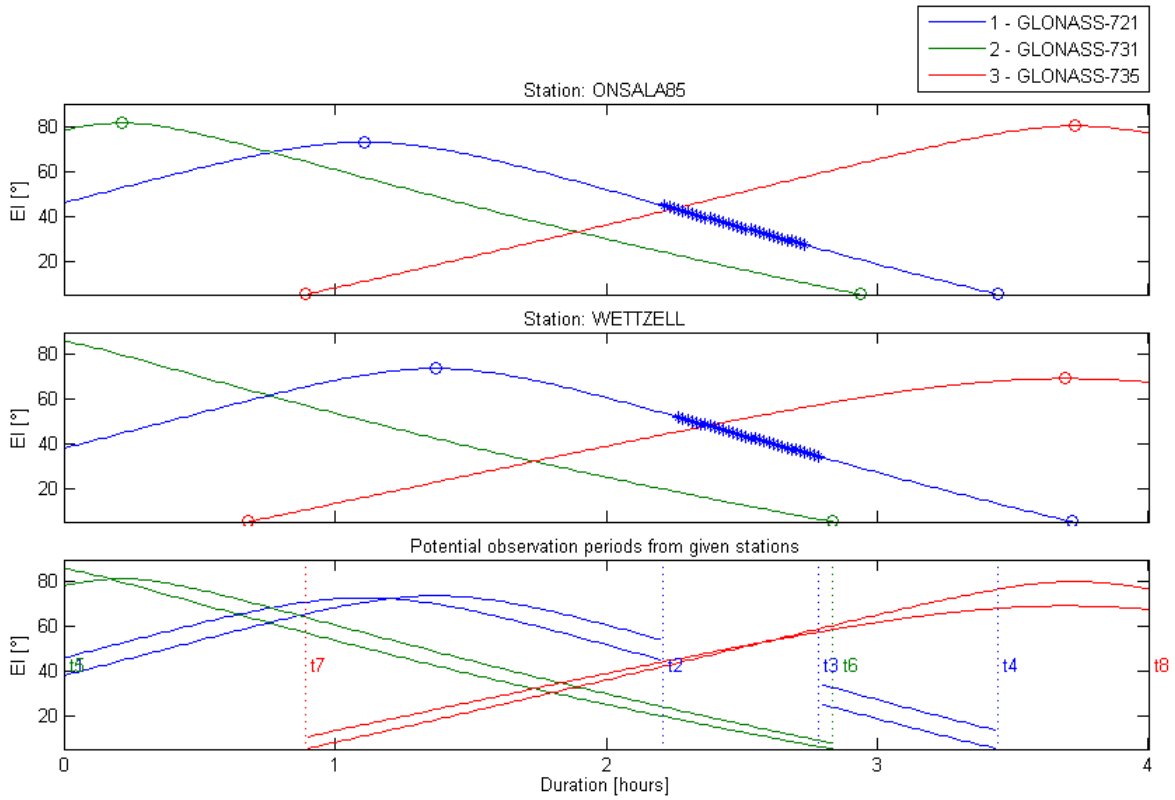

Figure 3.3: Satellite elevation plot for the stations Wettzell and Onsala85, showing the tracks of the satellites GLONASS-721 (blue), GLONASS-731 (green) and GLONASS-735 (red) in the period from 9 : 00 to 13 : 00 UTC on the 31st August 2014. The two upper sub-plots show the temporal progress of the topocentric elevation angles of the three GLONASS satellites, seen from both stations, as a function of the time elapsed since the session start. The cut-off elevation angle is 5°. The small circles mark three different satellite orbit events: *rise* (above the cut-off angle), *peak* (max. elevation during an overpass) and *set* (below cut-off angle). The highlighted parts of the tracks of GLONASS-721 (blue line) tag a violation of a condition for a valid satellite scan (the angular distance between satellite and sun is here smaller than 15°). The sub-plot on the very bottom summarizes the possible observation periods for the selected setup, marked with vertical dotted lines and time tags (t_x, also see Fig. 3.5) at the beginning and at the end.

in Fig. 3.5 shows. These time tags refer to the corresponding points in time in the elevation plot (see Fig. 3.3).

3.2.1.4 Scheduler interface

When the corresponding option in the GUI is selected, the scheduler interface appears in the MATLAB Command Window, after presenting the auxiliary scheduling information, as described in Sec. 3.2.1.3. Fig. 3.6 shows a screenshot of the scheduler interface with all entries according to the example defined on page 37. Although only one satellite scan is scheduled in Fig. 3.6, an arbitrary number of scans could be added in the same fashion. All entered parameters are checked for their reasonableness; e.g. for the entered scan period (between *t_start* and *t_stop*), it is checked, whether the satellite is actually observable. Additional commands, such as *"help"* (provides further information about the current parameter), or *"exit"* (closes the scheduler in-

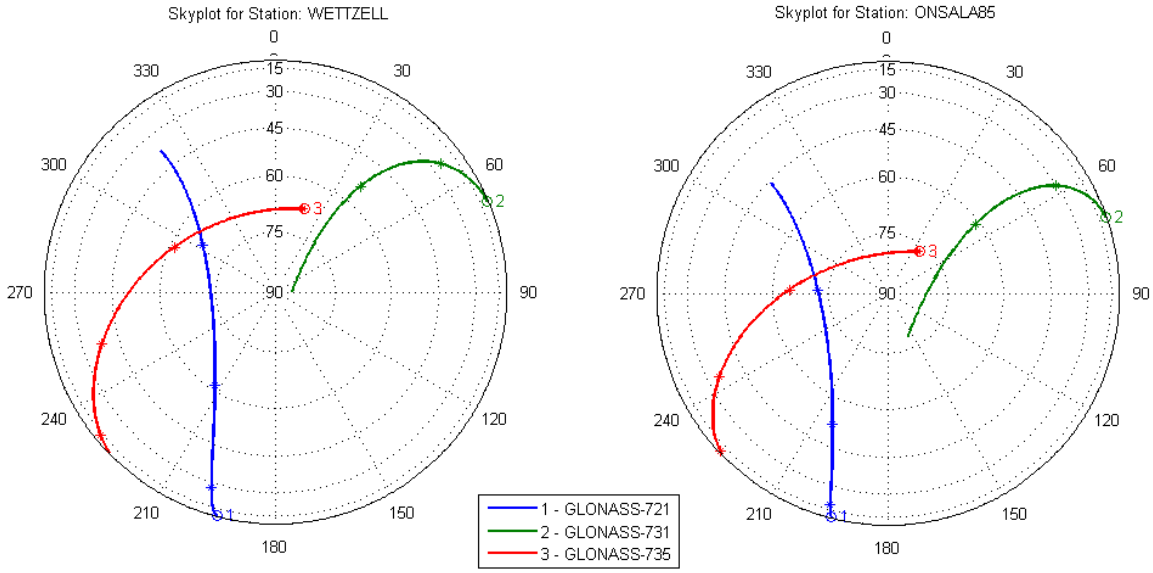

Figure 3.4: Skyplots for the stations Wettzell (left) and Onsala85 (right), showing the tracks of the satellites GLONASS-721 (blue) GLONASS-731 (green) and GLONASS-735 (red) in the period from 9 : 00 to 13 : 00 UTC on the 31^{st} August 2014. The satellite numbers near the tracks (1, 2, 3) are plotted on the beginning of the selected time period.

```
######  Available observation periods: ######
1 - GLONASS-721
  t1 - 2014  8 31  09:00:00.00 (start)
  t2 - 2014  8 31  11:12:40.20 (end)

  t3 - 2014  8 31  11:47:07.80 (start)
  t4 - 2014  8 31  12:26:33.51 (end)

2 - GLONASS-731
  t5 - 2014  8 31  09:00:00.00 (start)
  t6 - 2014  8 31  11:50:02.42 (end)

3 - GLONASS-735
  t7 - 2014  8 31  09:53:22.03 (start)
  t8 - 2014  8 31  12:59:60.00 (end)
```

Figure 3.5: Available observation times for the stations Wettzell and Onsala85, and the satellites GLONASS-721 GLONASS-731 and GLONASS-735 in the period from 9 : 00 to 13 : 00 UTC on the 31^{st} August 2014 (MATLAB Command Window screenshot). The time tags (t_x) refer to the corresponding points in time in Fig. 3.3.

terface without creating VEX files), provide additional functionalities. If no additional scan is entered, the scheduler interface closes and VEX files are created, as described in the next Section (3.2.1.5).

```
#### Type in an Experiment Name ####
  => Input Length: Between 1 and 4 characters
  => Legal characters: "A-Z", "a-z", "0-9", "_" and "-"
 Experiment name : test

#### Choose a satellite to schedule ####
 Satellite number : 1
  Choosen satellite: GLONASS-721

#### Choose the beginning of the observation periode - t_start ####
  => Input Format: <Time Tag Label>  or <yyyy-mm-dd HH:MM:SS>
 t_start = t1

#### Choose the end of the observation periode - t_stop ####
  => Input Format: <Time Tag Label>  or <yyyy-mm-dd HH:MM:SS>
 t_stop = 2014-08-31 09:14:45

#### Type in time interval for topo. Ra/Dec ans Az/El timeseries calculation ####
  => Input Format: <delta_t [seconds]>
 delta_t = 15

#### Record the schedule observation? (y=yes, n=no)  ####
 "y" or "n" : y

#### Schedule another observation? (y=yes, n=no)  ####
 "y" or "n" : n

#### Calculation of stepwise antenna pointing data for scheduled observation  ####.

Manual Scheduling Process => Finished!

-------------------------vie_sched output--------------------------
Creating VEX Files => Finished!
-------------------------------------------------------------------
```

Figure 3.6: Screenshot of the Scheduler interface in the MATLAB Command Window. A session with the experiment name *test* was scheduled, containing a single satellite observation to GLONASS-721 with a duration of $15 min$, starting on 9 : 00 UTC on the 31^{st} August 2014. VEX files were generated to track the satellite stepwise with a repositioning interval of $15 sec$.

3.2.1.5 Output data: VEX files

After finishing with the assembling of scans in the scheduler interface, schedule files in the current VEX format (version 1.5b1, Whitney *et al.*, 2002) are generated. Because the current VEX version does not provide the possibility to define satellites as sources explicitly by means of TLE orbit data, as already discussed in Sec. 3.1, the satellite orbits are approximated by sequences of discrete coordinates in the topocentric equatorial coordinate systems (see Appx. A.1.3) in terms of topocentric right ascension and declination. These positions are commanded consecutively in a defined time interval (*repositioning interval*) to implement a *stepwise tracking approach*, as it is described in Sec. 2.5.1. As discussed in Sec. 2.5, a so-called *cross-eyed schedule* (Duev *et al.*, 2012) is generated, because the topocentric satellite coordinates differ between different sites. This leads to the situation that the *$SOURCE block* (Whitney *et al.*, 2002), the part of the VEX file, where the source positions are defined, would contain a very large number of single source definitions. The already large number of source definitions needed for stepwise tracking

at one site[1] is additionally multiplied by the number of observing stations. The same applies to the *$SCHED block* of the VEX file, where the chronological order of the distinct scans is defined. Hence, if one VEX file is generated comprising the schedule data for all stations, this file will be confusing and difficult to handle because of its length. For this reason, the VieVS satellite scheduling module generates one separate VEX file per station, containing only the information needed at the particular sites.

A VEX file does not only contain the definition of source positions (*$SOURCE block*) and the timing (*$SCHED block*). It also defines the complete receiver setup and various procedures, which are carried out during a session, for all participating antennas. All information needed to include these definitions in the schedule files are provided in the form of catalog and configuration files (see Sec. 3.2.1.1), which have to be set up correctly before the program execution.

3.2.2 Technical program aspects

This section discusses the more technical aspects of the VieVS satellite scheduling module. After giving an initial overview of the program with a flowchart, particular important details are discussed within the following sub-sections.

A flowchart of the VieVS scheduling module is shown in Fig. 3.7. The left side (blue) illustrates the input data and the required parameters for each processing step, shown in the middle (gray). The program output is drawn on the right side of the figure (yellow). n denotes the number of selected satellites and m the number of VLBI stations.

(a) In a first processing step, the allocated TLE data are used to calculate state vectors for all n satellites, as discussed in Sec. 3.2.2.1.

(b) In a second step, the calculated satellite state vectors, together with required station-specific and general scheduling parameters, are used to calculate time series of a number of parameters for each available station/satellite combination.

(c) This derived data are required to determine the available observation periods for each satellite, as described in Sec. 3.2.2.2. The calculated information is then presented to the user by means of various output options, as shown in Sec. 3.2.1.3.

(d) By means of the provided information, the user has to compile the desired schedule for the satellite observations by applying the provided scheduler interface, described in Sec. 3.2.1.4.

(e) Finally, VEX files are generated – one for each station – as described in Sec. 3.2.1.5. The applied approach for the calculation of the precise topocentric satellite coordinates, required for the source definition in the generated VEX files, is outlined in Sec. 3.2.2.3.

[1] One hour of satellite tracking with the stepwise tracking approach and a repositioning interval of $15sec$ requires $3600sec/15sec = 240$ single source definitions per observing station.

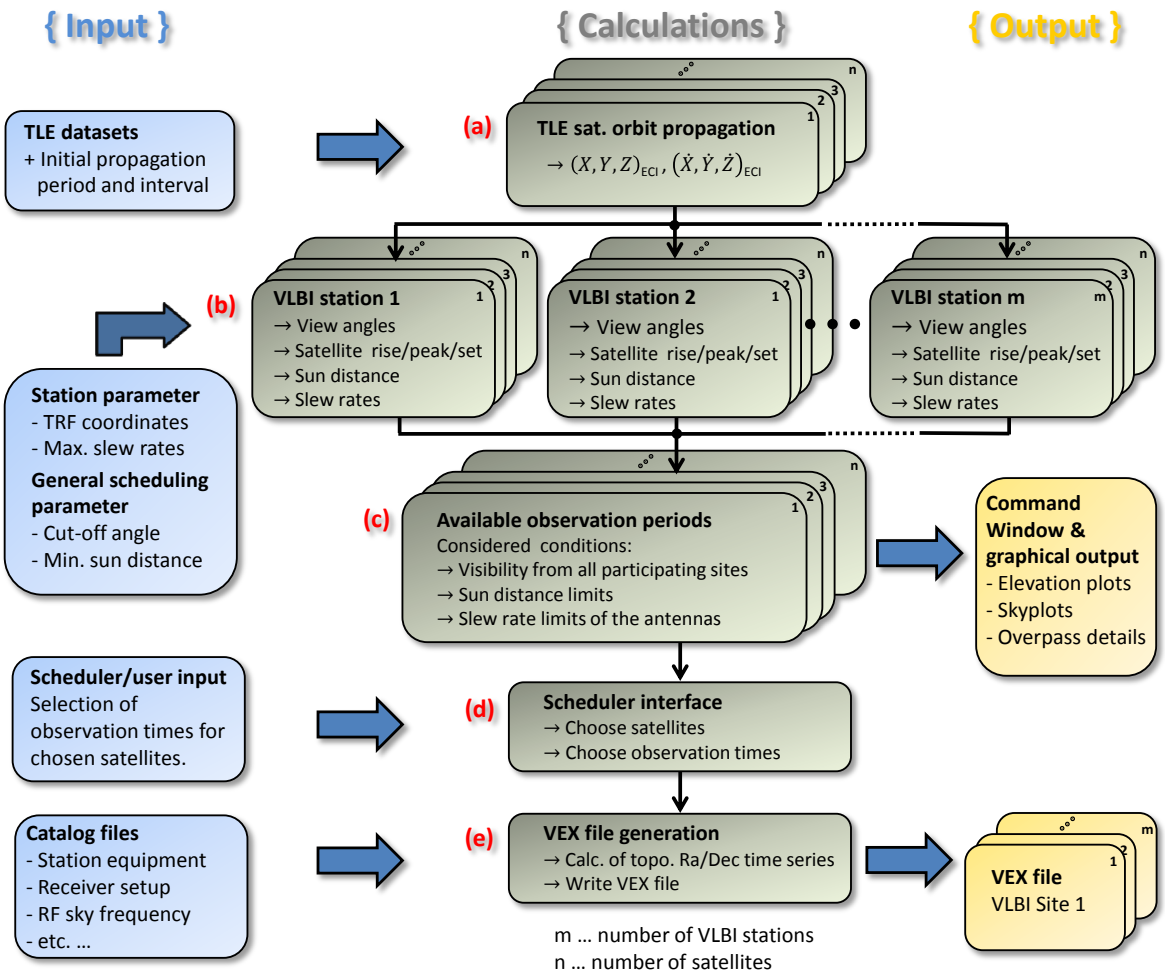

Figure 3.7: Flowchart of the VieVS satellite scheduling module. Input data and required parameters can be found on the left side (blue). The actual program flow is shown in the middle (gray) and the output on the right side (yellow).

3.2.2.1 Initial orbit propagation

After setting all parameters and executing the program via the GUI, stacks of *satellite state vectors* are computed for the defined session start time and durations (one stack per selected satellite, see Fig. 3.7 (a)).

Each state vector stack consists of consecutive satellite position and velocitie vectors, propagated in the defined time interval (parameter "*Initial Propagation Interval*" in the GUI) with the SGP4 models and the prepared TLE data (see Sec. 2.3.3). The state vectors are computed in the ECI TEME reference frame, described in Appx. A.1.1.1. These state vectors are the basis for all subsequent computations.

3.2.2.2 Derivation of available observation periods

As described above (Sec. 3.2.2.1), satellite state vectors are computed for the selected propagation period and interval. These discrete satellite position and velocity sets, available for each propagation epoch, are used to calculate several parameters, which are required to decide whether a satellite is observable at the particular epochs from a particular site (see Fig. 3.7 (b)). These parameters are:

- *View angles* by means of azimuth (β) and elevation (el). They are required to determine satellite visibilities and are needed to calculate further parameters. The formulae to compute the view angles are described by Escobal (1965) on page 29.
- The satellite *orbit events* rise, peak and set, as described in Sec. 2.7.1. The rise and set times identify the begin and the end of a passage. Peak labels the time of the maximal elevation. The times of these events are determined very accurately to the sub-second level using an iterative calculation approach, similar to the bisection method described by Kelso (1997).
- The required antenna *slew rates*, meaning the change rates of the actual view angles. Currently the software supports to schedule observations with HaDec and AzEl mounted antennas (see Sec. 2.6). Hence, it is necessary to compute the rates of azimuth and elevation($\dot{\beta}$, $\dot{el}$), and the rates of the local hour angle and topocentric declination ($\dot{LHA}$, $\dot{\delta}_t$), to be able to check whether an antenna with its limited axes slew rates is able to follow the satellite. The formulas to calculate the view direction rates are described by Vallado (2013) in the according chapters.
- The angular distance between the satellite target and the sun, referred to as *sun distance*, has to be larger than the user defined limits. The solar ephemeris are calculated with the formulas from the The Astronomical Almanac (1984) on page C24.

If the number of satellites is n and the number of observing stations is m, approximately $m \cdot n$ parameter sets are calculated per propagation epoch, leading to quite a lot of computational costs, especially for longer periods and small computation intervals.

These computed parameter sets are then used to find the available observation times (see Fig. 3.7 (c)). In this respect, a satellite counts as *observable* from one particular station, if all necessary observation conditions are met simultaneously, as illustrated in Fig. 3.8. A similar approach is applied to determine the available observation times for a whole station network, meaning that a satellite is observable from a network, for the periods, it is observable simultaneously from each single station of the network.

3.2.2.3 Calculation of topocentric equatorial coordinates for the source definition

For the definition of the source positions in the VEX files, implementing a stepwise tracking approach (see Sec. 2.5.1), precise topocentric equatorial coordinates in terms of topocentric right

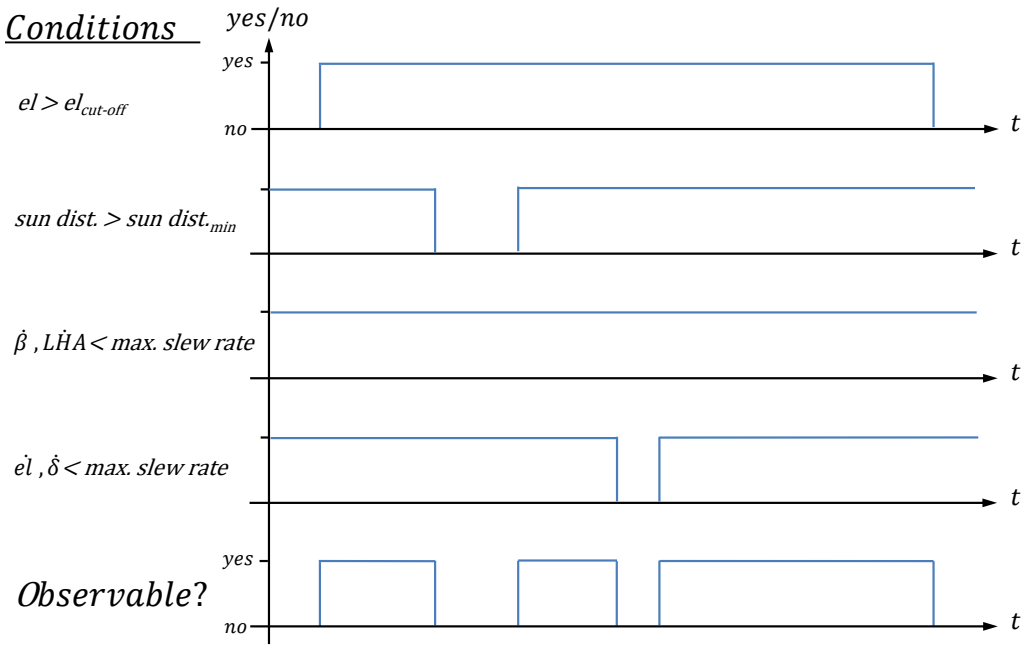

Figure 3.8: Observation conditions for a valid satellite scan at one station. If all conditions (satellite visibility, antenna axes slew rates and the minimal sun distance) are met simultaneously, the satellite counts as *observable* from the particular station.

ascension and declination (see Appx. A.1.3) are required in the J2000.0 standard epoch. After the user finished the arranging of the schedule in the dedicated interface (see Fig. 3.7 (d)), the observation times for all satellites are fixed and stored to be used as input for the generation of source positions for the final VEX files (see Fig. 3.7 (e)). The user is also asked to enter the desired antenna repositioning interval. Hence, all scheduled observation periods are segmented into discrete epochs, separated by the repositioning interval. For each of these epochs, satellite positions are computed using TLE data and the SGP4 orbit propagator (see Sec. 2.3.3).

In the first step, the resulting (X, Y, Z) satellite coordinates in the ECI TEME frame (see Appx. A.1.1.1) have to be converted to the J2000.0 standard epoch, as required for the antenna control. This coordinate transformation is outlined in Appx. A.1.1.1. The schedules are usually generated to be carried out in the future and, therefore, the availability of Earth orientation parameters (EOP) cannot be ensured for the epochs of observation. As long time predictions of EOP are potentially not available, an approximation is made: The value for dUT1 (used to translate between UT1 ant UTC) is set to zero for the computation of the required nutation and precession matrices using the IAU-76/FK5 formulae as described by McCarthy (1992a).

The second step comprises the transformation of the (X, Y, Z) J2000.0 satellite coordinates to topocentric right ascension and declination (see Appx. A.1.3). To compute topocentric view

directions, the position of the observing VLBI station is required. Station positions are available in terms of (X, Y, Z) ITRF coordinates and have to be converted to the same frame as the satellite positions are provided. Therefore, a conversion from the terrestrial to the celestial frame is necessary, which is done following the IAU 2006/2000 precession-nutation model (IERS Conventions, Chap. 5, Petit & Luzum, 2010). Also in this case the influences of the Earth orientation parameters dUT1, polar motion $(x_p,\ y_p)$ and the nutation corrections $(dX,\ dY)$ are neglected, because of the reasons mentioned above.

Now, the geocentric space fixed (X, Y, Z) position vectors in the ECI J2000.0 system ("mean equinox, mean equator") for the satellite $(\vec{r_{sat}})$ and the station $(\vec{r_{stat}})$ are available. To get a topocentric view direction, the origin of the satellite vector is moved to the station location by calculating the difference vector $(\vec{r_d})$ as shown in Fig. 3.9,

$$\vec{r_d} = \begin{bmatrix} r_d(1) \\ r_d(2) \\ r_d(3) \end{bmatrix} = \vec{r_{sat}} - \vec{r_{stat}}. \tag{3.1}$$

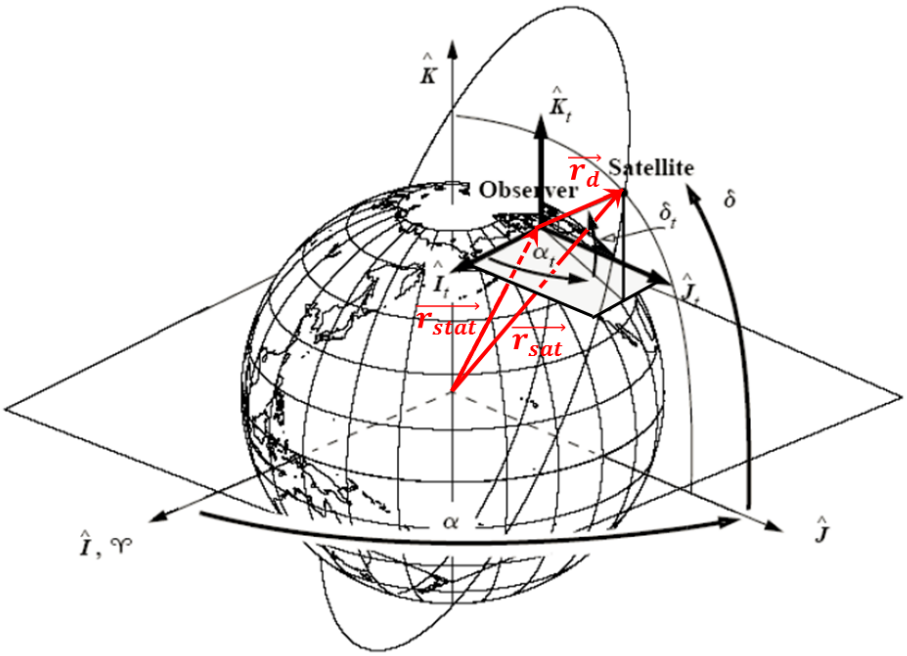

Figure 3.9: Topocentric satellite vector $\vec{r_d}$ in the ECI J2000.0 frame.

The formulae to finally calculate topocentric right ascension α_t and declination δ_t are provided by Escobal (1965) on pp. 397–398,

$$\alpha_t = \arctan\left(\frac{r_d(2)}{r_d(1)}\right), \tag{3.2}$$

$$\delta_t = \arctan\left(\frac{r_d(3)}{\sqrt{r_d(1)^2 + r_d(2)^2}}\right). \tag{3.3}$$

Chapter 4

Satellite tracking at Wettzell

This chapter describes how continuous satellite tracking with VLBI radio antennas is realized at the Geodetic Observatory Wettzell, Germany (GOW). After giving a general introduction on the GOW and its equipment in Sec. 4.1, the implementation of satellite tracking is discussed in Sec. 4.2.

4.1 Geodetic Observatory Wettzell

The Geodetic Observatory Wettzell (GOW) is jointly operated by the Federal Agency for Cartography and Geodesy (Bundesamt für Kartographie und Geodäsie, BKG) and the Forschungseinrichtung Satellitengeodäsie (FESG) (Research Facility Satellite Geodesy) of the Technische Universität München. The GOW represents an important co-location site, combining the space-geodetic techniques SLR, GNSS and VLBI at a single location, as shown in Fig. 4.1. Such co-location sites play a key-role in the ITRF combination (see Sec. 1.1) by providing geometric ties (*local ties*) in terms of vectors between the reference points of the different techniques.

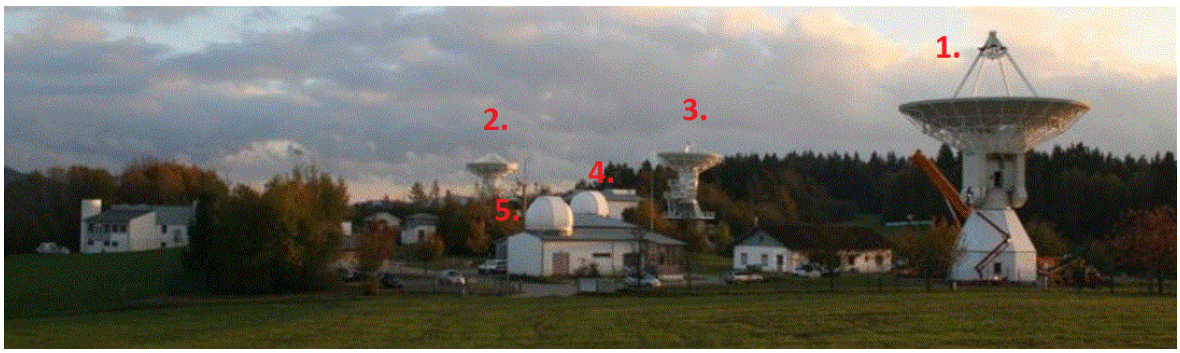

Figure 4.1: Panorama view of the Geodetic Observatory Wettzell, Germany. This important co-location site has three VLBI radio antennas: the 20*m* Radio Telescope Wettzell (RTW; 1.) and the two 13.2*m* Twin Telescopes Wettzell (TTW; 2. and 3.). Beside several IGS GNSS permanent stations, there is the Wettzell Laser Ranging System (WLRS; 4.) and the new Satellite Observing System Wettzell (SOS-W; 5.), which is in preparation for the regular operation (picture taken from Neidhardt *et al.*, 2010).

Three VLBI radio telescopes are located at the GOW: the older 20*m* Radio Telescope Wettzell (RTW) and the new 13.2*m* Twin radio Telescope Wettzell (TTW).

The RTW started its operation in the year 1983. Due to several technical changes, improvements and updates the reliability of the VLBI observation system could be increased steadily. The last large changes were carried out by Vertex Antennentechnik GmbH, Duisburg, Germany in summer 2013. The over-aged servo system and the gears of the azimuth and elevation axes were replaced, as well as the complete control rack including the Antenna Control Unit (ACU). The new Vertex ACU of the RTW is similar to those of the Twin telescopes and provides in general the same functionalities. In addition to the classical celestial tracking modes, the new ACU provides a new tracking mode for satellites (Two-Line Track mode), which is described in Sec. 4.2.1 (Neidhardt *et al.*, 2014). A new GNSS receiver unit (Kodet *et al.*, 2014) adds an additional receiver chain to acquire GNSS signals in the L1-band with the classical IVS-compatible S/X receiver system of the RTW (see Sec. 5.1). Nevertheless, at the time when all practical tests and observations described in this thesis were carried out, an older Field System version (9.10.4) was still installed and used to control the RTW system, which did not provide the dedicated satellite tracking commands described in Sec. 4.2.3.1.

The two identical radio antennas of the TTW are built in accordance with the VLBI2010 guidelines (Petrachenko *et al.*, 2009) in the recent years until 2013. With a 13.2*m* diameter they are smaller and faster[1] than the RTW, being able to serve the demands of the modern VLBI for short slew times and a maximum number of observations. The north tower of the TTW (TTW1, Wn) was already equipped with a new tri-band horn. The south tower (TTW2, Ws) was prepared for mounting a broadband feed (Elevenfeed), which is build by Omnisys, Sweden. The Elevenfeed is expected for 2014. The TTW started its operational test phase in April 2013 and the first operational test sessions were performed in August 2013 by the north tower (Neidhardt *et al.*, 2014). The Field system version 9.11.5 was installed at the TTW, which already provided the new satellite tracking SNAP-commands described in Sec. 4.2.3.1).

In addition to the three VLBI radio antennas two ILRS laser ranging system for SLR (the WLRS and the SOS-W), several IGS GNSS permanent stations, a large laser gyroscope (ringlaser G) and super conducting gravimeters are also operated at the GOW in combination with the required local techniques, such as atomic clocks for precise timing, meteorological sensors, etc.

4.2 Implementation of continuous satellite tracking

At Wettzell, satellites can be tracked continuously with all three antennas during observations, using the satellite tracking capabilities of the recently implemented Antenna Control Units (ACU) from the company Vertex Antennentechnik GmbH. First, the ACU tracking function is described in

[1] $12°/sec$ in azimuth and $6°/sec$ in elevation, compared to $4°/sec$ in azimuth and $1.5°/sec$ in elevation at the RTW.

general in Sec. 4.2.1, followed by a detailed description of Wettzell's satellite tracking procedure in Sec. 4.2.2.

4.2.1 Two-Line Track mode

All three VLBI radio antennas in Wettzell, the RTW and the Twin Telescopes, are equipped with similar Antenna Control Units (ACU), providing various tracking capabilities. Beside different tracking functions used to track space objects, such as quasars at the celestial rate, there is one mode offering the possibility to track satellites using TLE data, called Two-Line track mode.

A recent TLE dataset for the satellite, which should be tracked, is converted to a specific format, according to the ACU interface specification, on the station computer where the Field System runs. To start the Two-Line Track mode the prepared data are sent over the remote control interface to the ACU, where the satellite orbit is determined using the dedicated SGP4 propagation model (see Sec. 2.3.3). The ACU calculates an internal stack of antenna positions in terms of azimuth and elevation angles. These support points are calculated 2 seconds into the future (10 datasets with an interval of $\Delta t = 0.2s$) and stored on the stack with a capacity of 3000 sets of values. These calculations also require the correct time and the geographic position oft the antenna. To ensure a smooth tracking and antenna motion, the ACU applies additionally a cubic spline interpolation between the individual position samples in the stack and calculates the target velocity using the path gradient of the spline. Additionally, the next points of arise of sight (AOS) and loss of sight (LOS) of the currently tracked satellite are determined by the ACU. If the satellite is still below the local horizon at the time the Two-Line Track is started, i.e. it is not visible from the current location, the antenna moves to the next AOS position and waits there until the next overpass begins (Vertex, 2013).

Using the Two-Line Track mode provided by the Vertex ACU has the advantage, that the antenna movement is precisely adjusted to the internally predicted satellite movement, without the detour of calculating discrete satellite positions in the Field System.

4.2.2 Satellite tracking workflow

The satellite tracking workflow, which was implemented at the radio antennas at Wettzell, is illustrated in Fig. 4.2.

The starting point is a satellite observation schedule in the form of a *VEX* file, generated with the VieVS satellite scheduling module, described in Sec. 3.2. In such VEX files, which implement a stepwise tracking approach (see Sec. 2.5.1), the sources are defined as sequences of discrete topocentric right ascension/declination positions. *DRUDG*'ing a VEX file, issued by VieVS, generates a SNAP file (SNP_s), implementing a stepwise track by defining each satellite scan as a sequence of SNAP commands ($source = \langle source\_name \rangle, \langle Ra \rangle, \langle Dec \rangle, \langle epoch \rangle$), which point the antenna to the specified celestial positions. To enable the continuous tracking, a pearl script (*SNAP-file converter*) was written to convert these SNAP files by replacing the SNAP-command sequence for a stepwise antenna positioning (*source=...*) with a single SNAP command for satellite

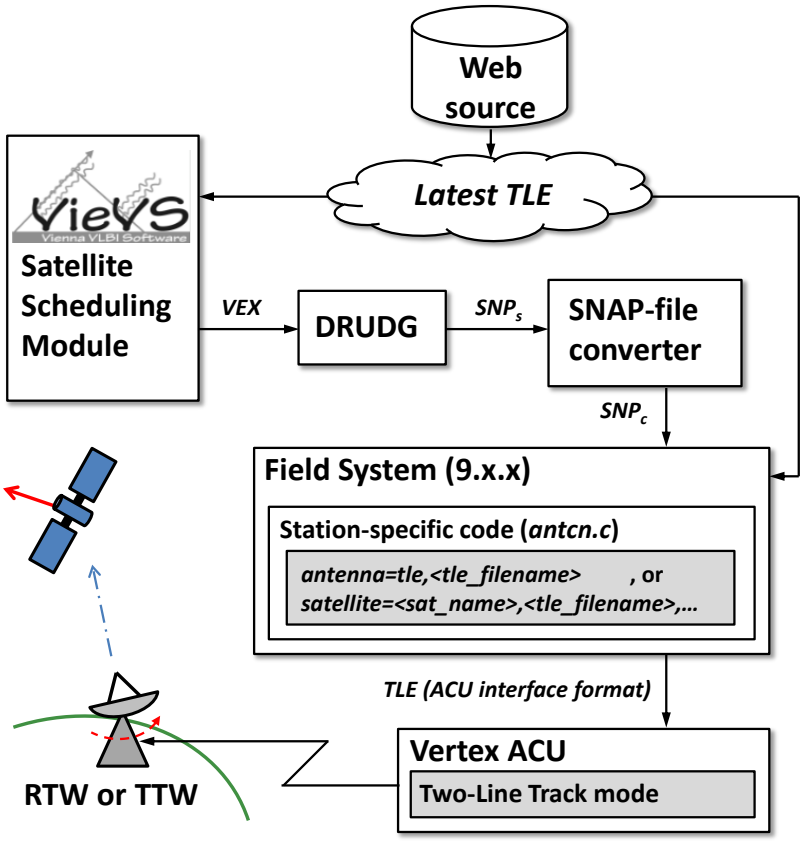

Figure 4.2: Satellite tracking workflow at Wettzell for the RTW and TTW. The latest TLE datasets are obtained from a web service prior to an experiment to be used by VieVS for generating the global observation schedules (*VEX*) and by the Field System to guide the antenna during the observations. A Perl script (*SNAP-file converter*) is used to convert the SNAP files intended for stepwise tracking (SNP$_s$) to enable a continuous tracking (SNP$_c$) with the new Field System functions in combination with the Two-Line Track mode of the Vertex ACU of the TTW or RTW.

tracking per satellite (for details see Sec. 4.2.4).

Two different Field System versions were installed at the RTW (version 9.10.4) respectively at the TTW (version 9.11.4) during our experiments between late 2013 and early 2014. At the TTW the newer FS version already provided a dedicated satellite SNAP-command ($satellite = \langle satellite\_name \rangle, \langle tle\_filename \rangle, \langle mode \rangle, \langle wrap \rangle$), while at the RTW a new SNAP command for satellite tracking ($antenna = tle, \langle tle\_filename \rangle$) had to be integrated into the station specific code of the Field System. The necessary modifications in the Field System to activate the already existing FS satellite tracking capabilities at the TTW, and to integrate the new SNAP command at the older FS version for the RTW, are described in the Sections 4.2.3.1 and 4.2.3.2.

Basically both, the "*satellite*" and the "*antenna=tle*" command, read the referred TLE dataset either from the shared memory of the FS ("*satellite*" command) or from a separate TLE file ("*antenna=tle*" command). Then they convert the TLE dataset to a specific *ACU interface format* and send them to the ACU via a remote control interface. There, a stack of tracking points is calculated and the mode is switched to Two-Line Track, as described in Sec. 4.2.1.

4.2.3 Field system modifications

4.2.3.1 Twin Telescope Wettzell (TTW)

The Field System version 9.11.4, installed at the TTW, provides the SNAP command $satellite = \langle satellite\_name \rangle, \langle tle\_filename \rangle, \langle mode \rangle, \langle wrap \rangle$ for satellite tracking (Himwich & Gipson, 2012), as described in Sec. 2.5.2. To provide the necessary orbit information a data file named "*tle_filename*", containing the current TLE datasets for all satellites, which should be tracked during a session, has to be stored in a specified directory on the FS computer. This file is read automatically when the satellite SNAP-command is executed by the FS and its content is available over the FS shared memory then.

In the original FS distribution only the entry point to the command selection (code skeleton) for the new satellite SNAP-command was provided in the antenna control program (antcn.c, see Sec. 2.2). Furthermore, additional functions that calculate a stack of topocentric satellite positions after the SNAP command execution, are provided. The topocentric satellite positions are computed on the basis of SGP4 orbit models (see Sec. 2.3.3) in an one second interval and stored on the stack in terms of azimuth/elevation values. This satellite position stack is then provided over the shared memory for the purpose of controlling the antenna. The actual communication between the FS and the ACU of the antenna had to be coded in the station-specific code during this work. Because the Two-Line Track mode provided by the ACU should be used for satellite tracking, the FS internally calculated stack with satellite position was not required. The calculation of the antenna pointing data was directly carried out by the ACU working in the Two-Line Track mode, as described in Sec. 4.2.1. To start tracking, only the TLE dataset of the satellite referred to by the parameter "*satellite_name*" of the satellite SNAP-command has to be forwarded to the ACU. On that account, a function was programmed and added to the station-specific part of the FS, that parses the TLE data provided in the FS shared memory as required and sends it to the ACU via the remote control interface, which switches to the Two-Line Track mode immediately.

4.2.3.2 Radio Telescope Wettzell (RTW)

At the RTW, the older FS version 9.10.4 was installed, which still does not provide the FS inherent satellite tracking capabilities, as used at the TTW (Sec. 4.2.3.1). Nevertheless, the RTW has an ACU identical to that of the TTW, capable to track satellites in the Two-Line Track mode (see Sec. 4.2.1).

On that account, a new code module ("*simple_tle_reader.cpp*") was prepared to read in TLE files from a local directory on the FS computer. Each of these local TLE files has to contain one TLE dataset for a particular satellite. Furthermore, a new SNAP command, $antenna = tle, \langle tle\_filename \rangle$, was added to the antenna control program of the FS *antcn.c* (see Sec. 2.2). On execution, the content of the local TLE file specified in the parameter "*tle_filename*" is loaded, using the *simple_tle_reader* module. The TLE data are formatted according to the ACU interface specifications and transferred to the ACU over the provided remote control interface. Then, the

ACU switches to the Two-Line track mode and starts tracking of the satellite, specified in the loaded TLE file.

4.2.4 Conversion of local control files

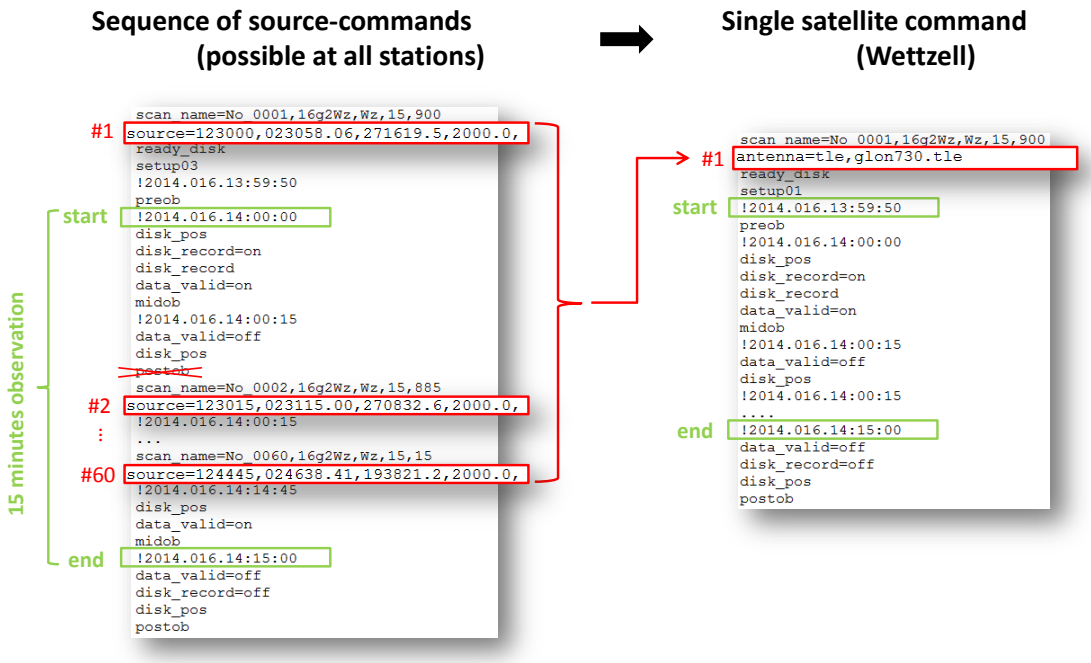

Figure 4.3: Illustration of the SNAP-file conversion scheme. The figure shows SNAP files of a scan on January 16, 2014, with 15 minutes duration, starting at 14 : 00 : 00 and ending at 14 : 15 : 00 UT. In the SNAP file, directly generated with DRUDG, using the VieVS satellite observation schedules (left side), each scan consists of numerous source commands (red), to realize a stepwise tracking (60 repositioning steps for this 15 minutes scan with $\Delta t = 15s$). After the conversion with a Perl script (right side), the sequence of 60 consecutive source commands is replaced by a single dedicated SNAP command to start the continuous satellite track (*antenna=tle,...*).

After adapting the FS code as describe above in Sec. 4.2.3, dedicated SNAP commands to track satellites were available for both FS versions, used for the antennas at the GOW.

The next task was, how to include these newly integrated SNAP commands to the local control files (SNAP files) generated with DRUDG on the basis of the VieVS satellite schedules, because these commands were not supported by the current DRUDG version. The provisional solution was to modify ("convert") the SNAP files after creating them with DRUDG with a simple Perl scrip, the *SNAP-file converter*. The conversion scheme is outlined in Fig. 4.3. In the first step, the VEX file issued by the VieVS satellite scheduling module is DRUDG'ed. In the resulting SNAP file (left side) each satellite scan (green) consists of a sequence of sub-scans containing a SNAP command (source=..., red boxes) to reposition the antenna in defined time intervals. SNAP files in this fashion could now be used directly to carry out a stepwise satellite tracking with the standard IVS station equipment. In a second step, the original SNAP file is modified, using the SNAP-file

converter script. This software replaces the source commands by a single “satellite=...” SNAP command at the beginning of the track, which starts the continuous track at the right time. In the case of the RTW with the older FS version, the included command was “*antenna=tle,...*”, as discussed in Sec. 4.2.3.2.

Although this approach was envisaged as a provisional solution until a new DRUDG version supporting satellite SNAP-commands is released, the conversion tool has its advantages. The SNAP commands used for satellite tracking may differ between different VLBI stations, because of specific local implementations of satellite tracking features. Hence, such a conversion script could be very flexible, because it is able to include arbitrary SNAP commands to the control files.

Chapter 5

Satellite observation experiments

To validate the proper functionality of the recently developed VieVS satellite scheduling module (Chapter 3) and the new satellite tracking features at Wettzell (Chapter 4),which allow to follow a satellite continuously, real satellite observation experiments were carried out in January 2014. Observations of L1 signals of several GLONASS satellites were planned and carried out on the baseline Wettzell-Onsala.

5.1 Station network

All observations were carried out on the Baseline Onsala (Sweden) - Wettzell (Germany). The observing antennas are depicted on Fig. 5.1.

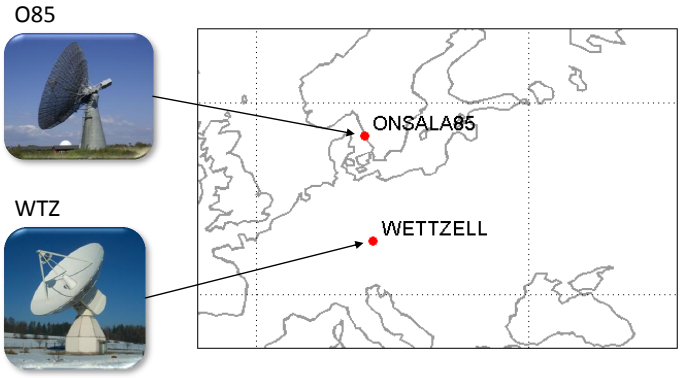

Figure 5.1: VLBI station network for the sessions G140116a, G140116b, G140121a and G140121b: The 20m telescope in Wettzell (WTZ, Germany) and the 25m telescope in Onsala (O85, Sweden).

Wettzell. In Wettzell (WTZ) the 20m Radio Telescope Wettzell (RTW) was used.

The existing S/X receiver system was extended, in order to be able to receive GNSS L1 signals[1],

[1]The GPS L1 signal is transmitted at 1575.42MHz and the GLONASS satellites transmit L1 signals in the band from 1592MHz to 1609MHz.

which are well below the lowest S-band frequency (Kodet *et al.*, 2014 and Kodet *et al.*, 2013). The RTW is equipped with a classical IVS-compatible S/X receiver system, designed to observe in the S- and X-band domain, as common in the geodetic VLBI. A simplified block diagram is shown in Fig 5.2. The incoming signal first passes through the antenna dish with the feed horn and the waveguides, where it is split up into an S- and an X-band signal path. The Low Noise Amplifiers (*LNA*), coolded down to $20K$ in a cryo-box to keep the noise level low, amplify the signal before it is bandpass filtered (*BP*) and frequency-shifted with the receiver mixers to the Intermediate Frequency (*IF*) domain. Concerning the possibility to receive L1 GNSS signals, the waveguide of the X-band receiver does not allow to route these signals, due to its dimensions; whereas over the S-band waveguide (cut-off frequency of $1.375GHz$) L1 transmission is still possible. Nevertheless, because of the unmatched frequency and waveguide combination in the S-band chain, the L1 signals are attenuated by approximately $60dB$ by the S-band feed chain (Kodet *et al.*, 2014). Therefore, the power level of typical GNSS signals is already about $30dB$ below the noise floor at the input of the LNA. This fact preludes the detection of GNSS signals with spectrum analyzers, as it would be possible with a separate L-band feed chain. The bottleneck of the complete S-band receiver chain for L1 signals is the bandpass filter after the LNA. In order to enable the reception of L1 GNSS signals, the main S-band receiver is bypassed by adding a power splitter (*PS*) behind the S-band LNA. One part of the signal is still used for the standard S-band receiver, while the other part is fed into the newly developed L1-band GNSS receiver, which is presented in terms of a block diagram in Fig. 5.3 (Kodet *et al.*, 2014). Splitting of the signal behind the LNA will not influence the standard VLBI observations since the system temperature is mainly defined by the noise temperature of the LNA. Hence, the acquisition of L1-band additionally to S/X-band is possible without changing the original receiver hardware. Another advantage is, that the phase calibration tones are also present in the L1 observations.

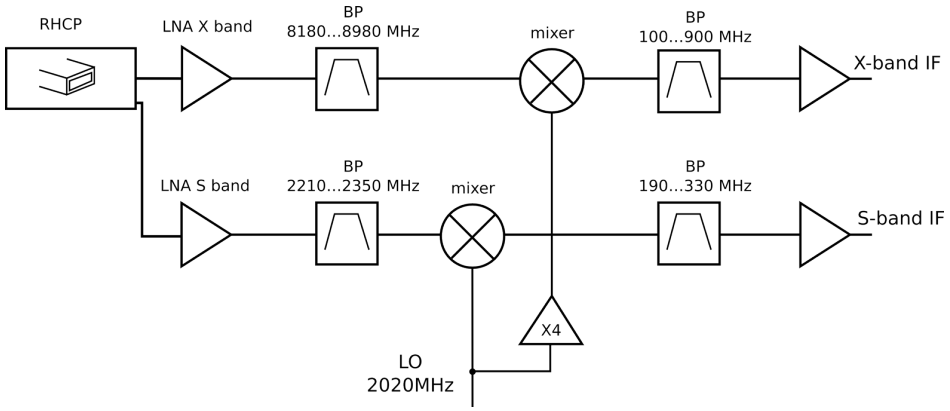

Figure 5.2: Simplified block diagram of the S/X IVS-compatible receiver of the $20m$ Radio Telescope Wettzell (from: Kodet *et al.*, 2014).

In the first experiment (G140116a), the antenna was guided applying a stepwise satellite tracking approach (see Sec. 2.5.1) directly controlled by the unaltered VEX files generated with the VieVS satellite scheduling module. This was done to test, if the scheduling is principally

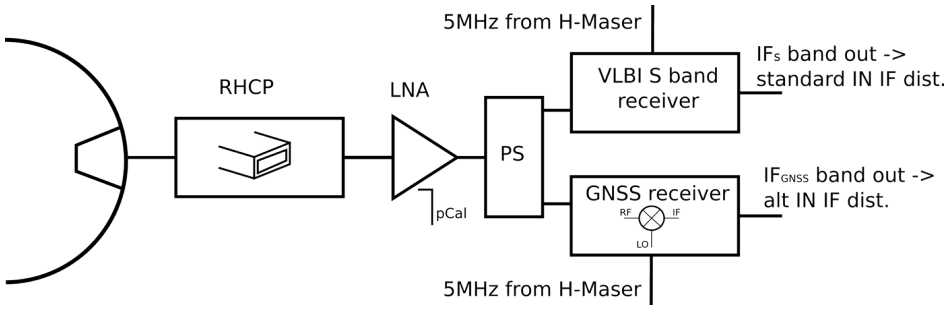

Figure 5.3: Block diagram showing the L1 GNSS receiver upgrade for the S/X receiver of the 20*m* Radio Telescope Wettzell (from: Kodet *et al.*, 2014).

functional. The antenna repositioning interval was 15 seconds. For the following three sessions (G140116b, G140121a, G140121b), the satellites were tracked continuously. During these experiments the most recent Field System version (9.11.2), which would have already provided dedicated satellite tracking capabilities, was not installed at the RTW. Therefore, the special implementations, described in Chapter 4, were necessary in order to track satellites continuously with the RTW.

Onsala. In Onsala the 25*m* radio telescope was used. As it was equipped with a dedicated L-band receiving system, the satellite signals had to be attenuated in the RF domain to avoid saturation of the receiver components. This was done by adding a 20*dB* attenuation module before the first session started. The L-band receiver qualifies to receive strong L1 signals, which are far above the noise level and, therefore, clearly visible in the IF domain with a spectrum analyzer. However, one drawback is, that an simultaneous acquisition of S/X-band signals is not possible without changing the receiver.

Because Onsala's SATTRACK module (Moya Espinosa & Haas, 2007) was not installed when the experiments were carried out, all satellites were tracked stepwise with a 15 second repositioning interval, directly controlled by the VEX schedule files.

5.2 Experiment Description

After several final tests at the station in Wettzell, where the antenna tracking functions were checked locally, two experiments were carried out on January 16, 2014 (G140116a, G140116b), respectively on January 21, 2014 (G140121a, G140121b) on the baseline Wettzell-Onsala. Each of these sessions had a duration of one hour and scheduled several GLONASS satellites consecutively. The PIs for the observations on-site during the experiments were Alexander Neidhardt[1] in Wettzell and Rüdiger Haas[2] in Onsala in close cooperation with the author.

We chose to observe satellites of the GLONASS constellation, because their L1 signals

[1]Forschungsgruppe Satellitengeodäsie, Technische Universität München, Geodetic Observatory Wettzell
[2]Chalmers University of Technology, Onsala Space Observatory

($1592MHz - 1609MHz$) are a bit closer to the S-band than the L1 signals of GPS satellites ($1575.42MHz$). Hence, signal attenuation due to the S-band feed-chain in Wettzell should be less with the GLONASS L1 signals. The duration was limited to one hour for each session. In order to avoid wasting too much time on the antenna repositioning between different sources, i.e. to keep the slew times in a low range, satellites with a relative short angular separation from one another were selected. This was especially important since the slew speeds of the HaDec-mounted axes (see Sec. 2.6.2) of the $25m$ telescope in Onsala were very low with only $17.6°/min$ about the equatorial axes and $14.7°/min$ about the declination axes. Hence, the antenna needs approximately 20 minutes for one full rotation in the azimuth (according to personal communication with Rüdiger Haas). Since the primary goal of these observations was to test the new tracking features in Wettzell and the scheduling with VieVS, no natural sources for calibration purposes were observed, as it was done in several previous experiments (e.g. Tornatore *et al.*, 2014).

The observation planning and further the creation of the schedule files in the VEX format were performed with the new VieVS satellite scheduling module (see Sec. 3.2). Appx. B.1 shows the auxiliary data (skyplots, elevation plots and listings of the available observation periods) generated by the VieVS module during the corresponding scheduling tasks. A listing that summarizes the observation schedules for all four sessions, showing the related observation periods for each selected GLONASS satellite and the emitted carrier frequency, can be found in Table 5.1.

All four sessions were carried out using the same receiver setup. Four IF channels with $8MHz$ bandwidth were observed with the center frequency set to the corresponding L1 carrier frequency emitted by the observed satellite, as listed in Table 5.1. This means, that the data recording was redundant, recording the same signal with all four IF channels simultaneously. In principle it would be sufficient to record the narrow-band GLONASS signals (L1 bandwidth is $\approx 1MHZ$) only with one IF channel with an adequate bandwidth.

Although four IF channels were recorded at Wettzell, only two of them contained GLONASS signals. Only two of four channels connected to the L1-band GNSS receiver could be allocated to the appropriate IF sub-band (HI sub-band at IF1, $216MHZ$ to $504MHz$) at the according IF distributor in the control room, because of hardware limitations. The GLONASS signals (centered at $\approx 400MHZ$ in the IF domain) were outside the recorded frequency band at the other two channels (LO sub-band at IF1, $96MHZ$ to $224MHz$) and had to be suppressed. Nevertheless, no data was lost, because all four recorded IF channels initially contained the same GLONASS signals. Hence, this recording configuration had no negative impact on the observation results.

At Onsala the observed GLONASS signals were lost at the last two scans (7 and 8) of the G140121a session, because the receiver setting was re-adjusted incorrectly by accident in the control room during the experiment. The recorded IF spectra of the corresponding scans are shown in Fig. B.21 and Fig. B.22 in the Appendix confirm the signal loss.

Table 5.1: Satellite observation schedules for the sessions on the 16^{th} and 21^{st} January 2014.

Session	Scan period [UTC]	Satellite name	NORAD ID	L1 carrier frequ. [MHz]
		16^{th} Jan. 2014		
G140116a	12:30 - 12:45	GLONASS-743	37869	1605.3750
	12:50 - 13:05	GLONASS-723	32395	1602.0000
	13:10 - 13:30	GLONASS-730	36111	1602.5625
G140116b	14:00 - 14:15	GLONASS-730	36111	1602.5625
	14:20 - 14:35	GLONASS-737	37138	1601.4375
	14:40 - 15:00	GLONASS-747	39155	1599.7500
		21^{st} Jan. 2014		
G140121a	13:30 - 13:35	GLONASS-743	37869	1605.3750
	13:37 - 13:43	GLONASS-732	36402	1603.6875
	13:44 - 13:49	GLONASS-743	37869	1605.3750
	13:51 - 13:56	GLONASS-732	36402	1603.6875
	13:59 - 14:04	GLONASS-743	37869	1605.3750
	14:08 - 14:13	GLONASS-735	36401	1603.1250
	14:14 - 14:19	GLONASS-735	36401	1603.1250
	14:25 - 14:30	GLONASS-732	36402	1603.6875
G140121b	15:00 - 15:04	GLONASS-735	36401	1603.1250
	15:05 - 15:09	GLONASS-735	36401	1603.1250
	15:10 - 15:14	GLONASS-735	36401	1603.1250
	15:20 - 15:24	GLONASS-746	37938	1604.2500
	15:25 - 15:29	GLONASS-746	37938	1604.2500
	15:30 - 15:34	GLONASS-746	37938	1604.2500
	15:45 - 15:49	GLONASS-723	32395	1602.0000
	15:50 - 15:54	GLONASS-723	32395	1602.0000
	15:55 - 16:00	GLONASS-723	32395	1602.0000

5.3 Observation results

As a first indicator to proof whether the satellites were tracked correctly in Onsala, the received signals were investigated with a spectrum analyzer directly at the Intermediate Frequency (IF) output of the recorder system. During all observations the signal spectra of the GLONASS satellites were clearly visible, indicating that the antenna was tracking correctly[1]. The received power spectrum of GLONASS-743 is shown exemplarily in Fig. 5.4 for the G140116a session. Due to the very high power level of the GLONASS signals (between $-13dBm$ and $-6dBm$, measured at the

[1] In Appx. B.2 plots of the received satellite signal spectra are shown – one plot per scan.

IF output) the input amplifiers overdrove, resulting in non-linear distortions in the acquired signal spectra, as clearly evident in the corresponding figure[1]. To avoid receiver saturation and signal corruption an additional $20dB$ attenuation module was installed in the RF signal path for the upcoming sessions on January 21^{st} (G140121a and G140121a), resulting in a total RF attenuation of $40dB$. Considering the received spectrum of GLONASS-743 during the 21g1 session, shown in Fig. 5.5, apparently the saturation effect has disappeared. The spectra were now symmetrical to the peak, without showing any saturation effects.

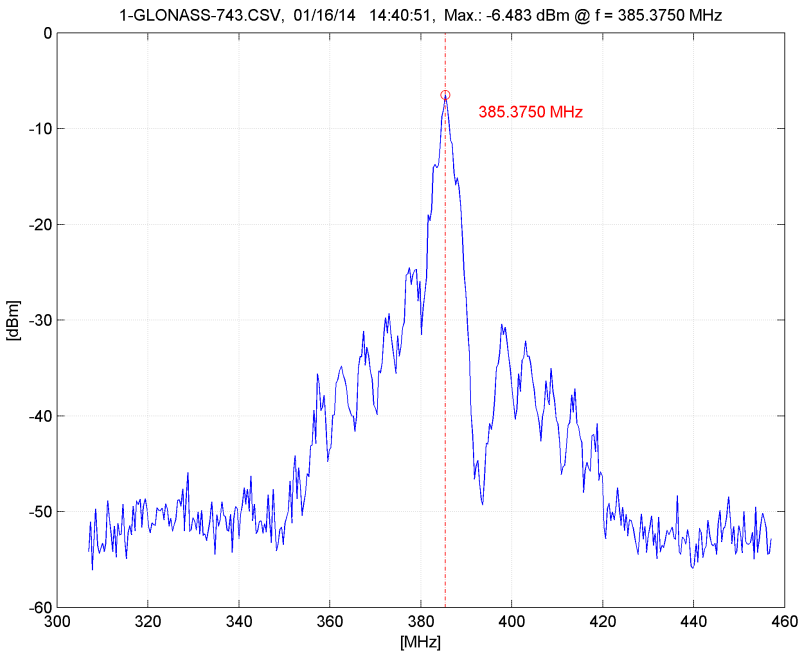

Figure 5.4: IF spectrum of the satellite GLONASS-743 recorded in Onsala during the G140116a session at $12:40:51$ UT on January 16, 2014. Due to the high power level of the received signal the receiver electronics were saturated, resulting in non-linear signal distortions (unsymmetrical to the peak), as evident in the shown diagram.

Using the new L1-band GNSS receiver at Wettzell, the GLONASS signals were strongly attenuated due to the hardware restrictions discussed in Sec. 5.1. Hence, it was not possible to visualize and examine the signals directly in the IF domain with a standard spectrum analyzer as done in Onsala, because they were below the noise floor. Another way had to be found to check, whether the VLBI antenna is detecting the satellite or not. On that account J. Kodet prepared a MATLAB software, which is able to correlate weak GNSS signals in the recorded VLBI data (Kodet *et al.*, 2014). The software implements GNSS signal acquisition based on cross-correlation between the recorded data and an artificially generated GNSS (GPS or GLONASS) ranging code. This is done by a parallel code phase search algorithm for the GPS or GLONASS satellite signals, where the

[1] According to personal communication with Rüdiger Haas.

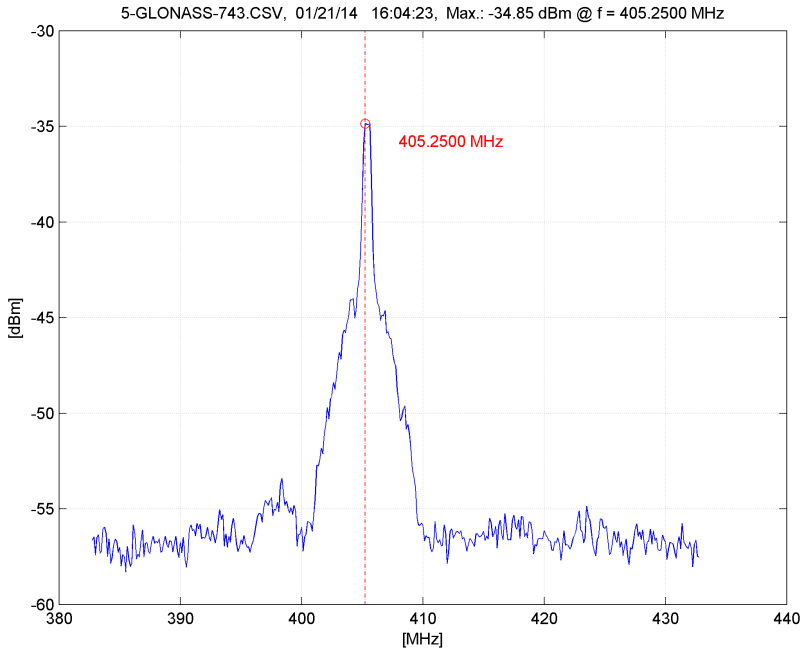

Figure 5.5: IF spectrum of the satellite GLONASS-743 recorded in Onsala during the G140121a session at $14:03:23$ UT on January 21, 2014. After increasing the added RF signal attenuation from $20dB$ to $40dB$ the receiver saturation effects vanished.

sensitivity was improved by coherent and non-coherent integration (for further information see Bao-Yen Tsui, 2005). Furthermore, this MATLAB software is able to calculate the carrier-to-noise ratio (C/N_0) and to calculate the system noise temperature. Having such a tool available to examine the recorded data almost in real-time was important to get a quick feedback after the actual observations, which played a major role for process optimization at Wettzell.

The correlation result for GLONASS-743, acquired during the 21g1 session (see Fig. 5.6), exemplarily shows a strong peak, indicating successful tracking and signal acquisition.

Finally, a preliminary analysis was carried out by Rüdiger Haas with the acquired data from both stations. The DiFX software (Deller *et al.*, 2007) was used to correlate the data with an integration time of 0.25 seconds. The correlation results were fringe-fitted with the Astronomical Image Processing System Software (AIPS; Greisen, 2014). The resulting fringe plot for the observation of GLONASS-732 during the G140121a session is exemplarily shown in Fig. 5.7. According to Rüdiger Haas continuous phases and strong amplitudes could be found for all satellite observations[1]. This indicates that the described concepts for scheduling and satellite tracking, and also the data acquisition, worked correctly at both stations.

[1]Except of the 7^{th} and 8^{th} scan of G140121a, where the signal was lost at Onsala due to unintended manual interaction during the observation.

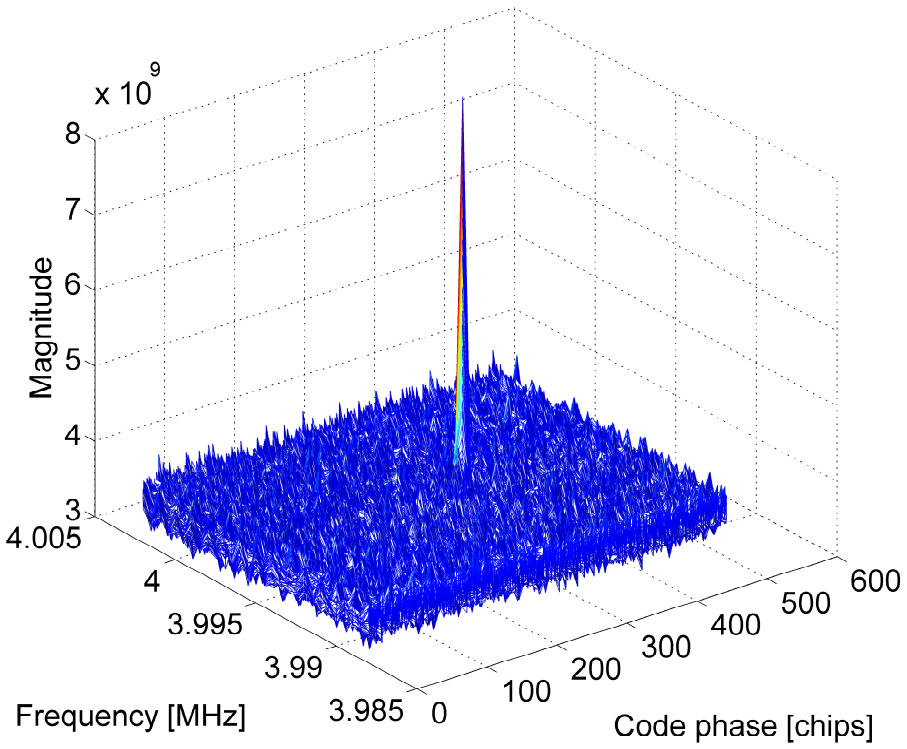

Figure 5.6: Signal acquisition of GLONASS-743 by a cross-correlation with an artificial ranging code. The data was acquired during the session G140121a in Wettzell. The correlation peak in the diagram indicates the existence of the GLONASS signal in the recorded data.

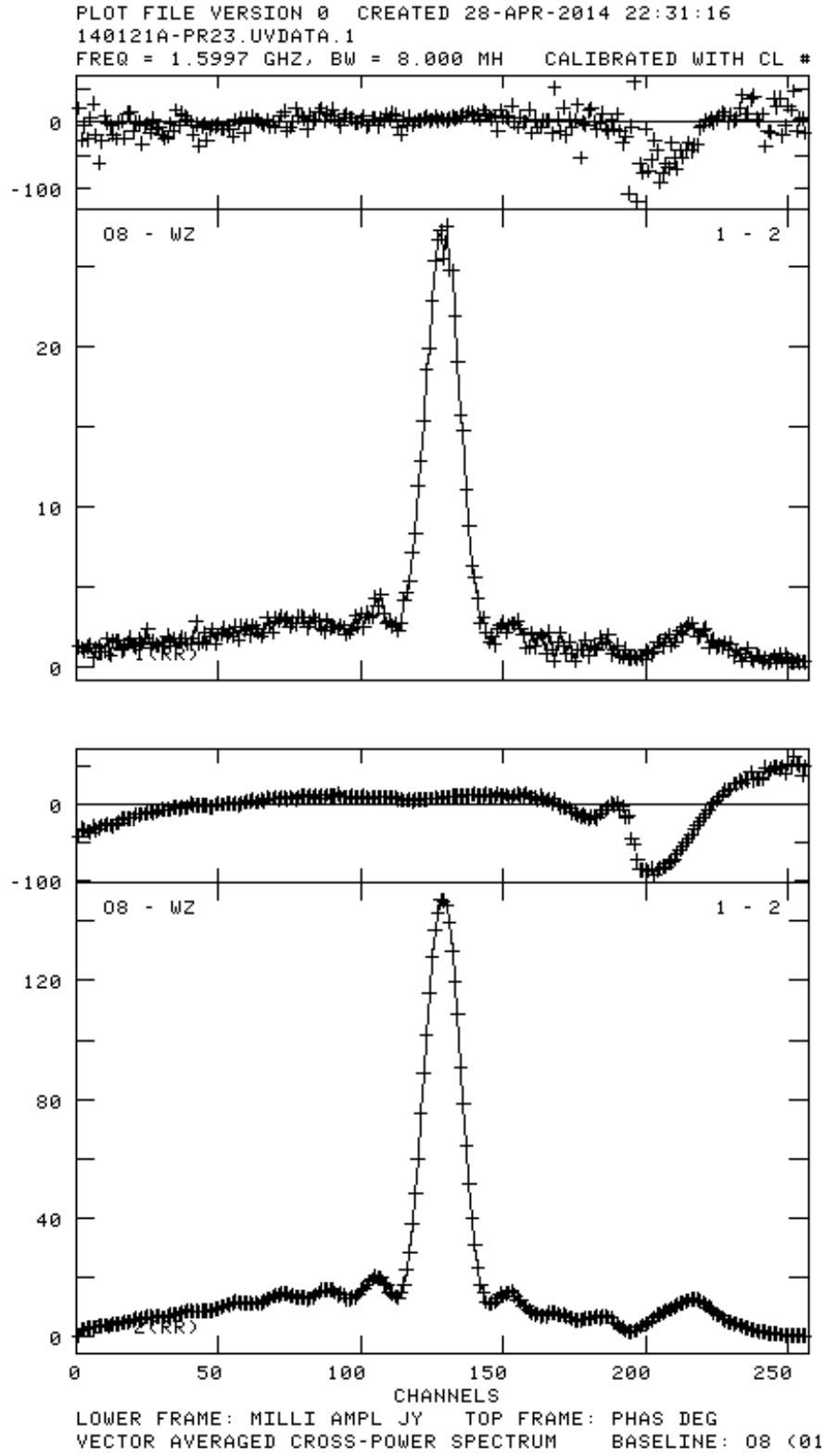

Figure 5.7: Fringe plot of GLONASS-732. The data was acquired during the G140121a session (2^{nd} scan). After correlation with DiFX (Deller *et al.*, 2007) the result was fringe fitted with AIPS (Greisen, 2014).

Chapter 6

Summary, conclusion and outlook

6.1 Summary

The aim of this thesis was to investigate options for an operational path to implement satellite observations with VLBI antennas. On that account, the whole process chain – from observation scheduling, over satellite tracking, to actual data acquisition – had to be considered. To manage this in a structured manner, it seemed convenient to split the task into the three basic sub-topics, summarized in the following paragraphs:

1. VieVS satellite scheduling module. A software tool for scheduling satellite observations with VLBI antennas had to be prepared. Therefore, VieVS was equipped with a new satellite scheduling module. The software leads the user through the whole scheduling process. Initially it calculates positions of all selected satellites on the basis of widely available TLE data and checks, if they have shared visibility from the selected station network for the chosen date and time. After checking of further conditions, e.g. observation restrictions due to limited antenna slew rates, a list of observable satellites is presented and the user is asked to assemble a sequence of sources to set up a complete observation schedule. Finally, VEX files are generated containing all required data to run the scheduled observations. Due to the inadequate satellite support of the current VEX format, the satellites are still defined as stepwise stationary sources, in terms of sequences of topocentric right ascension and declination.

2. Continuous satellite tracking at Wettzell. Using the VEX files, generated with VieVS directly, satellites can be tracked by consecutively repositioning of the radio antennas per defined time interval, virtually stepwise. To be able to follow the satellites continuously over the sky, special satellite tracking features have to be implemented at the VLBI antennas, as it was done at Wettzell. There are three VLBI radio antennas at the Geodetic Observatory Wettzell: the $20m$ Radio Telescope Wettzell (RTW) and the two $13.2m$ antennas of the Twin Telescope (TTW). After a hardware update in 2013 each of them is equipped with an identical Antenna Control Unit (ACU), being able to operate in a Two-Line Track mode, capable to process TLE data directly for satellite

tracking purposes. This ACU inherent tracking mode has the advantage, that the antenna movement is precisely adjusted to the internally calculated satellite movement, without the detour of calculating discrete satellite positions in an external software, resp. in the Field System (FS). This tracking mode was activated by adding additional functions to the station-specific part of the FS, which allows to start the Two-Line Track via a remote control interface by executing a dedicated SNAP command in the FS. Although, the new SNAP command for satellite tracking, provided by the official FS releases since version 9.11.2, could be activated for the TTW, they could not be used for the RTW, because an older FS version (9.10.4) was installed. For that reason a new satellite SNAP command had to be implemented there, doing the same.

3. Satellite tracking experiments. To validate the proper functionality of the newly implemented tracking features at Wettzell and the VieVS satellite scheduling module, several VLBI satellite experiments were scheduled in January 2014. Altogether four sessions with a duration of one hour for each session were carried out on the baseline Onsala-Wettzell, observing L1 signals of GLONASS satellites. At Wettzell all observations were done with the RTW, equipped with a recently developed GNSS receiver module, that enables L1 band signal acquisition with the existing IVS receiver system, additionally to the S- and X-bands. In Onsala the $25m$ antenna was used in combination with a dedicated L-band front end receiver. All sessions were run controlled with VEX files generated with the VieVS satellite scheduling module developed in this work. The satellites were tracked in a continuous fashion at Wettzell by means of the newly added tracking features and satellite snap commands, and stepwise at Onsala. The program DRUDG is used prior to a VLBI session at the stations to prepare the locally required information from the provided schedule files (VEX) and to create station specific control files, containing SNAP-command sequences that control all processes during an automatized experiment. Because DRUG is still not able to add the new SNAP commands for satellite tracking to the local control files, they had to be modified using a Perl script to add the required commands. Finally, a preliminary data analysis in terms of cross-correlating the recorded data showed, that during all experiments the GLONASS signals were acquired successfully, indicating that all developments worked properly.

Although, successful observations have been carried out, there are still some general limitations for observations of satellite signals with the VLBI antennas of the IVS network, emerging due to the specific characteristics of the observed signals. IVS-compatible antennas are usually equipped with S/X-band receivers, limiting the number of potential satellites to be observed drastically. Only a very small number of satellites transmit signals in those bands, e.g. some remote sensing satellites in LEO orbits. To be able to observe GNSS signals in the L-band for instance, as we did here, suitable receivers have to be installed, capable of handling the new frequency bands. Broadband receivers as proposed for future VLBI antennas in the context of the VLBI2010 campaign may give more opportunities related to the selection of observable satellites. Also the signal strength of satellite signals has to be considered, because they are usually several magnitudes stronger than natural radio signals from quasars. If the power level of the received radio

waves is too high, this causes signal corruption due to saturation effects in the receiver electronics, as it happened at the sessions G140116a and G140116b in Onsala (see Sec. 5.3). Hence, care has to be taken to adjust the signal attenuation level carefully before observations.

Finally please note, that all the discussed implementations at the station level, such as tracking capabilities, have to be carried out according to the specific requirements of the particular VLBI antennas. In some cases, there is no overall solution available. For instance concerning the activation of the satellite tracking functions delivered with the current official FS releases. Also in this case, at least the communication between the FS and the ACU has to be set up, which is strictly antenna specific.

6.2 Conclusion and outlook

The VieVS satellite scheduling module provides a flexible tool for the scheduling of real VLBI satellite observations, even for large station networks and arbitrary satellites. The required orbit calculations are carried out using TLE data, which potentially limits the available selection of satellites. Practically this is not an issue, because of the wide and easy availability of this type of orbit data. Nevertheless, more severe limitations in the satellite selection occur due to the restricted capabilities of the radio antennas in handling the specific characteristics of satellite signals (frequency bands, flux density, etc.). The satellite scheduling tool generates VEX files capable of performing satellite tracking directly in a stepwise fashion. They can be directly applied at all IVS-compatible VLBI stations, without any modifications – neither in the local control procedure, nor at the station's tracking capabilities. For the future it would be important to extend the current VieVS module with further functionalities, such as the possibility to combine satellite observations with classical observations to quasars. Combined schedules would give the opportunity to use the quasars as calibration sources. Another topic for further research is the implementation of an automated source selection, based on a dedicated scheduling optimization approach. For precisely such research topics it is greatly important that we already have the possibility to carry out real satellite experiments in order to collect valuable data and to test the new developments.

According to the discussions in Sec. 2.4, the accuracy of tracking data calculated with NORAD TLE datasets and the appropriate SGP4 models can be basically considered to be largely sufficient in order to use them for tracking GNSS satellites. The situation could be different, if further pointing errors are introduced, e.g. due to inaccurate transformations between the used coordinate frames (ECI TEME to a topocentric system in general). If satellites are tracked stepwise in terms of discrete topocentric Ra/Dec positions, substantial point errors are added, due to the limited position update rate of the applied tracking approach and the Earth rotation adaption per se. Nevertheless, preceding practical experiments as well as our own applications showed, that tracking of GNSS satellites with the stepwise approach is already possible and delivers good results, if the

repositioning interval is chosen adequately. The situation may look different, if faster satellites on lower orbits should be tracked. For such cases, further investigations are recommended.

Tracking satellites continuously would circumvent these pointing issues related to the position update rate, but raises other difficulties. The difficulty is, that the standard IVS-procedure for geodetic VLBI sessions, does not consider satellites as radio sources in the whole process chain. As a consequence, VLBI radio antennas do not support any satellite tracking features routinely. Hence, further efforts are required to implement similar approaches, as we did in Wettzell. In Wettzell the ACU of all antennas already enable the Two-Line Track mode, to track satellites on the basis of TLE data. This tracking mode was activated in the FS and can now be started by executing the related SNAP command in the FS. The next requirement is that DRUDG, which is used to generate local control files containing SNAP commands to control the station equipment automatized during VLBI sessions, is currently not able to write these new satellite SNAP commands. Also the current file format used for the global schedule files (VEX 1.5b1) does not provide the possibility to define satellites as observation targets in an appropriate way in terms of TLE data. To be able to carry out satellite observations applying the newly implemented functions for continuous tracking in Wettzell, a provisional solution was found. Satellite orbits have been defined in terms of stepwise discrete positions in the VEX files. Later on the derived local control files were modified by an external script to add the required commands.

Altogether this means, that fully operational application and process automation of VLBI satellite observations, comparable to traditional geodetic VLBI observation of quasars, is presently restricted due to limitations in the schedule file format (VEX) and generation of local control files (SNAP files) with DRUDG.

The new VEX2 schedule file format was already proposed, including a transition plan to move from VEX1 to VEX2[1]. This new format will provide all required parameters to define satellite orbits directly in terms of TLE datasets. Also DRUDG has to be updated during the transition period to be able to handle the new file format and its functions. Consequently, the complete process chain would be ready to carry out VLBI satellite observations in a fully operational manner.

Based on several successful satellite observation experiments on the baseline Wettzell-Onsala in January 2014, two things could be validated: 1) the schedule files in the current VEX format prepared with VieVS were applied successfully to control the satellite observations and 2), satellite tracking with both approaches, stepwise and continuous, worked properly at the involved stations. Hence, we already have all tools available to carry out satellite observations with VLBI antennas, although some interim solutions have to be applied.

[1]For more information we refer to https://safe.nrao.edu/wiki/bin/view/VLBA/Vex2.

All the described developments related to satellite tracking and scheduling allow to conduct VLBI satellite observations in an easy and nearly operational manner. This is an important step to promoting further developments and research activities in the field of satellite observations with VLBI. Actual observation experiments are strongly required to investigate further important aspects. They are needed for investigations related to the satellite-antenna link budget, for examining signal characteristics, to test new correlation approaches for satellite signals, etc., and finally to investigate potential improvements of the frame ties between different space-geodetic techniques.

Appendix A

Coordinate systems

The content of this chapter is mainly taken from the according sections in the book *Fundamentals of Astrodynamics and Applications* from Vallado (2013).

A.1 Earth-based Coordinate systems

Earth-based coordinate systems are the basis for many operations and applications related to the observation of near Earth objects, such as Earth-orbiting satellites. The origin of Earth-based systems may be either the Earth's center (*geocentric*), or a site on the Earth's surface (*topocentric*).

A.1.1 Geocentric equatorial coordinate system

The fundamental plane of this system is the Earth's equator and the origin is located in the Earth's center (geocentric), as shown in Fig. A.1. The three orthogonal axes are designated with the letters IJK. The I axis points towards the vernal equinox (Υ), the J axis is 90° to the east in the equatorial plane and the K axis extends through the North Pole. This geocentric *IJK* frame is often used interchangeably with an *Earth-Centerd Inertial (ECI)* or *Coventional Inertial System (CSI)* nomenclature. Because the equinox and the equator move slightly over time, the term "inertial" can cause confusion. A "pseudo" Newtonian inertial system can be achieved by referring to the equator and equinox at a particular epoch, such as the standard epoch J2000.0 (Vallado, 2013).

A.1.1.1 ECI TEME frame

According to Vallado *et al.* (2006) and Vallado (2013) the Air Force Space Command (ASFC) analytical theory (SGP4) produces ephemerides in *a "true equator, mean equinox" (TEME)* system. Hence, this topic is particularly important for the treatment of the results of all orbit propagation applications done in the context of this work.

The intent of TEME was to provide an efficient, although approximate, coordinate system for the ASFC analytical theories. An exact operational definition of TEME is difficult to find in the

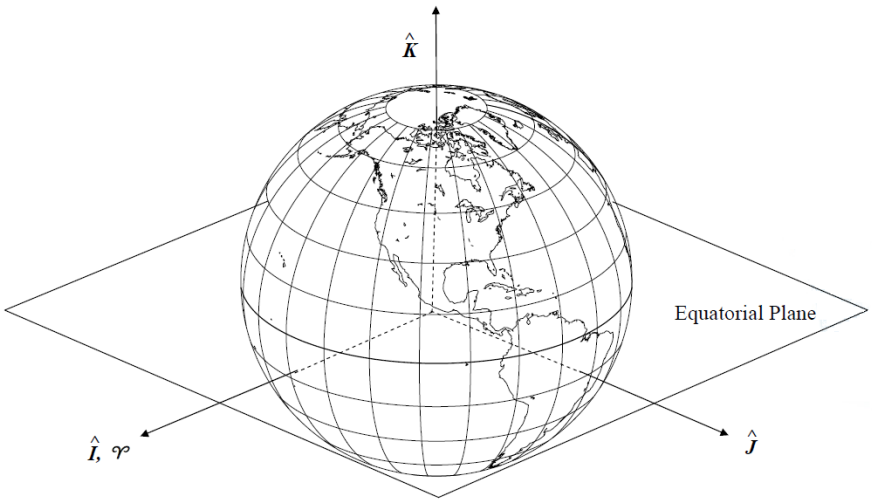

Figure A.1: Geocentric equatorial coordinate system, IJK. This sytem uses the Earth's equator, the vernal equinox (♈) and the Earth's rotation axis to define an orthogonal set of vectors, designated with the letters IJK (Vallado, 2013)

literature, but conceptually its primary direction is related to the "uniform equinox", described by Seidelmann (1992) on page 116. Technically, the direction of the uniform equinox resides along the true equator "between" the origin of the intermediate Pseudo Earth Fixed (PEF) and True of Date (TOD) frames (Vallado, 2013, pp. 236–240). Thus,

$$\vec{r}_{TOD} = ROT3(-Eq_{Equinox1982})\vec{r}_{TEME}, \tag{A.1}$$

$$\vec{r}_{PEF} = ROT3(\Theta_{GMST1982})\vec{r}_{TEME}. \tag{A.2}$$

Vallado (2013) recommends to convert TEME coordinates, derived by applying the analytical SGP4 model, to a truly standard coordinate frame before interfacing with external programs. For this purpose the preferred approach is to rotate to the PEF frame using the Greenwich Mean Sidereal Time ($\Theta_{GMST1982}$) by applying Equ. A.2, and then convert to other standard coordinate frames. For implementation simply a rotation about the Z-axis by $\Theta_{GMST1982}$ (Seidelmann, 1992, p. 162) is required (using UT1). Because the polar motion has been historically neglected for General Perturbation applications, it is assumed that the PEF frame is the closest conventional frame.

The rotation to the TOD frame is done by applying Equ. A.1, using the equation of equinoxes $\Theta_{GMST1982}$ (McCarthy, 1992b, p. 30). However, it is important to note that for the determination of $\Theta_{GMST1982}$ several approximations may be introduced with the calculation of the nutation of the longitude ($\Delta\psi$) and the obliquity of the ecliptic (ϵ). For details the author refers to Vallado (2013) p. 238.

There is an additional nuance, concerning the epoch of the TEME frame (Vallado, 2013, pp. 238–240), which has to be considered for frame conversions:

TEME of Date: The epoch of the TEME frame is always the same as the epoch of the associated ephemeris generation time. The transformation to an Earth Centered Earth Fixed (ECEF) frame is done by firstly applying the conversion from TEME to TOD with Equ. A.1, and secondly the standard IAU-76/FK5 transformation from TOD to ECEF. Another possibility is to directly convert TEME coordinates to the ITRF over the PEF frame by applying Equ. A.3 to A.5.

TEME of Epoch: The epoch of the TEME frame is held constant. Subsequent rotation matrices must therefore account for the change in precession and nutation from the epoch of the TEME frame to the epoch of the transformation. This is accomplished by finding a static transformation from TEME to J2000.0, including the equation of equinoxes, the nutation, and the precession – all calculated at the epoch of the TLE data. The J2000.0 vector can then be converted to other coordinate systems.

Vallado (2013) states that "Researchers generally believe the *of-date* option is correct, but confirmation from official sources is uncertain, and others infer that the *of-epoch* option is correct".

Transformation from TEME to ITRF over PEF. The transformation from the TEME frame to the ITRF over the PEF frame is outlined by Vallado *et al.* (2006). It is found by using the polar motion values (x_p, y_p) and the GMST. [1]

$$[W]_{ITRF-PEF} = ROT1(y_p)ROT2(x_p) \tag{A.3}$$

$$\vec{r}_{ITRF} = [W]^T \left[ROT3(\Theta_{GMST1982})\right]^T \vec{r}_{TEME} \tag{A.4}$$

$$\vec{v}_{ITRF} = [W]^T \left\{\left[ROT3(\Theta_{GMST1982})\right]^T \vec{r}_{TEME} + \vec{\omega_\oplus} \times \vec{r}_{ITRF}\right\} \tag{A.5}$$

Transformation from TEME to ECI J2000.0 over TOD. The conversion from TEME to the J2000.0 standard frame over the TOD frame is described by Vallado *et al.* (2006). It can be found by applying Equ. A.6. The values for the nutation ($[N]$) and precession ($[P]$) reductions are computed using the complete IAU-76/FK5 formulae (IERS Conventions, McCarthy, 1992a). Depending on whether the "TEME of epoch" or the "TEME of date" approach should be followed, all reductions have to be calculated for the time of the TLE epoch, and for the actual TLE propagation time respectively.

$$\vec{r}_{J2000} = [P][N]ROT3(-Eq_{Equinox1982})\vec{r}_{TEME} \tag{A.6}$$

[1] Note, that the PEF frame ("pseudo" Earth fixed) does not consider polar motion.

A.1.2 Topocentric horizon coordinate system

This system rotates with the site and is extensively used for satellite observations, because it provides the possibility to define *look angles*, in terms of azimuth (β) and elevation (*el*) to view a satellite from a ground station. The fundamental plane is formed by the local horizon and the origin is at the site on the Earth's surface, as shown in Fig. A.2. The S axis points towards south. The E axis points east and is undefined for the North and for the South Pole, while the Z axis (zenith) points radially outwards along the site's local vertical. The (north-)azimuth β is measured from north, clockwise to the location beneath the object of interest in the ES-plane, with a value range from 0° to 360°. The elevation angle *el* is measured from the ES-plane (local horizon), positive up to the object of interest with a value range of −90° to +90° (Vallado, 2013).

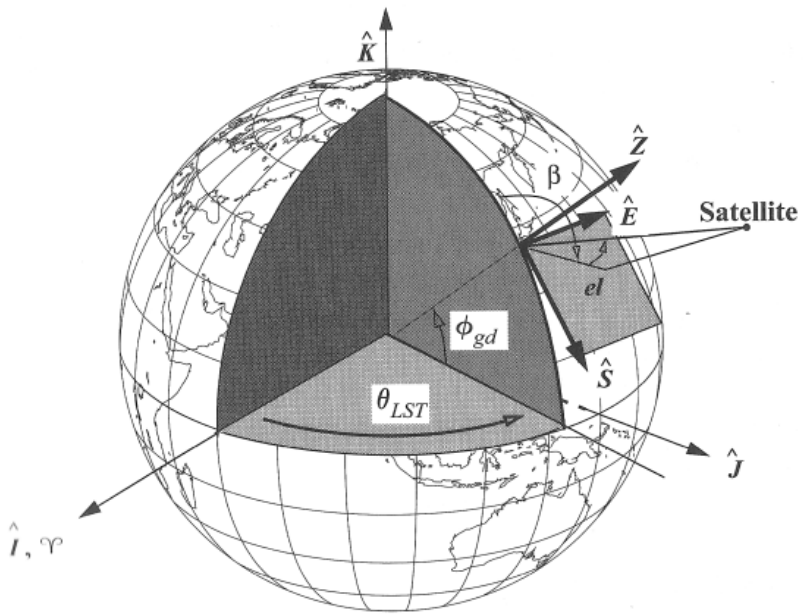

Figure A.2: Topocentric horizon coordinate system, SEZ. This system moves with the Earth and allows to define *look angles* in terms of azimuth β and elevation *el*, used for many observation applications. The Local Hour Angle Θ_{LST} is required to orient the SEZ system to a fixed location. Commonly, the geodetic latitude ϕ_{gd} is used, but the geocentric latitude is used in many systems too (Vallado, 2013)

.

A.1.3 Topocentric equatorial coordinate system

The topocentric equatorial system, denoted by the letters $I_tJ_tK_t$, is basically equal to the geocentric equatorial system, as described in Sec. A.1.1, with the origin translated from the Earth's center to the origin of the topocentric horizon system (see Sec. A.1.2). The orientation of the $I_tJ_tK_t$ axes is the same as the IJK system, only the origin differs. This system provides the possibility to determine positions of space objects in terms of topocentric right ascension (α_t) and declination (δ_t), as illustrated in Fig. A.3. At a first glance, the $I_tJ_tK_t$ system seems to be useless, because for stars the right ascension (α) and declination (δ) values are almost the same, even

when viewed from different places on the Earth's surface, due to the virtually infinite distance. However, satellite observations are performed in the topocentric equatorial system, where the direction to the target can be defined in terms of α_t and δ_t. If objects near to Earth, such as satellites, are observed, α and δ would differ between different observation locations (Vallado, 2013).

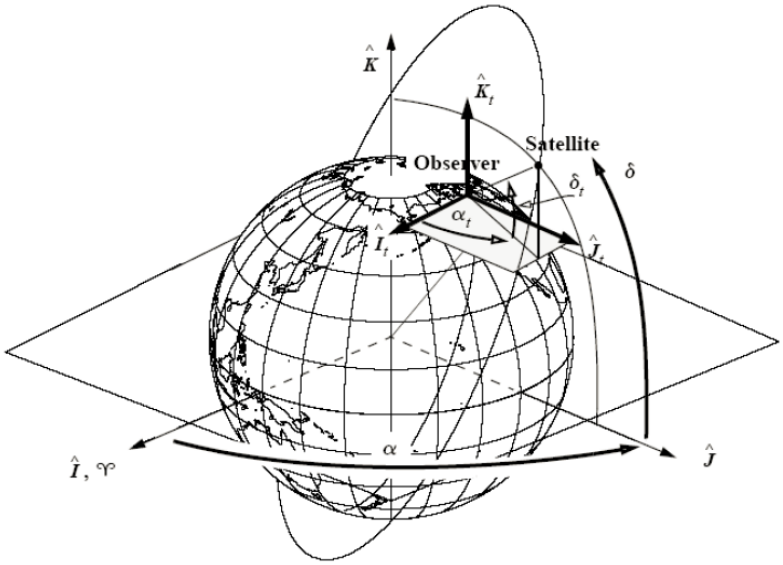

Figure A.3: Topocentric equatorial coordinate system, $I_tJ_tK_t$. This system uses the axes orientation oft the IJK system and the origin of the SEZ system. The origin rotates with the Earth, but maintains the fixed orientation (Vallado, 2013).

A.2 Satellite-based coordinate systems

Satellite based systems are based on the plane of a satellite's orbit. True anomaly and classical orbit elements are used to describe the location of objects (Vallado, 2013).

A.2.1 Satellite coordinate system

The satellite coordinate system, which moves with the satellite, is defined through an orthogonal axis triple, designated by the letters RSW, as shown in Fig. A.4. R always points from the Earth's center along the radius vector towards the satellite. The S axis points in the direction of the velocity vector $\vec{v}$ and is perpendicular to the radius vector. S is aligned with the velocity vector $\vec{v}$ only for circular orbits. W is normal to the orbit plane and completes the right-handed orthogonal system RSW.

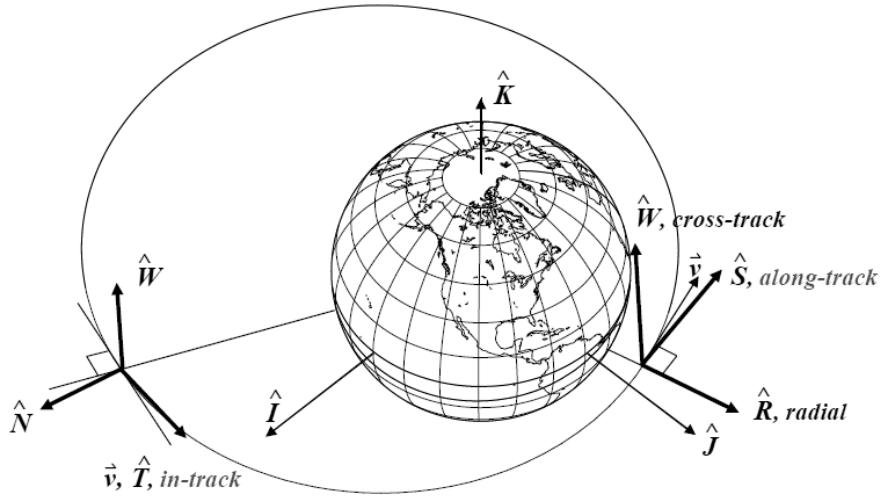

Figure A.4: Satellite coordinate system, RSW. The RSW system moves with the satellite. The R axis points in radial direction, W is normal to the orbit plane and S is orthogonal to the RW plane positive in the direction of the velocity vector $\vec{v}$ (Vallado, 2013).

Appendix B

Satellite observation experiments

This section contains a collection of Listings and Figures related to the satellite observation experiments (G140116a, G140116b, G140121a and G140121b) described in Sec. 5.

B.1 Auxiliary scheduling data generated with VieVS

Within this section the auxiliary scheduling data generated with the VieVS satellite scheduling module for the actual experiments are shown: elevation plots, skyplots and listings of the available observation periods.

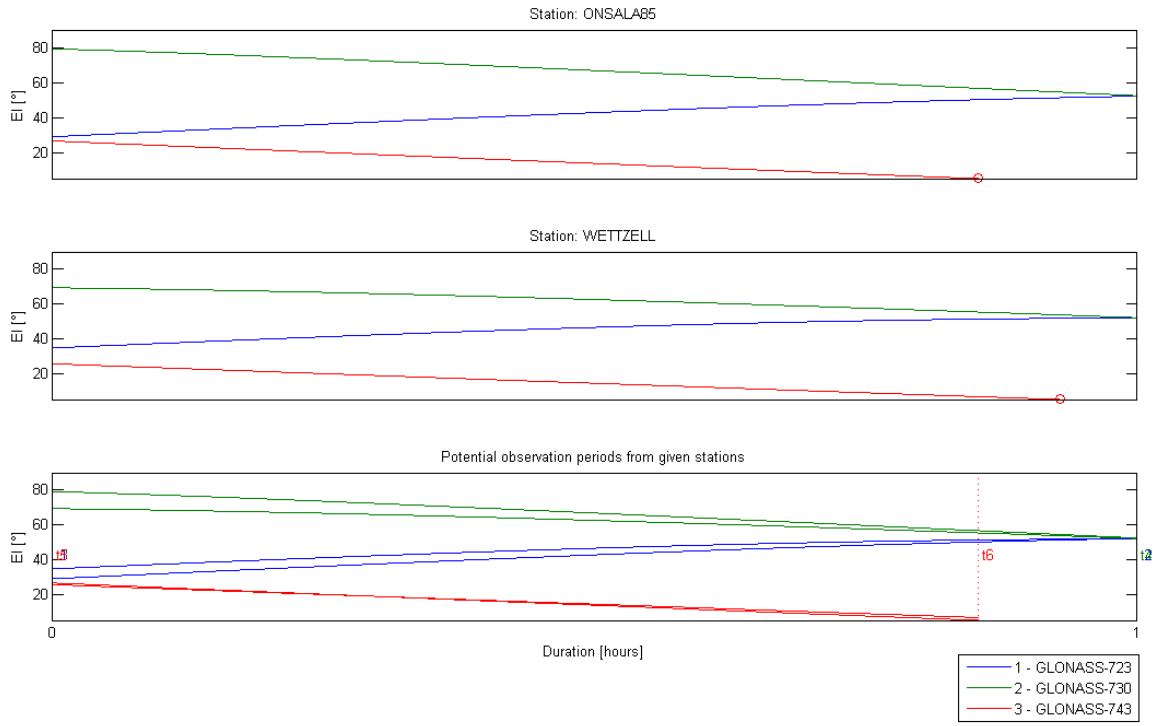

Figure B.1: Elevation plot for the session G140116a, from 12:30 to 13:30 UTC on the 16^{th} January 2014.

Listing B.1: Available observation times for the session G140116a.

```
1 - GLONASS-723
  t1 - 2014  1 16  12:30:00.00 (start)
  t2 - 2014  1 16  13:30:00.00 (end)

2 - GLONASS-730
  t3 - 2014  1 16  12:30:00.00 (start)
  t4 - 2014  1 16  13:30:00.00 (end)

3 - GLONASS-743
  t5 - 2014  1 16  12:30:00.00 (start)
  t6 - 2014  1 16  13:21:12.07 (end)
```

Listing B.2: Available observation times for the session G140116b.

```
1 - GLONASS-730
  t1 - 2014  1 16  14:00:00.00 (start)
  t2 - 2014  1 16  15:00:00.00 (end)

2 - GLONASS-737
  t3 - 2014  1 16  14:00:00.00 (start)
  t4 - 2014  1 16  15:00:00.00 (end)

3 - GLONASS-747
  t5 - 2014  1 16  14:00:00.00 (start)
  t6 - 2014  1 16  15:00:00.00 (end)
```

Listing B.3: Available observation times for the session G140121a.

```
1 - GLONASS-735
  t1 - 2014  1 21  13:30:00.00 (start)
  t2 - 2014  1 21  14:29:60.00 (end)

2 - GLONASS-732
  t3 - 2014  1 21  13:30:00.00 (start)
  t4 - 2014  1 21  14:29:60.00 (end)

3 - GLONASS-743
  t5 - 2014  1 21  13:30:00.00 (start)
  t6 - 2014  1 21  14:29:60.00 (end)
```

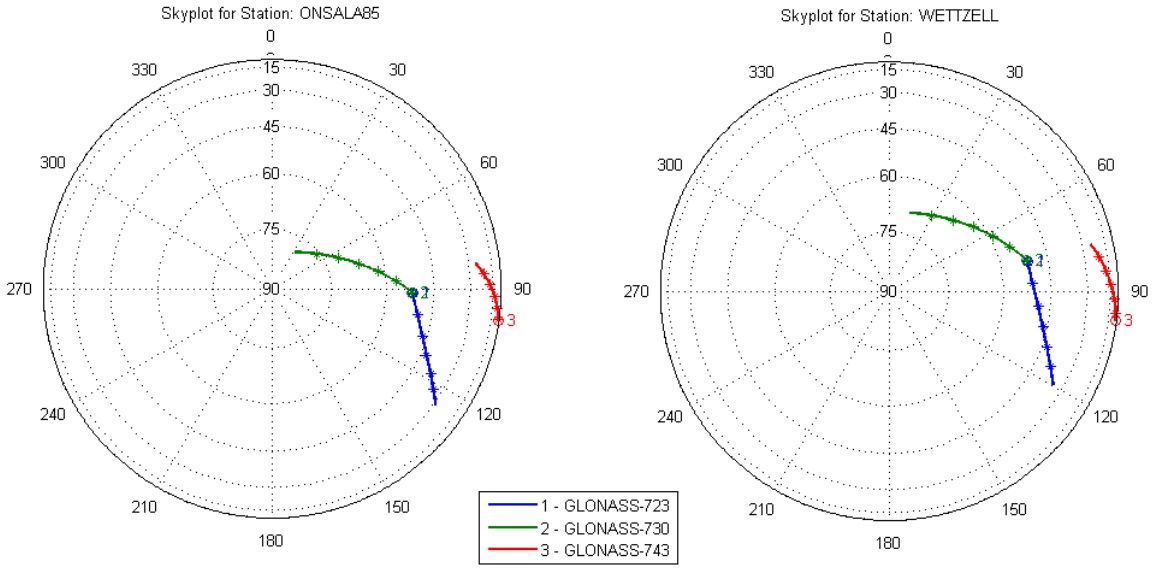

Figure B.2: Skyplots for the session G140116a, from 12:30 to 13:30 UTC on the 16^{th} January 2014. Plotted with $10min$ tick interval.

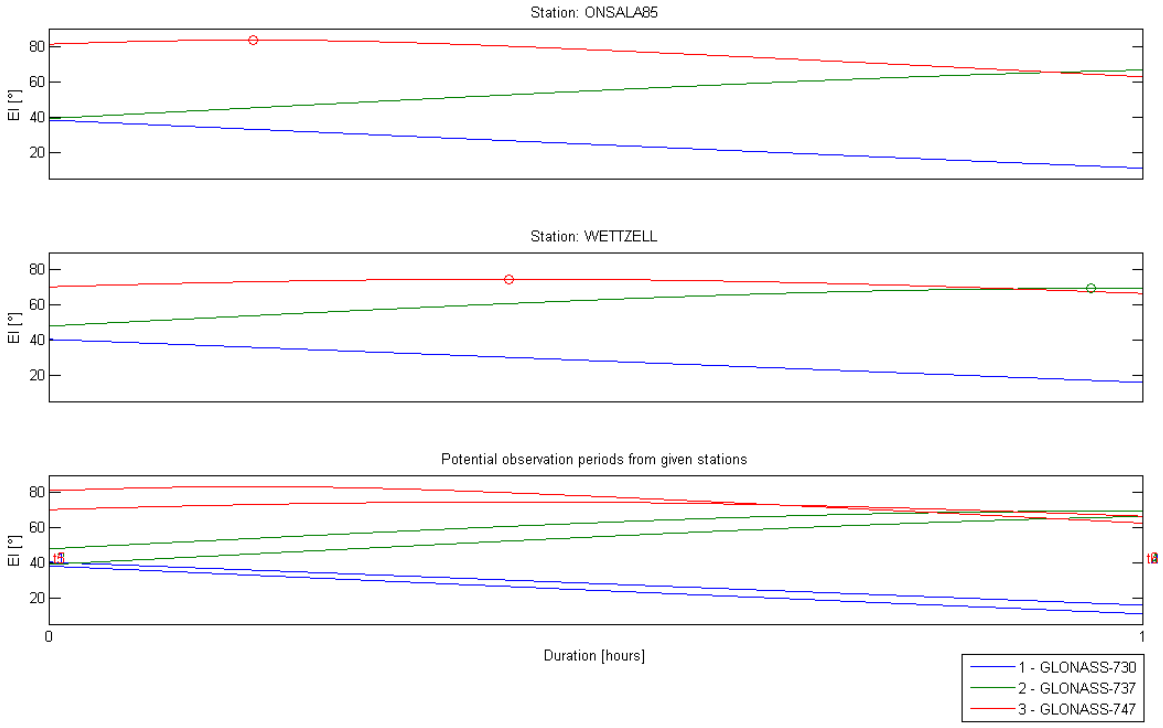

Figure B.3: Elevation plot for the session G140116b, from 14:00 to 15:00 UTC on the 16^{th} January 2014.

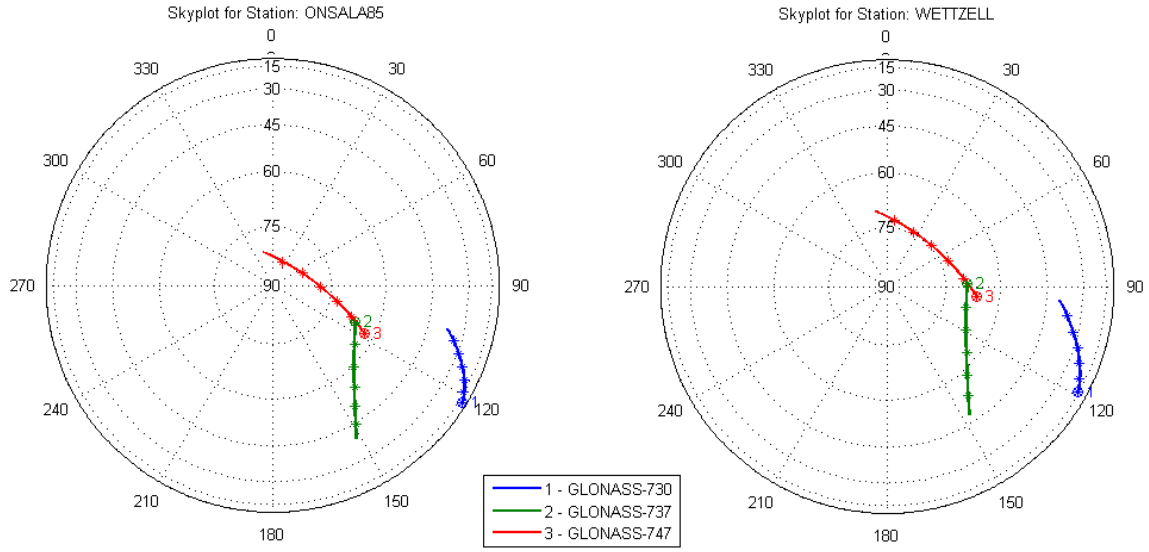

Figure B.4: Skyplots for the session G140116b, from 14:00 to 15:00 UTC on the 16^{th} January 2014. Plotted with $10min$ tick interval.

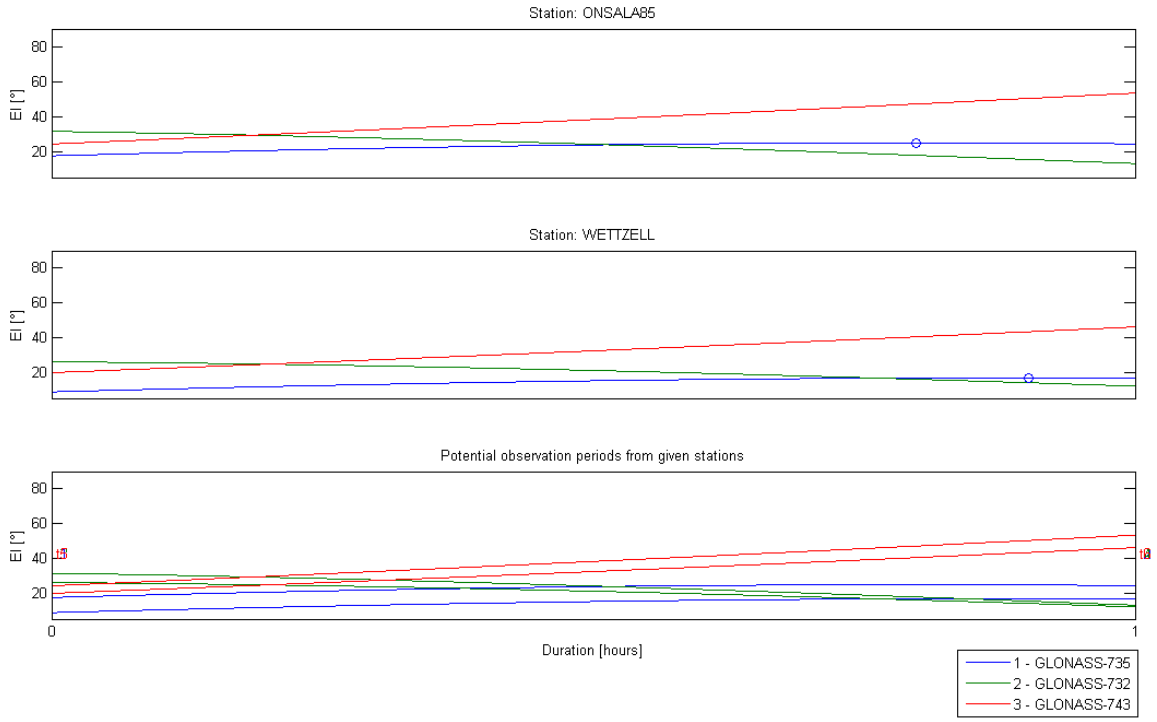

Figure B.5: Elevation plot for the session G140121a, from 13:30 to 14:30 UTC on the 21^{st} January 2014.

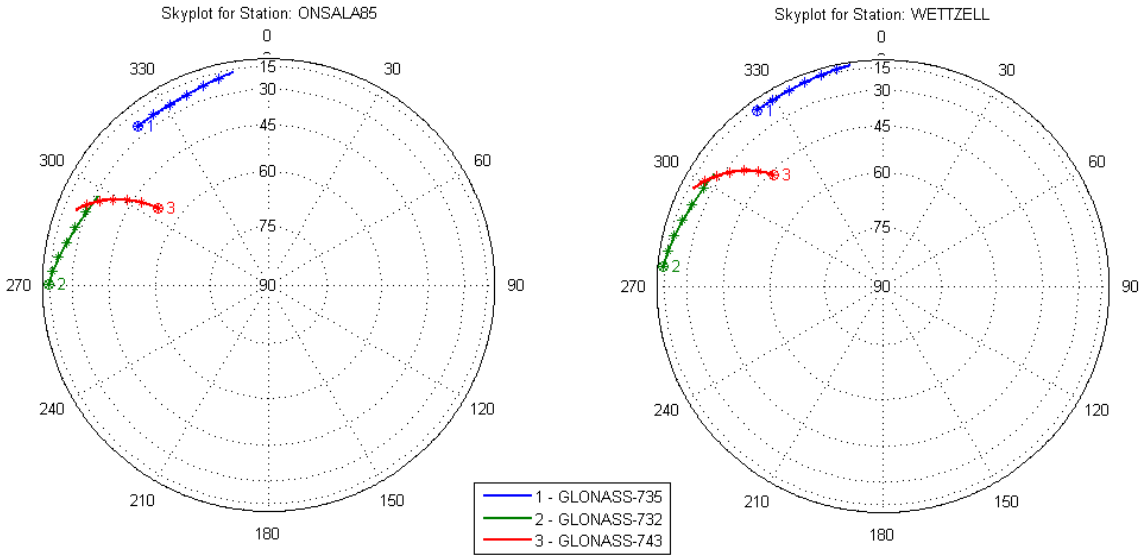

Figure B.6: Skyplots for the session G140121a, from 13:30 to 14:30 UTC on the 21^{st} January 2014. Plotted with $10min$ tick interval.

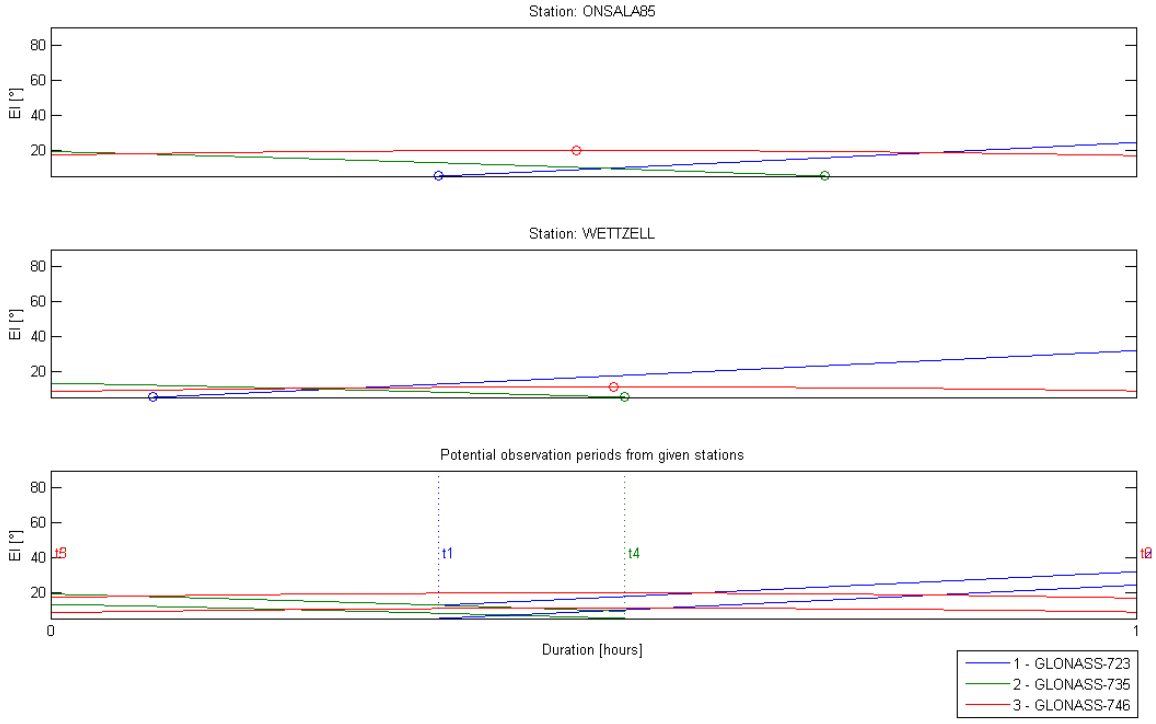

Figure B.7: Elevation plot for the session G140121b, from 15:00 to 16:00 UTC on the 21^{st} January 2014.

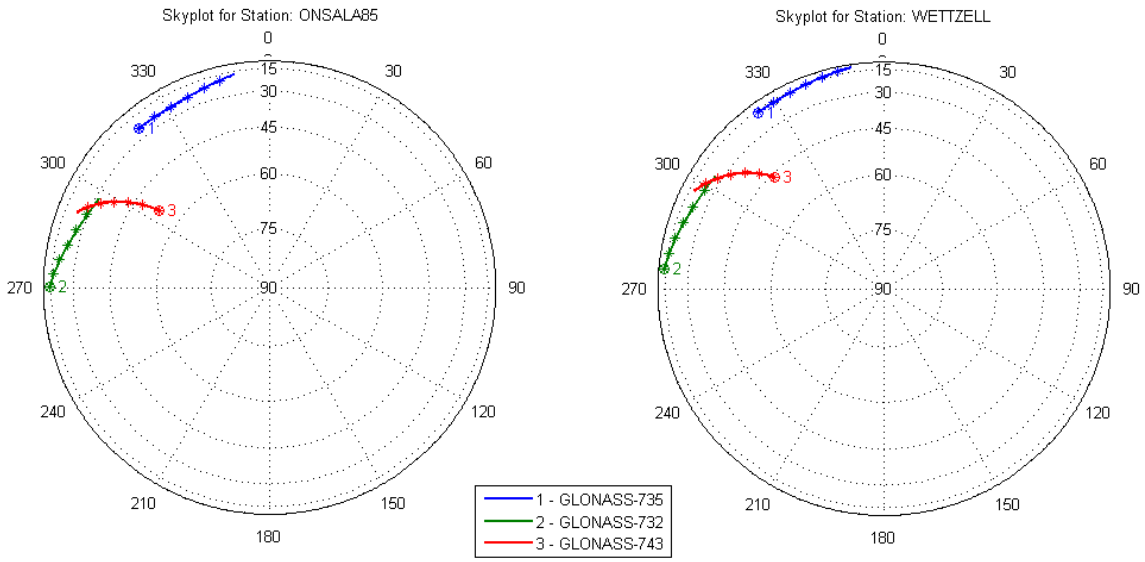

Figure B.8: Skyplots for the session G140121b, from 15:00 to 16:00 UTC on the 21^{st} January 2014. Plotted with $10min$ tick interval.

Listing B.4: Available observation times for the session G140121b.

```
1 - GLONASS-723
   t1 - 2014   1 21   15:21:27.88 (start)
   t2 - 2014   1 21   15:59:60.00 (end)

2 - GLONASS-735
   t3 - 2014   1 21   15:00:00.00 (start)
   t4 - 2014   1 21   15:31:44.16 (end)

3 - GLONASS-746
   t5 - 2014   1 21   15:00:00.00 (start)
   t6 - 2014   1 21   15:59:60.00 (end)
```

B.2 IF spectra acquired at Onsala

This section contains plots of IF spectra, acquired with a spectrum analyzer connected to the L-band IF channel during the observations in Onsala. The received spectra of the GLONASS satellite signals were recorded once per satellite scan using the spectrum analyzer. Please note, that the time designations at the IF spectrum plots are made in Central European Summer Time ($CEST = UTC + 2hours$).

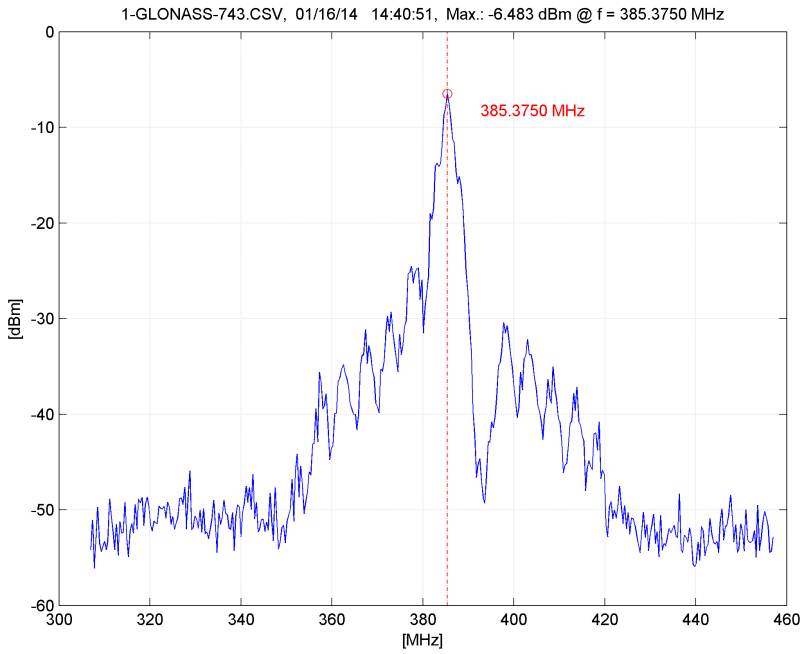

Figure B.9: Frequency spectrum of the satellite GLONASS-743 in the IF domain recorded in Onsala during the G140116a session (1^{st} scan).

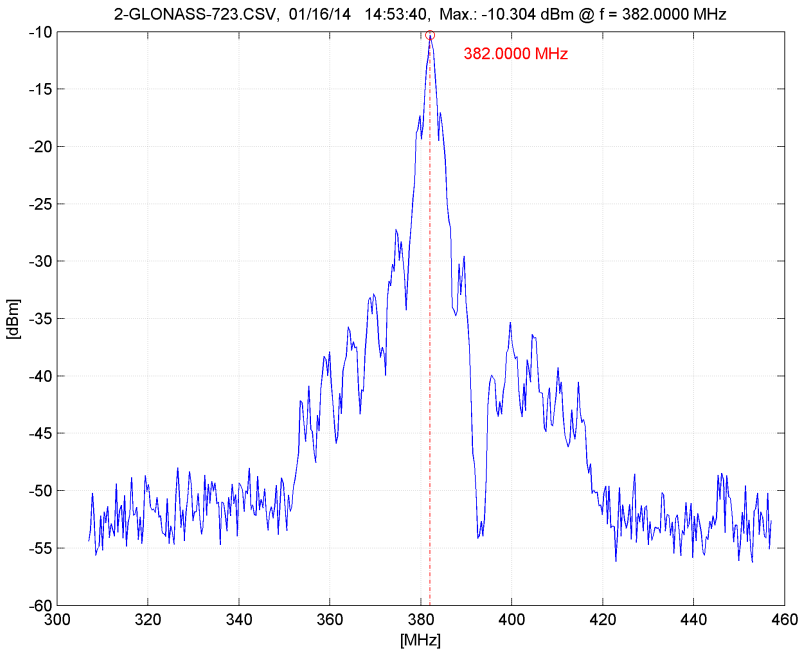

Figure B.10: Frequency spectrum of the satellite GLONASS-723 in the IF domain recorded in Onsala during the G140116a session (2^{nd} scan).

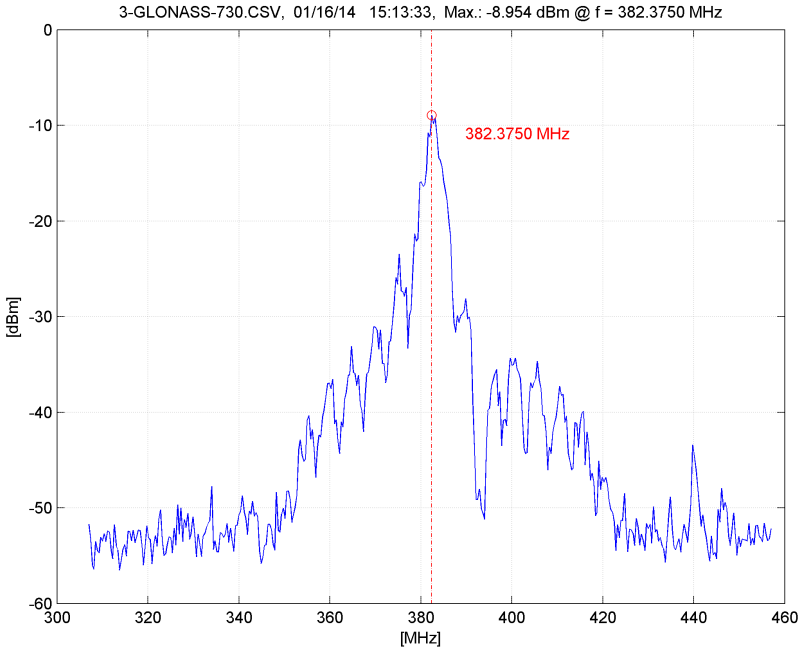

Figure B.11: Frequency spectrum of the satellite GLONASS-730 in the IF domain recorded in Onsala during the G140116a session (3^{rd} scan).

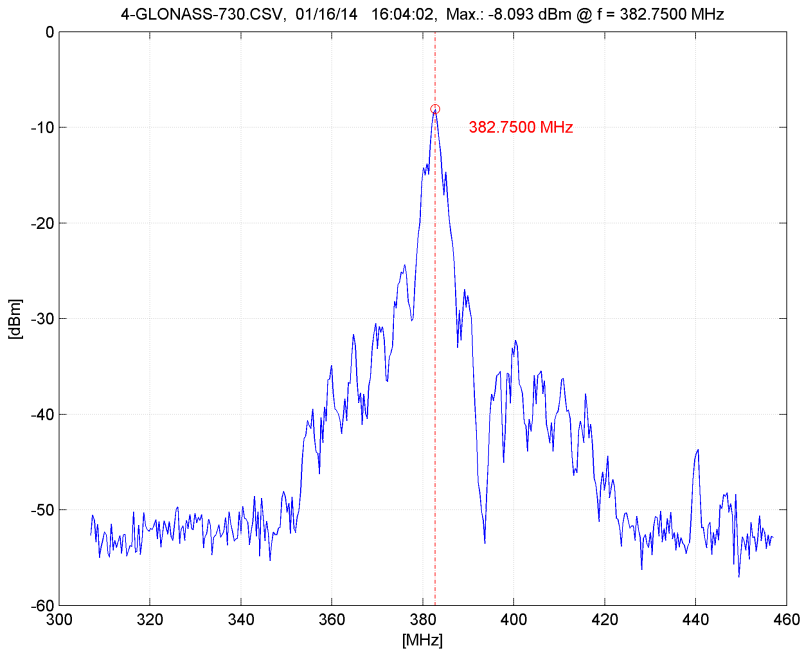

Figure B.12: Frequency spectrum of the satellite GLONASS-730 in the IF domain recorded in Onsala during the G140116b session (1^{st} scan).

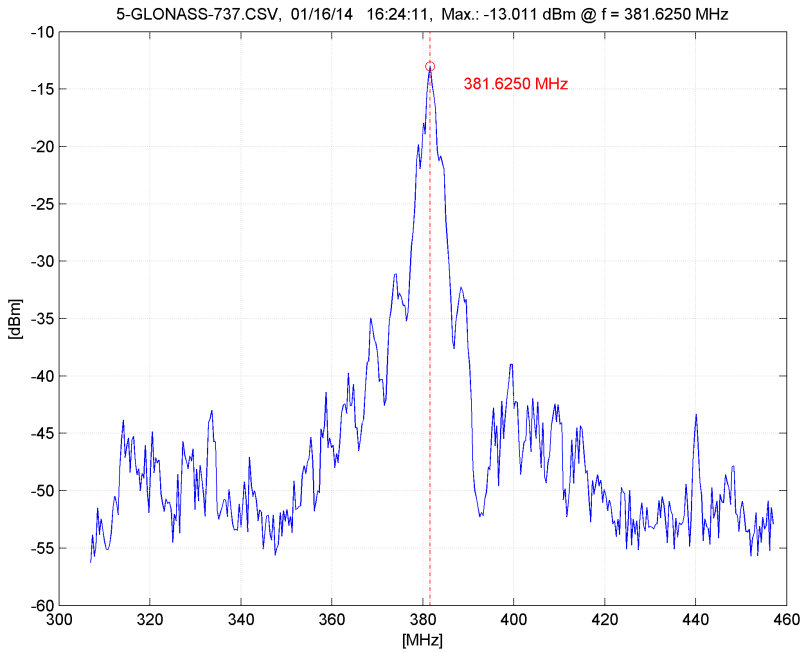

Figure B.13: Frequency spectrum of the satellite GLONASS-737 in the IF domain recorded in Onsala during the G140116b session (2^{nd} scan).

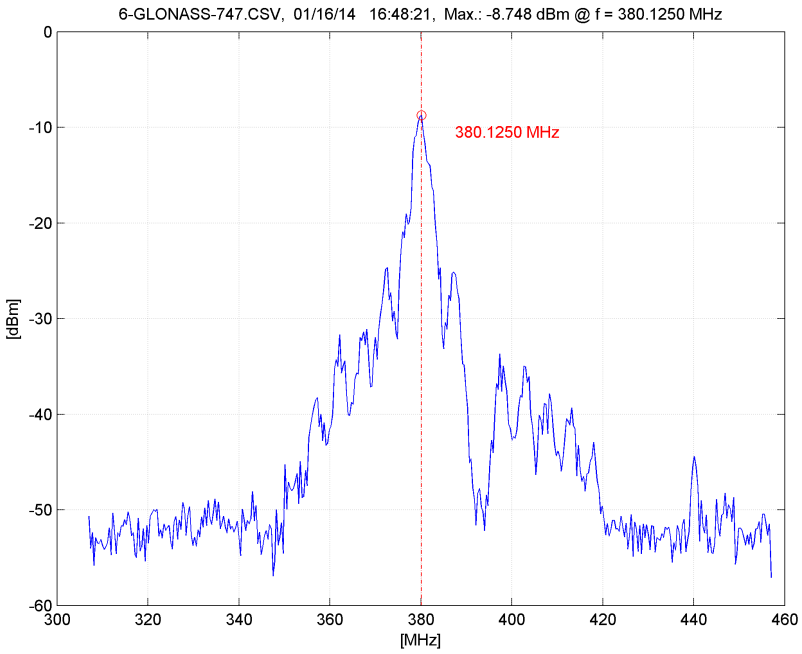

Figure B.14: Frequency spectrum of the satellite GLONASS-747 in the IF domain recorded in Onsala during the G140116b session (3^{rd} scan).

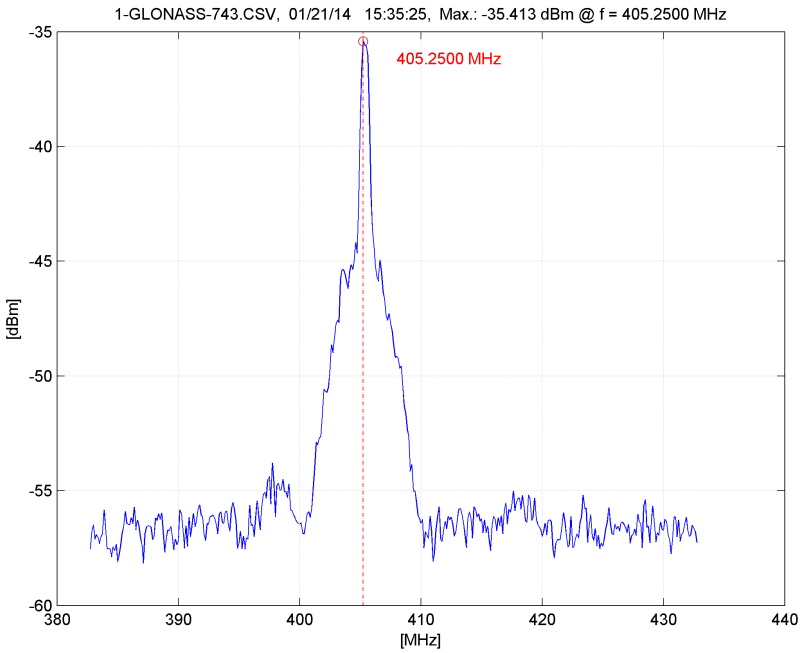

Figure B.15: Frequency spectrum of the satellite GLONASS-743 in the IF domain recorded in Onsala during the G140121a session (1^{st} scan).

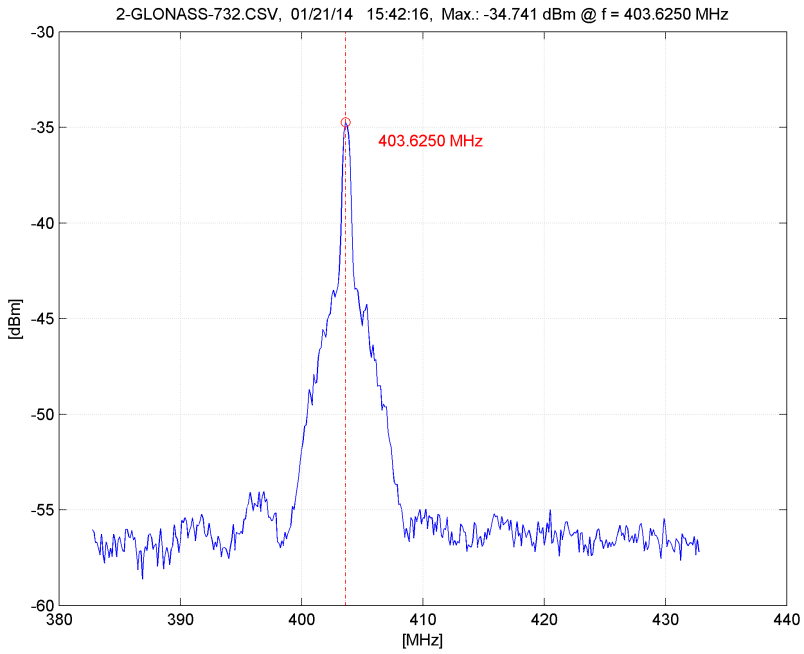

Figure B.16: Frequency spectrum of the satellite GLONASS-732 in the IF domain recorded in Onsala during the G140121a session (2^{nd} scan).

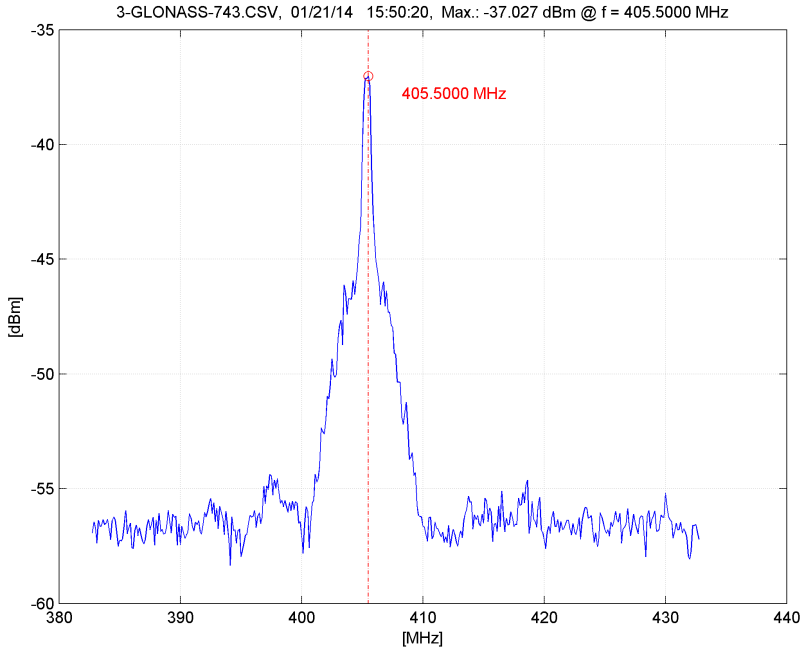

Figure B.17: Frequency spectrum of the satellite GLONASS-743 in the IF domain recorded in Onsala during the G140121a session (3^{rd} scan).

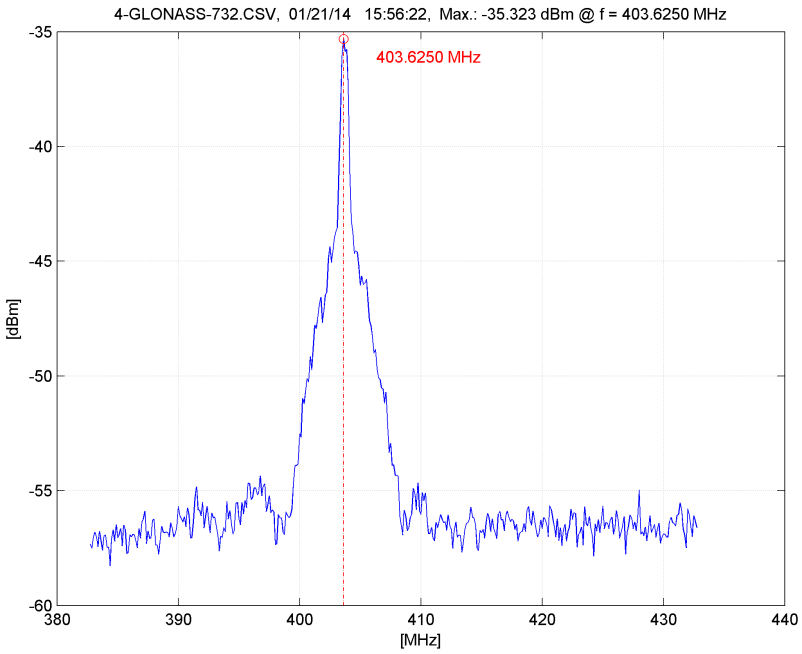

Figure B.18: Frequency spectrum of the satellite GLONASS-732 in the IF domain recorded in Onsala during the G140121a session (4^{th} scan).

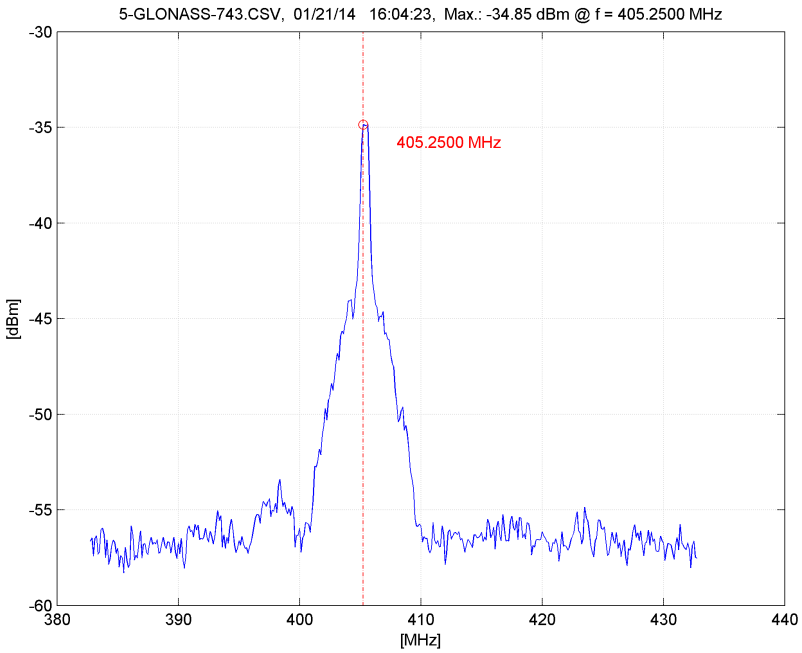

Figure B.19: Frequency spectrum of the satellite GLONASS-743 in the IF domain recorded in Onsala during the G140121a session (5^{th} scan).

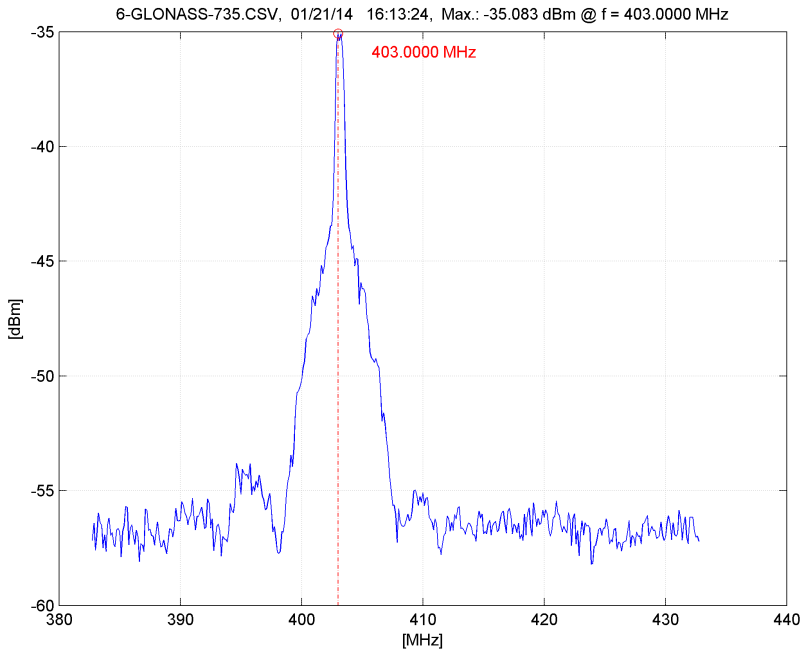

Figure B.20: Frequency spectrum of the satellite GLONASS-735 in the IF domain recorded in Onsala during the G140121a session (6^{th} scan).

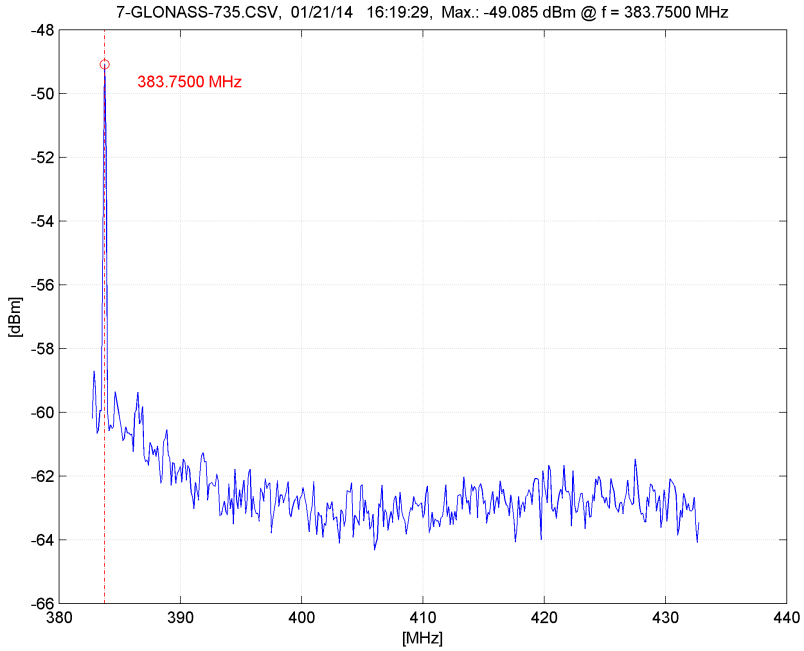

Figure B.21: Frequency spectrum of the satellite GLONASS-735 in the IF domain recorded in Onsala during the G140121a session (7^{th} scan).

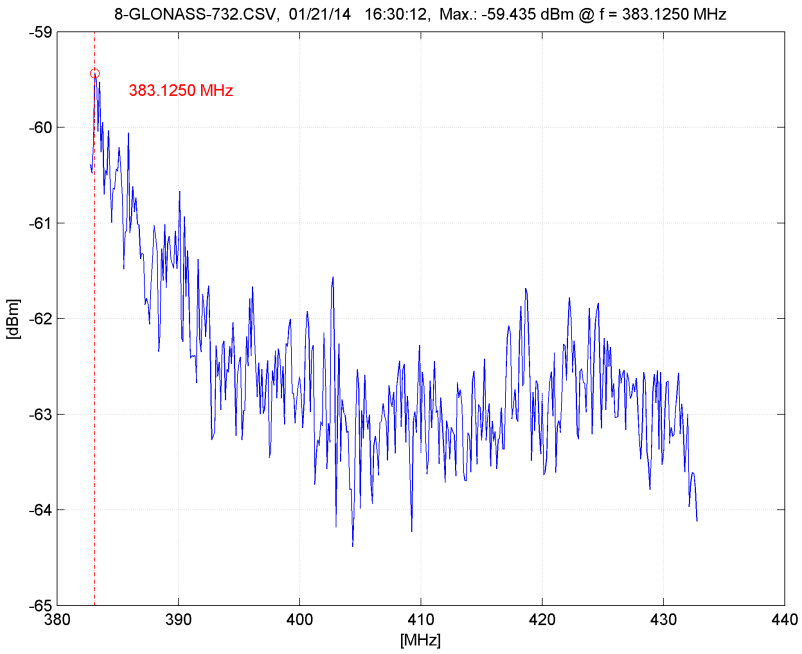

Figure B.22: Frequency spectrum of the satellite GLONASS-732 in the IF domain recorded in Onsala during the G140121a session (8^{th} scan).

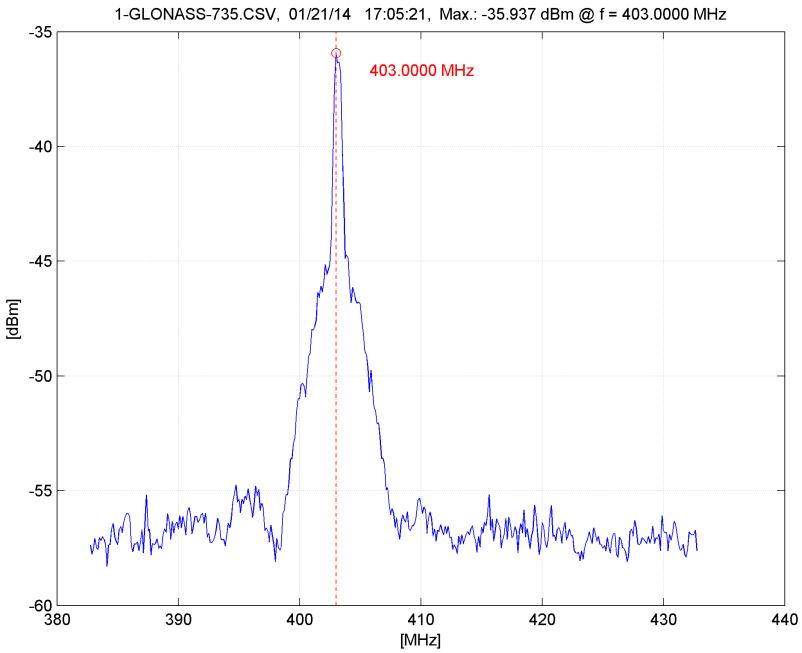

Figure B.23: Frequency spectrum of the satellite GLONASS-735 in the IF domain recorded in Onsala during the G140121b session (1^{st} scan).

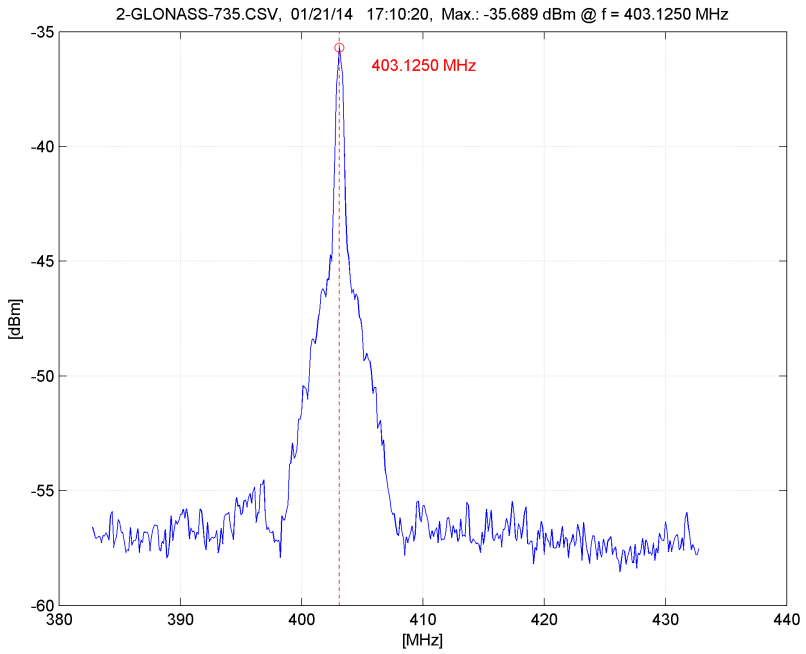

Figure B.24: Frequency spectrum of the satellite GLONASS-735 in the IF domain recorded in Onsala during the G140121b session (2^{nd} scan).

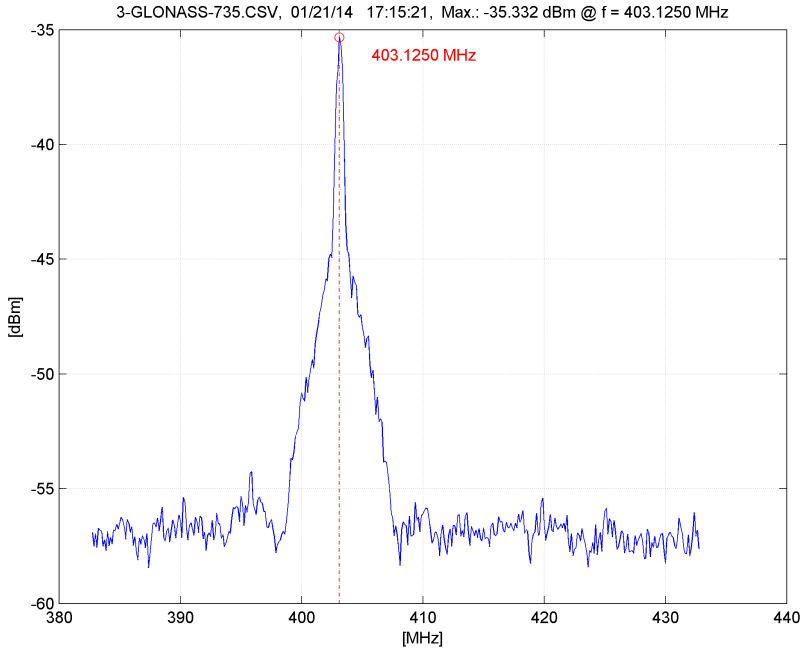

Figure B.25: Frequency spectrum of the satellite GLONASS-735 in the IF domain recorded in Onsala during the G140121b session (3^{rd} scan).

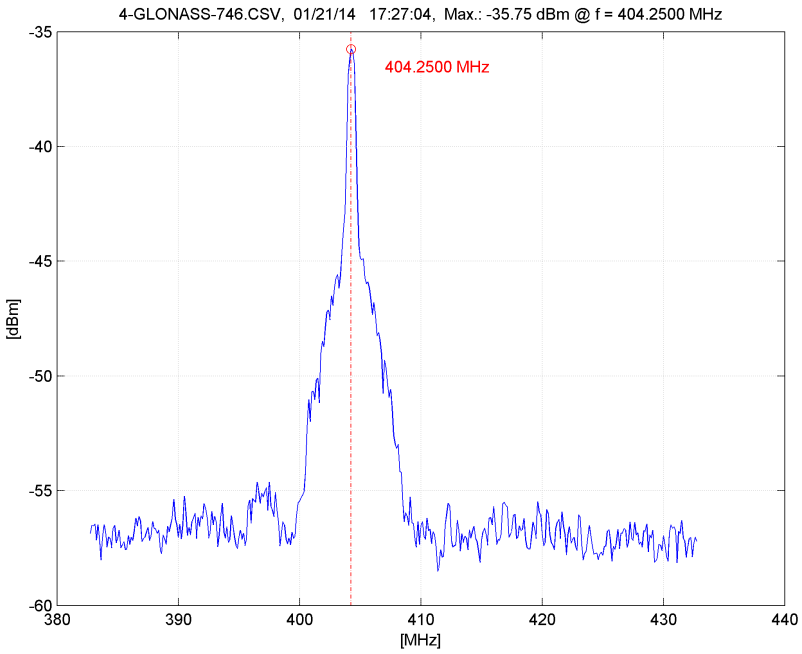

Figure B.26: Frequency spectrum of the satellite GLONASS-746 in the IF domain recorded in Onsala during the G140121b session (4^{th} scan).

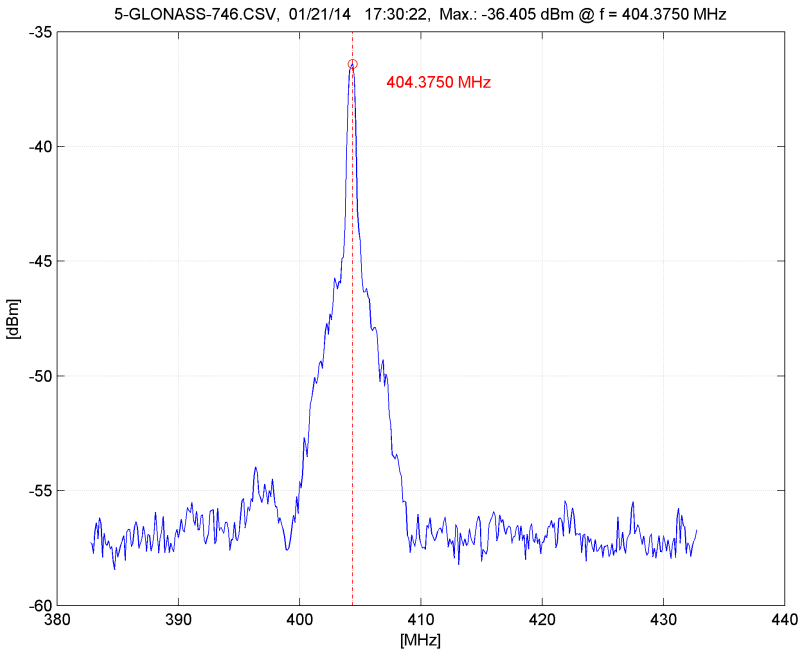

Figure B.27: Frequency spectrum of the satellite GLONASS-746 in the IF domain recorded in Onsala during the G140121b session (5^{th} scan).

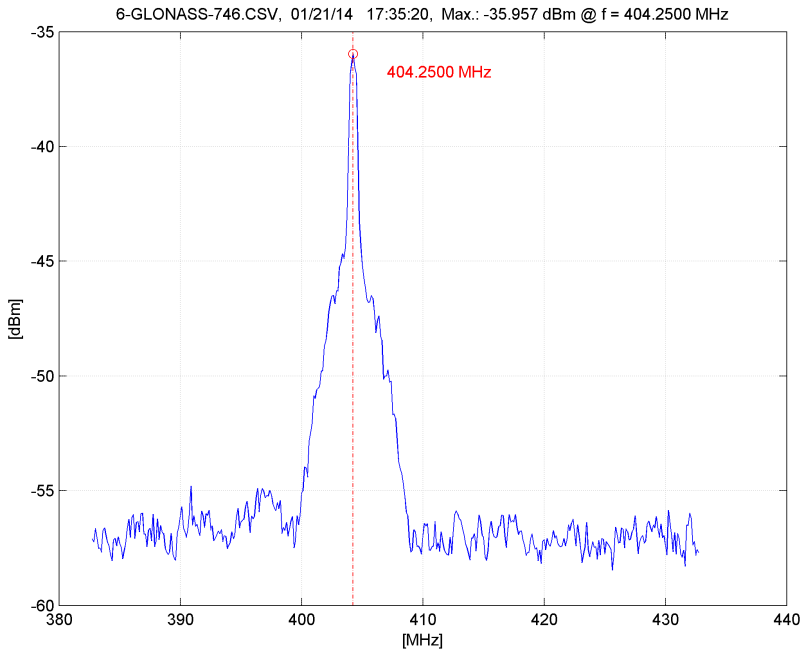

Figure B.28: Frequency spectrum of the satellite GLONASS-746 in the IF domain recorded in Onsala during the G140121b session (6^{th} scan).

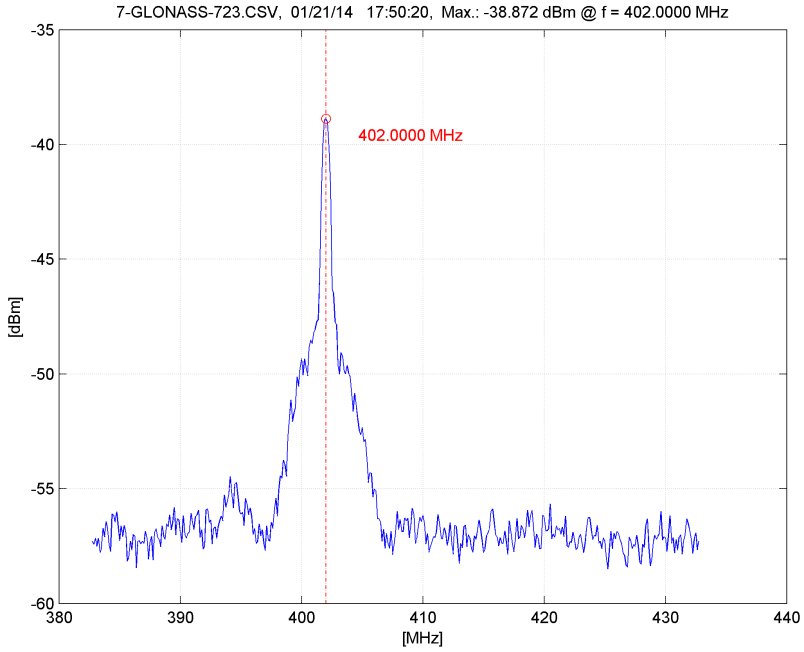

Figure B.29: Frequency spectrum of the satellite GLONASS-723 in the IF domain recorded in Onsala during the G140121b session (7^{th} scan).

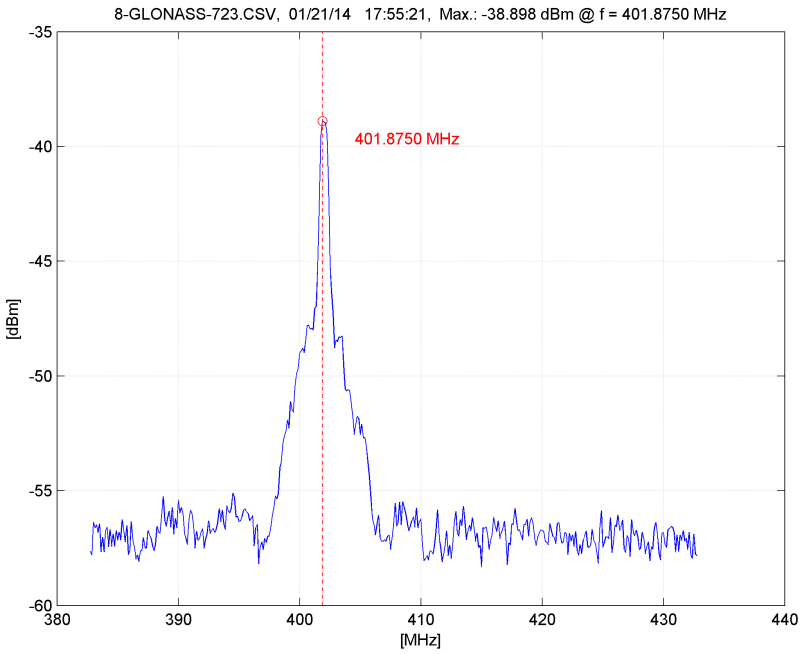

Figure B.30: Frequency spectrum of the satellite GLONASS-723 in the IF domain recorded in Onsala during the G140121b session (8^{th} scan).

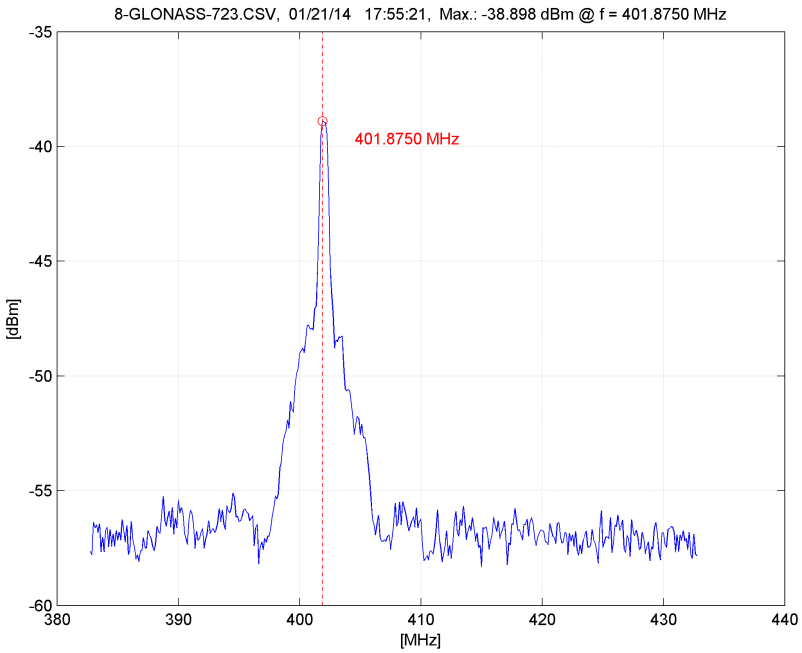

Figure B.31: Frequency spectrum of the satellite GLONASS-723 in the IF domain recorded in Onsala during the G140121b session (9^{th} scan).

Acronyms

C/N_0	Carrier-to-Noise ratio
ACU	Antenna Control Unit
AOS	Arise of Sight
ASFC	Air Force Space Command
BKG	Bundesamt für Kartographie und Geodäsie
BW	Beamwidth
CEST	Central European Summer Time
CIS	Coventional Inertial System
CPF	Consolidated Prediction Format
Dec	Declination
DEF	Pseudo Earth Fixed
DoD	United States Department of Defense
DORIS	Doppler Orbitography and Radiopositioning Integrated by Satellite
ECEF	Earth Centered Eath Fixed
ECI	Earth Centered Inertial
EOP	Earth Orientation Parameters
FESG	Forschungseinrichtung Satellitengeodäsie
FS	Field System
GGOS	Global Geodetic Observing System
GLONASS	Globalnaja Nawigazionnaja Sputnikowaja Sistema
GMST	Greenwich Mean Sidereal Time
GNSS	Global Navigation Satellite Systems
GOW	Geodetic Observatory Wettzell
GPS	Global Positioning System
GRASP	Geodetic Reference Antenna in Space
GSFC	Goddard Space Flight Center
GUI	Graphical User Interface
IAG	International Association of Geodesy
ICRF	International Celestial Reference Frame
IERS	International Earth Rotation and Reference Systems Service
IF	Intermediate Frequency

IGS	International GNSS Service
ILRS	International Laser Ranging Service
ITRF	International Terrestrial Reference Frame
IVS	International VLBI Service for Geodesy and Astrometry
JIVE	Joint Institute for VLBI in Europe
LEO	Low Earth Orbit
LNA	Low Noise Amplifier
LOS	Loss of Sight
NNR	No Net Rotation
NNT	No Net Translation
NORAD	North American Aerospace Defense Command
NRAO	National Radio Astronomy Observatory
PLC	Programmable Logic Control
Ra	Right ascension
RF	Radio Frequency
RTW	Radio Telescope Wettzell
SGP	Simplified General Perturbation
SLR	Satellite Laser Ranging
SNAP	Standard Notation for Astronomical Procedures
SNR	Signal to noise ratio
SOS-W	Satellite Observing System Wettzell
SP3	Standard Product 3
TEME	True Equator, Mean Equinox
TLE	Two Line Elements
TOD	True of Date
TTW	Twin Telescope Wettzell
UT1	Universal Time No. 1
UTC	Coordinated Universal Time
UT	Universal Time
VieVS	Vienna VLBI Software
VLBI	Very Long Baseline Interferometry
VTRF	VLBI Terrestrial Reference Frame
WLRS	Wettzell Laser Ranging System

List of Figures

List of Tables

List of Listings

Bibliography

ALTAMIMI, Z., SILLARD, P. AND BOUCHER, C. (2002). ITRF2000: a new release of the international terrestrial reference frame for earth science applications. *Journal of Geophysical Research (Solid Earth)*, 107j, 1.

ALTAMIMI, Z., COLLILIEUX, X. AND MÉTIVIER, L. (2011). ITRF2008: an improved solution of the international terrestrial reference frame. *Journal of Geodesy.*, 85:8, 457–473.

ANON. (1984). The Astronomical Almanac. With a preface by Charles K. Roberts, Superintendent, United States Naval Observatory, Washington, and Alexander Bokenseberg, Director, Royal Greenwich Observatory.

BAO-YEN TSUI, J. (2005). *Fundamentals of Global Positioning System Receivers: A Software Approach*. Wiley, 2nd edn.

BÖHM, J., BÖHM, S., NILSSON, T., PANY, A., PLANK, L., SPICAKOVA, H., TEKE, K. AND SCHUH, H. (2012). The new Vienna VLBI Software VieVS. In *Proceedings of the 2009 IAG Symposium, Buenos Aires, Argentina*, Vol. 136, International Association of Geodesy Symposia, 31 August - 4 September 2009.

DELLER, A., TINGAY, S., BAILES, M. AND WEST, C. (2007). DiFX: A Software Correlator for Very Long Baseline Interferometry Using Multiprocessor Computing Environments. *The Publications of the Astronomical Society of the Pacific*, 119, 318–336.

DICKEY, J.M. (2010). How and Why do VLBI on GPS. In D. Behrend and K. Baver, eds., *IVS 2010 General Meeting Proceedings, Hobart, Australia*, 65–69, NASA/CP 2010-215864.

DOW, J.M., NEILAN, R.E. AND RIZOS, C. (2009). The International GNSS Service in a changing landscape of Global Navigation Satellite Systems. *Journal of Geodesy.*, 83, 191–198, doi: 10.1007/s00190-008-0300-3.

DUEV, D.A., MOLERA CALVÉS, G., POGREBENKO, S.V., GURVITS, L.I., CIMÓ, G. AND BOCANEGRA BAHAMON, T. (2012). Spacecraft VLBI and Doppler tracking: algorithms and implementation. *Astronomy & Astrophysics*, 541, A43+.

ESCOBAL, P. (1965). *Methods of orbit determination*. New York, J. Wiley.

FEY, A., GORDON, D. AND JACOBS, C.S., eds. (2009). The second realization of the international celestial reference frame by very long baseline interferometry. Frankfurt am Main: Verlag des Bundesamts für Kartographie und Geodäsie, Presented on behalf of the IERS / IVS Working Group, IERS Technical Note 35.

GIPSON, J. (2010). An Introduction to SKED. In *IVS 2010 General Meeting Proceedings, Hobart, Australia*, 77–84, feb. 7–13.

GIPSON, J. (2012). *Sked - VLBI Scheduling Software*. NASA/Goddard Space Flight Center, ftp://gemini.gsfc.nasa.gov/pub/sked/sked_Manual_v2012May09.pdf.

GREISEN, E.W. (2014). Astronomical image processing system. web resource, http://www.aips.nrao.edu/index.shtml.

HAAS, R., NEIDHARDT, A., KODET, J., PLÖTZ, C., SCHREIBER, K., KRONSCHNABL, G., POGREBENKO, S., DUEV, D., CASEY, S., MARTI-VIDAL, I., YANG, J. AND PLANK, L. (2014). The Wettzell-Onsala G130128 experiment – VLBI-observations of a GLONASS satellite. In *Proceedings of the 8th IVS General Meeting, Shanghai*, in print.

HASE, H. (1999). Phase Centre Determinations at GPS-Satellites with VLBI. In W. Schlüter and H. Hase, eds., *Proceedings of the* 13^{th} *Working Meeting of the European VLBI for Geodesy and Astrometry*, 273–277, Bundesamt für Kartographie und Geodäsie, Wettzell, 1999, held at Viechtach, February 12-13, 1999.

HIMWICH, E. AND GIPSON, J. (2012). GSFC Technology Development Center Report. *IVS Annual Report*, 280–282.

HIMWICH, E. AND VANDENBERG, N. (2001). *SNAP Commands - Operations Manual, Version 9.5*. NASA/Goddard Space Flight Center, Space Geodesy Program, ftp://gemini.gsfc.nasa.gov/pub/fsdocs/snapcmd9518.pdf, VLBI Software Documentation, Field System.

HIMWICH, E., VANDENBERG, N., GONZALEZ, R. AND HOLMSTRÖM, C. (2003). New Development in the NASA Field System. In M. Y.C., ed., *New technologies in VLBI, Proceedings of a symposium of the International VLBI Service for Geodesy and Astrometry held in Gyeong-ju, Korea, 5-8 November 2002.*, Vol. 306 of *ASP Conference Series, San Francisco, CA: Astronomical Society of the Pacific*, 193–198.

HOOTS, F. AND ROEHRICH, R. (1980). Spacetrack Report number 3: Models for Propagation of NORAD Element Sets. Tech. rep., US Airforce Aerospace Defense Command, Colorado Springs, CO.

KAPLAN, E. AND HEGARTY, C., eds. (2005). *Understanding GPS - Principles and applications*. Artech House, 2nd edn.

KELSO, T. (1994). Orbit Propagation: Part 1. *Satellite Times*, 1, 70–71.

KELSO, T. (1997). Sunrise...Sunset. *Satellite Times*, 3, 66–67.

KELSO, T. (2007). Validation of SGP4 and IS-GPS-200D Against GPS Precision Ephemerides. In *17th AAS/AIAA Space Flight Mechanics Conference, Sedona, AZ, 2007 January 29*.

KODET, J., PLÖTZ, C., SCHREIBER, U., NEIDHARDT, A., POGREBENKO, S., HAAS, R., MOLERA CALVÉS, G. AND PROCHAZKA, I. (2013). Co-location of space geodetics techniques in space and on the ground. In N. Zubko and M. Poutanen, eds., *Proceedings of the 21st Working Meeting of the European VLBI Group for Geodesy and Astrometry*, 223–226, Finnish Geodetic Institute.

KODET, J., SCHREIBER, K., PLÖTZ, C., NEIDHARDT, A., KRONSCHNABL, G., HAAS, R., MOLERA CALVÉS, G., POGREBENKO, M., ROTHACHER, B., MAENNEL, B., PLANK, L. AND HELLERSCHMIED, A. (2014). Colocations of Space Geodetic Techniques on Ground and in Space. In *Proceedings of the 8th IVS General Meeting, Shanghai*, in print.

KWAK, Y., GOTOH, T., AMAGAI, J., TAKIGUCHI, H., SEKIDO, M., ICHIKAWA, R., SASAO, T., CHO, J. AND KIM, T. (2010). The First Experiment with VLBI-GPS Hybrid System. In D. Behrend and K. Baver, eds., *International VLBI Service for Geodesy and Astrometry 2010 General Meeting Proceedings*, 330–334, NASA/CP 2010-215864.

LOVELL, J., MCCALLUM, J., REID, P., MCCULLOCH, P., BAYNES, B., DICKEY, J., SHABALA, S., WATSON, C., TITOV, O., RUDDICK, R., TWILLEY, R., REYNOLDS, C., TINGAY, S., SHIELD, P., ADADA, R., ELLINGSEN, S., MORGAN, J. AND BIGNALL, H. (2013). The AuScope geodetic VLBI array. *Journal of Geodesy.*, 87, 527–538.

MCCARTHY, D., ed. (1992a). *IERS Conventions*. No. 21 in IERS Technical Note, Central Bureau of IERS - Observatoire de Paris.

MCCARTHY, D., ed. (1992b). *IERS Standards*. No. 13 in IERS Technical Note, Central Bureau of IERS - Observatoire de Paris.

MOYA ESPINOSA, M. AND HAAS, R. (2007). SATTRACK A Satellite Tracking Module for the VLBI Field System. In J. Böhm, A. Pany and H. Schuh, eds., *Proceedings of the 18th European VLBI for Geodesy and Astrometry Working Meeting, 12-13 April 2007, Vienna*, Vol. 79, 53–58, Schriftenreihe der Studienrichtung Vermessung und Geoinformation, Technische Universität Wien, ISSN 1811-8380.

NEIDHARDT, A., KRONSCHNABL, G. AND SCHATZ, R. (2010). Geodetic Observatory Wettzell: 20-m Radio Telescope and Twin Telescopes. *IVS Annual Report*, 113–116.

NEIDHARDT, A., KRONSCHNABL, G., SCHATZ, R. AND SCHÜLER, T. (2014). Geodetic Observatory Wettzell - 20-m Radio Telescope and Twin Telescopes. *IVS Annual Report*, 187–190.

NEREM, R.S. AND DRAPER, R.W. (2011). Geodetic Reference Antenna in Space. *GRASP proposal submitted in response to NNH11ZDA0120*, prepared for National Aeronautics and Space Administration Science Mission Directorate September 29, 2011.

PERLMAN, M., DEGNAN, J. AND BOSWORTH, J. (2002). The international laser ranging service. In *Advances in Space Research*, Vol. 30, No. 2, 135–143, Elsevier.

PETIT, G. AND LUZUM, B., eds. (2010). *IERS Conventions*. No. 36 in IERS Technical Note, Verlag des Bundesamts für Kartographie und Geodäsie.

PETRACHENKO, B. (2013). Radio antennas, feed horns, and front-end receivers. presentation, EGU and IVS Training School on VLBI for Geodesy and Astrometry, March 2-5, 2013, Aalto University, Espoo, Finland.

PETRACHENKO, B., NIELL, A., BEHREND, D., COREY, B., BÖHM, J., CHARLOT, P., COLLIOUD, A., GIPSON, J., HAAS, R., HOBIGER, T., KOYAMA, Y., MACMILLAN, D., MALKIN, Z., NILSSON, T., PANY, A., TUCCARI, G., WHITNEY, A. AND WRESNIK, J. (2009). Progress Report of the IVS VLBI2010 Committee: Design Aspects of the VLBI2010 System. *NASA/TM-2009-214180*, ftp://ivscc.gsfc.nasa.gov/pub/misc/V2C/TM-2009-214180.pdf.

PLANK, L. (2014). *VLBI satellite tracking for the realization of frame ties*. Geowissenschaftliche Mitteilungen, Heft 95, Geowissenschaftliche Mitteilungen, Wien.

PLANK, L., BÖHM, J. AND SCHUH, H. (2014). Precise station positions from vlbi observations to satellites: a simulation study. *Journal of Geodesy*, 88, 659–673.

RICKLEFS, R. (2006). *Consolidated Laser Ranging Prediction Format Version 1.01*. International Laser Ranging Service, Prediction Format Study Group, http://ilrs.gsfc.nasa.gov/docs/2006/cpf_1.01.pdf.

ROTTMANN, H. (2011). Field system overview. Presentation slides, ALMA Phasing Kickoff Meeting, Haystack, 13–14 December 2011.

SALZBERG, I. (1967). Mathematical relationships of the MFOD ANTENNA axes. Tech. Rep. 67N39334, NASA Goddard Space Flight Center, Greenbelt, MD, United States, report/Patent Number: NASA-TM-X-55956, X-553-67-213.

SARTI, P., ABBONDANZA, C., PETROV, L. AND NEGUSINI, M. (2011). Height bias and scale effect induced by antenna gravitational deformations in geodetic VLBI data analysis. *Journal of Geodesy.*, 85:1-8, doi:10.1007/s00190-010-0410-6.

SCHUH, H. AND BEHREND, D. (2012). VLBI: A fascinating technique for geodesy and astrometry. *J. of Geodynamics*, 61, 68–80.

SCHUH, H. AND BÖHM, J. (2013). Very long baseline interferometry for geodesy and astrometry. In G. Xu, ed., *Sciences of Geodesy II, Innovations and Future Developments*, 339–376, Springer Verlag.

SEIDELMANN, P., ed. (1992). *Explanatory Supplement to the Astronomical Almanac*. University Science Books, U.S.

SEITZ, M., ANGERMANN, D., BLOSSFELD, M., DREWES, H. AND GERSTL, M. (2012). The 2008 DGFI realization of the ITRS: DTRF2008. *Journal of Geodesy.*, 86:12, 1097–1123.

SPOFFORD, P. AND REMONDI, B. (1999). *The National Geodetic Survey Standard GPS Format SP3*. NOAA, National Geodetic Survey, NOAA, National Geodetic Survey, SSMC3, N/CG112, 1315 East-West Highway, Silver Spring, Maryland 20910-3282, USA.

SUN, J. (2013). VLBI scheduling strategies with respect to VLBI2010. *Geowissenschaftliche Mitteilungen*, 92, Schriftenreihe der Studienrichtung Vermessung und Geoinformation, Technische Universität Wien, ISSN 1811-8380.

SUN, J., BÖHM, J., NILSSON, T., KRÁSNÁ, H., BÖHM, S. AND SCHUH, H. (2014). New vlbi2010 scheduling strategies and implications on the terrestrial reference frames. *Journal of Geodesy*, 88, 449–461.

THALLER, D., DACH, R., SEITZ, M., BEUTLER, G., MAREYEN, M. AND RICHTER, B. (2011). Combination of GNSS and SLR observations using satellite co-locations. *Journal of Geodesy.*, 85, 257–272.

TORNATORE, V. AND HAAS, R. (2009). Considerations on the observation of GNSS-signals with the VLBI2010 system. In G. Bourda, P. Charlot and A. Collioud, eds., *Proceedings of the* 19^{th} *European VLBI for Geodesy and Astrometry Working Meeting*, 151–155, Université Bordeaux 1 - CNRS Observatoire Aquitain des Sciences de l'Univers Laboratoire d'Astrophysique de Bordeaux, 24-25 March 2009, Bordeaux.

TORNATORE, V., TUCARI, G. AND WEI, E. (2008). First considerations on the Feasibility of GNSS Observations by the VLBI Technique. In A. Finkelstein and D. Behrend, eds., *Measuring the Future, Proceedings of the Fifth IVS General Meeting*, 439–444.

TORNATORE, V., HAAS, R., MACCAFERRI, G., CASEY, S., POGREBENKO, S., MOLERA, G. AND DUEV, D. (2010a). Tracking of GLONASS satellites by VLBI radio telescopes. In *Proc. of the 5th ESA International Workshop on Tracking, Telemetry and Command Systems for Space Applications, TTC 2010, ESA-ESTEC, Noordwijk*.

TORNATORE, V., HAAS, R., MOLERA, G. AND POGREBENKO, S. (2010b). Planning of an Experiment for VLBI Tracking of GNSS satellites. In D. Behrend and K. Baver, eds., *International VLBI Service for Geodesy and Astrometry 2010 General Meeting Proceedings, Hobart, Tasmania, Australia, February 7–13*, 70–74, Goddard Space Flight Center Greenbelt, MD 20771-0001.

TORNATORE, V., HAAS, R., DUEV, D., POGREBENKO, S., CASEY, S., MOLERA CALVÉS, G. AND KEIMPEMA, A. (2011). Single baseline GLONASS observations with VLBI: data processing and first results. In W. Alef, S. Bernhart and A. Nothnagel, eds., *Proceedings of the* 20^{th} *Meeting of the European VLBI Group for Geodesy and Astrometry*, Vol. 22, 162–165, Institut für Geodäsie und Geoinformation der Universität Bonn.

TORNATORE, V., HAAS, R., CASEY, S., POGREBENKO, S. AND MOLERA CALVÉS, G. (2014). Direct VLBI Observations of Global Navigation Satellite System Signals. In C. Rizos and P. Willis, eds., *Earth on the Edge: Science for a Sustainable Planet, Proceedings of the IAG General Assembly, Melbourne, Australia, June 28 – July 2, 2011*, Vol. 6 of *International Association of Geodesy Symposia*, 247 – 252, Springer Berlin Heidelberg.

VALLADO, D. (2013). *Fundamentals of Astrodynamics and Applications*. Microcosm Press, 4th edn.

VALLADO, D., CRAWFORD, P., HUJSAK, R. AND KELSO, T. (2006). Revisiting Spacetrack Report number 3. In *AIAA/AAS Astrodynamics Specialist Conference, Keystone, CO, 2006 August 21–24*.

VANDENBERG, N. (1997). *sked's Catalogs - Program Reference Manual*. NASA/Goddard Space Flight Center, Space Geodesy Program, ftp://gemini.gsfc.nasa.gov/pub/sked/docs/skcat.pdf, VLBI Software Documentation, Scheduling Program.

VANDENBERG, N. (2000). *drudg: Experiment Preparation Drudge Work - Program Reference Manual*. NASA/Goddard Space Flight Center, Space Geodesy Program, ftp://gemini.gsfc.nasa.gov/pub/fsdocs/drudg.pdf, VLBI Software Documentation, Scheduling Program.

VERTEX (2013). *Umrüstung 20m RTW. Betriebshandbuch Servo-Subsystem, Technische Beschreibung und Allgemeine Betriebsanleitung, OM-1012043-30000-01*. Vertex Antennentechnik GmbH, Duisburg, Germany, pp. 78–79.

WALKER, R.C. (2014). *The SCHED User Manual - Version 11.2 of Jan. 22, 2014*. http://www.aoc.nrao.edu/software/sched/.

WHITNEY, A., LONSDALE, C., HIMWICH, E., VANDENBERG, N., VAN LANGEVELDE, H., MUJUNEN, A. AND WALKER, C. (2002). *VEX File Definition/Example, Rev. 1.5b1*. http://www.vlbi.org/vex/docs/vex